Stony Brook University

Studies on p53: From Discovery of Novel Functions to Improving p53-Based Therapies

A Dissertation Presented

by

Angelina Vasileva Vaseva

to

The Graduate School

in Partial Fulfillment of the

Requirements

for the Degree of

Doctor of Philosophy

in

Molecular and Cellular Biology

(Biochemistry and Cell Biology)

Stony Brook University

December 2011

Stony Brook University

The Graduate School

Angelina Vasileva Vaseva

We, the dissertation committee for the above candidate for the

Doctor of Philosophy degree, hereby recommend

acceptance of this dissertation.

Dr. Ute Moll, Professor
Department of Pathology, Dissertation Advisor

Dr. Wei-Xing Zong, Associate Professor
Department of Molecular Genetics and Microbiology
Chairperson of Defense

Dr. Stella Tsirka, Professor
Department of Pharmacology

Dr. Jingfang Ju, Associate Professor
Department of Pharmacology

Dr. Michael Frohman, Professor
Department of Pharmacology

Dr. Basil Rigas, MD, DSc
Professor of Medicine and Pharmacological Sciences
Chief, Division of Gastroenterology and Hepatology

This dissertation is accepted by the Graduate School

Lawrence Martin
Dean of the Graduate School

Abstract of the Dissertation

Studies on p53: From Discovery of Novel Functions to Improving p53-Based Therapies

by

Angelina Vasileva Vaseva

Doctor of Philosophy

in

Molecular and Cellular Biology

(Biochemistry and Cellular Biology)

Stony Brook University

2011

p53 is one of the most important and most frequently mutated tumor suppressors in human cancers and as such has been intensively studied for a long time. p53, which also has roles beyond cancer in normal tissues, is a major orchestrator of the cellular response to a broad array of stress types by regulating apoptosis, cell cycle arrest, senescence, DNA repair and genetic stability. These diverse actions of p53 rely on its function as a transcription factor, as well as on its transcription independent cytosolic functions. An example of transcription independent p53 function is the direct mitochondrial p53 pathway where p53 regulates the intrinsic apoptotic machinery by several direct interactions with members of the Bcl-2 family. Today, an exciting venue in p53 research is the development of p53-reactivating compounds such as Nutlin for the treatment of human cancers that retained wtp53. Although Nutlin-type compounds hold great promise, improvements are still necessary before they can be established in the clinic.

During my dissertation research I conducted three studies related to p53. The first shows a critical role of the direct mitochondrial p53 pathway during Nutlin-induced apoptosis in wild-type p53 retaining cancer cells, therefore establishing this pathway as a therapeutically relevant mechanism in p53-based therapies. My second project identifies the Hsp90 inhibitor 17AAG as a potent synthetic lethal synergistic partner of Nutlin for treatment of difficult-to kill solid human tumors. My third project describes a completely novel and exiting function of mitochondrial p53 in inducing tissue necrosis during oxidative stress. Upon such stress, p53 translocates to the mitochondrial matrix and regulates (induces opening of) the mitochondrial Permeability Transition Pore by direct interaction with the pore's essential regulatory protein Cyclophilin D. This unsuspected new function of p53 impacts brain ischemia-reperfusion injury during stroke in vivo.

Table of contents

List of Figures…… vi

List of Abbreviations…… viii

Acknowledgements…… x

Publications…… xi

I. Introduction…… 1

A. Domain organization of the p53 protein…… 2

B. p53 as a transcription factor…… 4

1. Regulation of apoptosis…… 4

2. Regulation of cell proliferation and growth…… 5

3. Regulation of ROS…….... 6

4. Regulation of metabolism…… 7

5. Inhibition of angiogenesis…… 8

6. Regulation of DNA repair…… 9

7. Functions of p53 not associated with tumor suppression…… 9

C. Regulation of p53 cellular levels and activity…… 11

D. Mitochondria mediated cell death…… 13

1. Regulation of intrinsic apoptotic pathway by Bcl-2 family members.. 13

2. Permeability transition pore (PTP)…… 14

E. The mitochondrial p53 pathway…… 16

1. p53 translocates to mitochondria upon various stress stimuli…… 16

2. Direct interaction with BCL-2 family members…… 17

3. Monoubiquitination of cytoplasmic p53 promotes mitochondrial translocation…… 18

4. The mitochondrial p53 pathway in pathophysiology…… 19

F. p53 based therapies and Nutlin…… 23

II. Results…….. 27

A. The transcription-independent mitochondrial p53 program is a major contributor to Nutlin-induced apoptosis in tumor cells…..…..……..... 28

B. Blockade of Hsp90 by 17AAG antagonizes MDMX and synergizes with Nutlin to induce p53-mediated apoptosis in solid tumors…….……... 33

C. p53 protein regulates the mitochondrial permeability transition pore during oxidative stress-induced necrosis and ischemic stroke.……. 41

III. Discussion……. 50

IV. Future Directions…….……...…….……. 61

V. Materials and Methods……...……. 67

References……. 78

Appendix…….....……...……. 92

List of Figures

Figure 1. Nutlin stabilizes p53, resulting in induced p53 transcriptional activity and apoptosis in ML-1 cells.

Figure 2. Nutlin stabilizes p53 protein levels in both nucleus and cytoplasm, does not prevent mono-ubiquitination of p53 and disrupts partially the p53-MDM2 complex formation.

Figure 3. Nutlin promotes mitochondrial translocation of p53.

Figure 4. Specific blocking of mitochondrial p53 significantly reduces the apoptotic response to Nutlin.

Figure 5. Blocking of Nutlin-induced transcription with αAmanitin does not block apoptotic response to Nutlin.

Figure 6. Specific blocking of p53-mediated transcription with PFTα does not block apoptotic response to Nutlin.

Figure 7. 17AAG increases wtp53 and p21, but decreases MDMX and MDM2 protein levels.

Figure 8. 17AAG stabilizes p53 protein and induces transcription of p53 targets.

Figure 9. Destabilization of MDMX by 17AAG is caspase-independent and proteasome-dependent, while destabilization of MDM2 is a caspase-dependent event.

Figure 10. 17AAG disrupts the p53-MDMX and MDMX-MDM2 interactions.

Figure 11. 17AAG kills cancer cells in a p53 dependent manner.

Figure 12. 17AAG induces transcription of p53 targets p21, PUMA and MDM2 in p53+/+ but not in p53-/- cells.

Figure 13. Combining Nutlin and 17AAG significantly increases cell death as compared to single treatments.

Figure 14. Combination of Nutlin and 17AAG dramatically increases cell death in p53+/+ but not in p53-/- cells.

Figure 15. Synergistic induction of cell death upon combination of Nutlin and 17AAG.

Figure 16. 17AAG modulates Nutlin-induced signaling.

Figure 17. The effect of 17AAG on Nutlin-induced signaling is p53 dependent.

Figure 18. 17AAG enhances Nutlin-induced apoptosis through inhibition of MDMX.

Figure 19. 17AAG enhances Nutlin-induced apoptosis through inhibition of PI3K pathway.

Figure 20. In vivo activity of the Nutlin and 17AAG drug combination on established RKO tumor xenografts in nude mice.

Figure 21. In contrast to tBid, p53's MOMP activity can be independent of Bax and Bak.

Figure 22. p53, but not tBid opens the PTP and induces physical alterations of VDAC.

Figure 23. p53, but not tBid induces mitochondrial swelling in a CypD-dependent and Bax/Bak-independent manner.

Figure 24. Mitochondrial p53 Interacts with CypD, but not with VDAC or ANT.

Figure 25. Mapping the CypD interaction on p53

Figure 26. Upon oxidative stress p53 is rapidly stabilized.

Figure 27. Upon oxidative stress p53 translocates to mitochondria.

Figure 28. p53 deficiency renders cells resistant to H_2O_2-induced and CsA-dependent loss of mitochondrial membrane potential ($\Delta\Psi m$).

Figure 29. p53 deficiency renders primary MEFs resistant to PTP opening.

Figure 30. In primary MEFs, oxidative stress induces necrosis that depends on p53 and CypD.

Figure 31. p53 deficiency and silencing of CypD protects HCT116 cells from H_2O_2-induced necrosis.

Figure 32. Mitochondrial matrix-targeted p53 (Leader p53-Lp53) reduces $\Delta\Psi m$ in a CypD dependent manner.

Figure 33. Mitochondrial matrix-targeted p53 (Lp53) renders p53-/- cells more sensitive to H_2O_2-induced necrotic death in a CypD dependent manner.

Figure 34. Blocking of transcription does not prevent H_2O_2 -induced PTP opening or cell death.

Figure 35. Lp53 renders Bax/Bak double knock out MEFs sensitive to oxidative stress in a CypD dependent manner.

Figure 36. The p53-CypD complex has a pathophysiologic role in ischemic stroke.

Figure 37. Expression of apoptotic proteins PUMA and Noxa and p73 family members upon MCAO.

List of Abbreviations

WT	wild type
ATM	ataxia telangiectasia mutated
ATR	ataxia-telangiectasia-mutated and Rad3-related
MDM2	murine double minute 2
MDMX	murine double minute X
Hsp90	heat shock protein 90
17AAG	17-allylamino-17-demethoxygeldanamycin
17DMAG	17-dimethylaminoethylamino-17-demethoxy-geldanamycin
PUMA	p53 up-regulated modulator of apoptosis
Bcl-2	B-cell lymphoma 2
BH	Bcl-2 homology
PARP	poly(ADP-ribose)polymerase;
PI3K	phosphatidylinositol-3-Kinase;
AKT	serine/threonine protein kinase B
PI	propidium iodide
FACS	fluorescence-activated cell sorting
ANT	adenine nucleotide translocase
VDAC	voltage dependent anion channel
CypD	cyclophilin D
PTP	permeability transition pore
mPT	mitochondrial permeability transition

MCAO	middle cerebral artery occlusion
HMGB1	high-mobility group box 1 protein
MEF	mouse embryonic fibroblast
DMEM	dulbecco's modified essential medium
RPMI	roswell park memorial institute medium
ROS	reactive oxygen species
CTB	cell titer blue assay
TUNEL	terminal transferase dUTP end labeling assay
MOMP	mitochondrial outer membrane permeabilization
HAUSP	herpes-virus-associated ubiquitin- specific protease
PFTα	pifithrin α
OD	optical density
TMRM	tetramethyl rhodamine methyl ester
Calcein AM	calcein acetomethoxy
SH3	src homology 3 domain
HIF-1	hypoxia inducible factor 1
VEGF	vascular endothelial growth factor
MAPK	mitogen activated protein kinase
Chk2	check point kinase 2

Acknowledgements

I would like to thank my advisor Dr. Ute Moll for advise and guidance; my committee members Dr. Wei-Xing Zong, Dr. Stella Tsirka, Dr. Jingfang Ju, Dr. Michael Frohman and Dr. Basil Rigas for support and advising; Natasha Marchenko, Alisha Yallowitz, Sulan Xu for help with projects; other Moll lab members for support; my husband Raehum Paik and my mother Nadka Vaseva for support and help; Susan Vanhorn and the Central Microscopy Imaging Center at Stony Brook University for sample processing and electron microscopy imaging; Stony Brook University FACS facility for assistance with flow cytometry; and the Molecular and Cellular Biology program at Stony Brook University.

Some material in this dissertation is reprinted with permission from articles published in Biochimica et Biophysica Acta, Cell Cycle and Cell Death and Disease.

Permission from Biochimica et Biophysica Acta was granted through the copyright agreement: Elsevier journals grant to authors the right to include the journal article, in full or in part, in a thesis or dissertation.

Permission from Cell Cycle was granted through the copyright agreement: authors retain the following non-exclusive rights: Use of all or part of the Contribution (after publication in the Journal) in any book, article, thesis or dissertation written by the authors without first requiring permission from Landes Bioscience.

Permission from Cell Death and Disease was granted through the copyright agreement: For journals published by Nature Publishing Group authors retain the non-exclusive rights to reproduce the Contribution in whole or in part in any printed volume (book or thesis) of which they are the author(s).

Publications

1**. Vaseva AV**, Wolf S, Ju K, Tsirka SE, Moll UM. p53 regulates the mitochondrial PTP pore during oxidative stress-induced necrosis. (submitted)

2. Zuber J, Rappaport AR, Luo W, Wang E, Chen C, **Vaseva AV**, Shi J, Weissmueller S, Fellmann S, Taylor MS, Graeber TG, Kogan SC, Vakoc CR, Lowe SW. An integrated approach to dissecting oncogene addiction implicates a Myb coordinated self-renewal program as essential for leukemia maintenance. Genes Dev. 2011 Aug 1;25(15):1628-40.

3. **Vaseva AV**, Moll UM. Detection of Mitochondrial Localization of p53. Book chapter from: Methods in Molecular Biology : p53 Protocols. Edited by: S. Deb and S. P. Deb © Humana Press Inc., Totowa, NJ

4. **Vaseva AV**, Yallowitz AR, Marchenko ND, Xu S, Moll UM. Blockade of Hsp90 by 17AAG antagonizes MDMX and synergizes with Nutlin to induce p53-mediated apoptosis in solid tumors. Cell Death Dis. 2011 May 12;2:e156.

5. Talos F, Abraham A, **Vaseva AV**, Holembowski L, Tsirka SE, Scheel A, Bode D, Dobbelstein M, Brück W, Moll UM. p73 is an essential regulator of neural stem cell maintenance in embryonal and adult CNS neurogenesis. Cell Death Differ. 2010 Dec;17(12):1816-29

6. Kimple RJ, **Vaseva AV**, Cox AD, Baerman KM, Calvo BF, Tepper JE, Shields JM, Sartor CI. Radiosensitization of epidermal growth factor receptor/HER2-positive pancreatic cancer is mediated by inhibition of Akt independent of ras mutational status. Clin Cancer Res. 2010 Feb 1;16(3):912-23.

7. Hagn F, Klein C, Demmer O, Marchenko N, **Vaseva A**, Moll UM, Kessler H. BclxL changes conformation upon binding to wild-type but not mutant p53 DNA binding domain. J Biol Chem. 2010 Jan 29;285(5):3439-50

8. Zimmer Y**, Vaseva AV**, Medová M, Streit B, Blank-Liss W, Greiner RH, Schiering N, Aebersold DM. Differential inhibition sensitivities of MET mutants to the small molecule inhibitor SU11274. Cancer Lett. 2010 Mar 28;289(2):228-36

9. **Vaseva AV**, Marchenko ND, Moll UM. The transcription-independent mitochondrial p53 program is a major contributor to Nutlin-induced apoptosis in tumor cells. Cell Cycle. 2009 Jun 1;8(11):1711-9

10. **Vaseva AV**, Moll UM. The mitochondrial p53 pathway. Biochim Biophys Acta. 2009 May;1787(5):414-20.

11. Palacios G, Crawford HC, **Vaseva A**, Moll UM. . Mitochondrially targeted wild-type p53 ind
duces apoptosis in a solid human tumor xenograft model. Cell Cycle. 2008 Aug 15;7(16):2584-90.

12. Freemantle SJ, **Vaseva AV**, Ewings KE, Bee T, Krizan KA, Kelley MR, Hattab EM, Memoli VA, Black CC, Spinella MJ, Dmitrovsky E. Repression of cyclin D1 as a target for germ cell tumors. Int J Oncol. 2007 Feb;30(2):333-40.

13. White KA, Yore MM, Warburton SL, **Vaseva AV**, Rieder E, Freemantle SJ, Spinella MJ. Negative feedback at the level of nuclear receptor coregulation. Self-limitation of retinoid signaling by RIP140.J Biol Chem. 2003 Nov 7;278(45):43889-92.

I. Introduction

A. Domain organization of the p53 protein

The structure of the p53 protein reflects its functional complexity. p53 consists of 393 residues and is active as a homo-tetramer when binding DNA. The N-terminal region includes a transactivation domain (TAD) followed by a proline-rich region and the central DNA-binding core domain that is responsible for sequence-specific DNA binding. The DNA-binding domain is connected to a short tetramerization domain that regulates the oligomerization state of p53. At its C-terminus p53 contains the so-called regulatory domain, which is rich in basic amino acids (mainly lysines) and binds DNA nonspecifically.

The N-terminal region of p53 is unfolded and consists of an acidic TAD (residues 1-61) and a proline-rich region (residues 64–92). The TAD is a binding site for interacting proteins, such as components of the transcriptional machinery, transcriptional coactivators p300/CBP (CREB-binding protein), and the negative regulators MDM2 and MDMX (1-3). Since p300 and MDM2 compete for the same binding site, binding of the negative regulators MDM2 and MDMX occludes TAD and prevents the coactivator p300 or components of the transcriptional machinery from binding, thereby regulating the transcriptional activity of p53. The TAD is a site for multiple posttranslational modifications by several kinases, which also determine the activation state of p53 (4).

The proline-rich region that links the TAD to the DNA-binding domain in human p53 contains five PXXP motifs. Such motifs bind to SH3 domains (Src homology 3 domains) and mediate numerous protein-protein interactions in signal transduction. The exact role of the proline-rich region is not well understood. Mutational studies have determined that this region is dispensable for tumor suppression, and instead may function as a spacer between the TAD and DNA-binding domains (5).

The DNA binding domain-DBD (also called core domain) consists of an immunoglobulin-like β-sandwich. Besides binding to DNA, this domain also participates in interaction with other proteins through the loops that separate the β-sandwiches in the fold (6). Most of the cancer-associated naturally occurring p53 mutations are found in DBD and disturb the interaction of p53 with DNA, therefore impairing its ability to activate target genes and exert tumor suppressive functions. Of note, these mutations also disturb interactions with Bcl-2 family members. Thus, DBD mutations appear to be double hit mutations simultaneously inactivating both the nuclear and the mitochondrial tumor suppressive activities of p53 (6).

The tetramerization domain of p53 is located in the C-terminal region and spans residues 325-356. It consists of a short β-strand and α-helix and is followed by the extreme C-terminus. The C-terminal region of p53 is subject to extensive posttranslational modifications, including acetylation, ubiquitination, phosphorylation, sumoylation, and methylation that regulate p53 function and cellular levels (4). The extreme C-terminus binds to DNA nonspecifically, which inhibits specific DNA binding of the core domain, thereby creating a negative autoregulation.

B. p53 as a transcription factor

Numerous genes have been discovered as transcriptional targets of p53, regulating multiple cellular processes such as cell death, cell cycle, senescence, DNA repair etc. Most of these genes have been considered to mediate the tumor suppressive functions of p53. However, recently it was recognized that p53 is also important for normal biological events in unstressed tissues, such as metabolism, reproduction, and various aspects of differentiation and development.

1. Regulation of apoptosis

Many models consider that apoptosis induction is an essential function of p53 as a tumor suppressor. Loss of p53-dependent apoptosis accelerates brain tumorigenesis in mice (7) and promotes lymphomagenesis in Eμ-Myc mice (8) without the need to inactivate p53 itself. Several Bcl-2 family proteins were discovered as critical mediators of p53-dependent apoptosis. The first identified was BAX, a crucial mediator of the mitochondrial apoptotic machinery, which upon stimuli forms dynamic lipid pores on the outer mitochondrial membrane that enable the release of apoptogenic factors (9). In a brain tumor model, loss of BAX causes accelerated tumor growth due to loss of p53 (10). BAX mediates p53-dependent apoptosis induced by 5-FU in colorectal

cancer cells (11). However, BAX is dispensable for apoptosis induced by γ-irradiation in thymocytes and intestinal epithelial cells and in many tissues BAX induction is not strictly dependent on p53 (12). The BH3-only proteins PUMA and Noxa that belong to the Bcl-2 family have also been described as critical mediators of p53 pro-apoptotic functions. Both proteins are activated in a p53-dependent manner following DNA damage (13-15) but are also induced by other pathways. Induction of PUMA by p53 is necessary for the apoptotic response in many tissues (16) and PUMA knockout mice recapitulate the acute apoptosis deficiencies observed in p53 knockout mice (17, 18). Noxa knockout mice also exhibit impaired apoptosis, albeit to a much lower extent (18).

At the same time, studies have also suggested that besides induction of apoptosis, other functions of p53 may be equally important to prevent cancer development. For example, despite the fact that in many tissues p53-mediated induction of PUMA is necessary for the acute apoptotic DNA damage response to p53 activation, *PUMA* null mice do not develop tumors (16, 19). Furthermore, mice harboring a specific p53 mutant (R175P) which is devoid of apoptotic functions are still protected from tumor development compared to p53 null littermates (20). Thus, p53 can retain tumor suppressive functions even in the absence of a robust apoptotic response.

2. Regulation of cell proliferation and growth

Other targets of p53 that were shown to contribute to tumor suppressive functions are genes that participate in regulation of cell proliferation and growth. Indeed, the most sensitive p53 transcriptional target is the cyclin-dependent kinase inhibitor p21, which blocks cell

proliferation by causing cell cycle arrest at the G1/S transition of the cell cycle. The induction of p21 expression is extremely sensitive to even low levels of p53 protein, and a temporary G1 block, induced by mild damage or stress might allow cells to survive until the damage has been resolved or the stress removed, therefore preventing accumulation of oncogenic lesions (21, 22). However, it was proposed that this might be a risky strategy, since a cell with oncogenic damage that cannot be repaired would be allowed to survive and resume proliferation. Other p53 targets that also contribute to cell cycle arrest especially at the G2/M border are 14-3-3 sigma and GADD45 (23).

Another p53-mediated cellular response to stress is senescence, an irreversible cell cycle arrest. Irreversible senescence induced by DNA damage and oncogene activation could be a more desirable outcome of p53 activation for inhibition of tumor initiation and/or progression than reversible cell cycle arrest. Studies have demonstrated that senescence is an important response to p53 activation, even in established tumors (24, 25). In mouse models, senescence induced by reactivation of p53 and subsequent engagement of the immune system can result in tumor clearance (24). Although not yet well established, several genes regulated by p53 are thought to mediate the senescence response. Some candidate genes include plasminogen activator inhibitor 1 (PAI-1) (26) and p21 (27).

3. Regulation of ROS

In addition to eliminating damaged cells, p53 can also contribute to cell survival. These functions of p53 are also associated with its tumor suppressor activity. For example, many antioxidant genes are activated by p53 to suppress endogenous ROS production. Among those

are Sestrins, Catalase, Manganese Super Oxide Dismutase, TIGAR etc (28). The activity of these genes is critical for protection from lower levels of oxidative stress, transformation and genomic instability. Conversely, upon severe stress p53 target genes such as the quinone oxidoreductase homolog TP53I3 (also known as PIG3) are involved in the generation of ROS to promote induction of cell death (28). Therefore, depending on the conditions p53 can activate seemingly opposing cellular processes, which in both cases would mediate its tumor suppressive activities either by preventing the accumulation of oncogenic lesions or by eliminating damaged cells through cell death or senescence.

4. Regulation of metabolism

Changes in cell metabolism also play a vital role in supporting tumor development. Cancer cells engage in reprogramming metabolic pathways that provides them with many benefits, including the ability to survive under unfavorable conditions (such as low oxygen and starvation), the ability to utilize anabolic pathways necessary for growth, and the ability to limit oxidative damage.

Starvation causes p53 stabilization. This in turn activates a set of genes which negatively regulate the kinase mTOR (mammalian target of rapamycin), which has a central positive role in the control of protein synthesis (28). Additionally, upon starvation p53 target genes such as the lysosomal protein DRAM (damage-regulated autophagy modulator) can promote autophagy, a process during which damaged proteins and organelles are eliminated, thereby promoting short-term cell survival under starvation conditions (29). Autophagy can also be regulated through negative regulation of mTOR signaling.

Additionally, several studies have shown that p53 has a role in the regulation of both glycolysis and oxidative phosphorylation. p53 can slow glycolysis and therefore counteract the increase in glycolysis that is characteristic of cancer cells. These functions of p53 are the result of its ability to inhibit the expression of the glucose transporters GLUT1 and GLUT4 and decrease the levels of phosphoglycerate mutase (PGM), while increase the expression of TIGAR (30), all of which result in suppressing glycolysis at various steps of the glycolytic pathway. While not yet clear exactly how, p53 can also indirectly inhibit glycolysis through modulating NFkB pathway (31).

5. Inhibition of angiogenesis

p53 also exerts tumor suppressor effects through inhibition of new blood vessel development (angiogenesis). p53 has been shown to limit angiogenesis by at least three mechanisms: (1) by modulating regulators of hypoxia that mediate angiogenesis. p53 promotes Mdm2-mediated ubiquitination and proteasomal degradation of the HIF-1α subunit of hypoxia-inducible factor 1 (HIF-1), a heterodimeric transcription factor that regulates cellular energy metabolism and angiogenesis in response to hypoxia (lack or low levels of oxygen). (2) By inhibiting production of angiogenic factors, such as negatively regulating the expression of vascular endothelial growth factor/vascular permeability factor (VEGF/VPF), a factor that stimulates the proliferation of endothelial cells. (3) by directly increasing the production of endogenous angiogenesis inhibitors. For example, p53 can stimulate the expression of thrombospondin-1 (TSP-1) gene trough positive regulation of TSP-1 promoter sequences. TSP-1 is a large, multifunctional matrix glycoprotein, which is a potent inhibitor of neovascularization

(32). The combination of these effects allows p53 to efficiently inhibit the angiogenic potential of cancer cells. This is evident in tumors carrying inactivating p53 mutations, which appear more vascularized and are often more aggressive.

6. Regulation of DNA repair

Besides reducing endogenous ROS, which can reduce DNA lesions and therefore maintain genomic stability and prevent tumorigenicity, p53 was shown to directly regulate DNA repair. A gene target of p53 called p53-inducible ribonucleotide reductase small subunit 2 (p53R2) encodes a protein similar to the R2 subunit of an enzyme that catalyzes the production of deoxyribonucleotide triphosphates (dNTPs). Therefore, p53 is able to regulate the synthesis of dNTPs, necessary during DNA-repair (33).

7. Functions of p53 not associated with tumor suppression

It is increasingly recognized that p53 also possess functions distinctive from its tumor suppressor functions. A role of p53 in negatively regulating stem cell renewal has been described by several studies. For example, p53 can limit the self-renewal of adult neural stem cells most likely through regulation of p21 expression (34, 35). Also, p53 can modulate quiescence in hematopoietic stem cells through direct targeting of the Gfi-1 and Necdin genes, which are important for regulation of cell cycle progression in hematopoietic stem cells (35).

p53 also represses the expression of CD44 cell surface proteins involved in regulating cell migration and survival (36). Because basal levels of p53 control CD44, this function of p53

most likely does not contribute to tumor suppression, but rather suggests that p53 would be involved in regulating normal functions of CD44, such as epithelial development or stem cell renewal. In other studies, p53 has been shown to contribute to maternal reproduction in mice by directly regulating the expression of leukemia inhibitory factor (LIF), a protein required for blastocyst implantation (37).

C. Regulation of p53 cellular levels and activity

Normally, p53 protein is maintained at very low levels due to constant degradation via ubiquitin-mediated proteolysis, a process where several copies of the small protein ubiquitin are attached to the protein that is destined for degradation, a process called poly-ubiquitination. The attached ubiquitin chain acts as a signal, enabling p53 to be detected by the proteasome, where protein digestion occurs. The MDM2 (mouse double minute 2) protein is the major ubiquitin E3 ligase involved in tagging p53 with ubiquitin. Disruption of the interaction between MDM2 and p53 or deletion of MDM2 results in rapid p53 stabilization and dramatic increase in p53 protein levels. Stabilized p53 translocates to the nucleus where it activates target genes. This process is subject to a negative feedback loop, since one of the genes whose transcription is activated by p53 is MDM2 itself. MMDM2 also directly inhibits p53 binding to targeted DNA sequences, thereby directly inhibiting p53's transcriptional function (38).

Another important regulator of p53 levels and activity is the protein MDMX. MDMX shows high similarity to MDM2; however it does not possess its own ubiquitin ligase activity. The most widely accepted model suggests that MDMX plays a major role in inhibiting the transcriptional activities of p53, as it has been detected at p53-responsive promoter elements. It

has been also suggested that MDMX plays a role in promoting MDM2 E3 ligase activity toward p53 via MDM2 hetero-oligomerization, thereby indirectly controlling p53 levels as well (38).

Several pathways lead to p53 stabilization. One pathway is activated upon DNA damage following ionizing irradiation. Two protein kinases play central roles: ATM (ataxia telangiectasia mutated) and Chk2. ATM activity is stimulated by double-strand breaks, and Chk2 is in turn stimulated by activated ATM. They phosphorylate p53 at amino-terminal sites that are close to the MDM2-binding region, thereby blocking its interactions with MDM2 and leading to stabilization of p53 (39). The second pathway activating p53 involves the expression of oncogenes such as Ras and Myc in the absence of DNA damage. These oncogenes stimulate the transcription of the p14ARF gene or stabilization of the p14ARF protein, which then binds to and inhibits MDM2. A third classical pathway is activated during UV-exposure, where ATR (ataxia telangiectasia related) plays a central role. Many other kinases can also modify p53, MDM2 or MDMX (for example AKT, PI3K, p38 MAPK, ERK MAPK, c-Abl etc.), providing additional pathways for activation of p53 signaling in the absence of DNA damage or oncogene activation, such as during starvation, hypoxia, oxidative stress, response to chemotherapeutic drugs, kinase inhibitors etc. (38). Numerous other modifications such as acetylation, sumoylation and monoubiquitination of lysine residues on p53, MDM2 and MDMX have also been described as important determinants for their activities and add tremendous complexity to the tight regulation of the p53 signaling pathway.

D. Mitochondria mediated cell death

Two modes of cell death can be mediated via mitochondria. The first is the intrinsic apoptotic cell death pathway that is regulated by Bcl-2 family members and induced by various stimuli. The second, regulated by the so-called mitochondrial permeability transition pore (PTP), is a regulated necrotic pathway and is activated upon Ca^{2+} overload or ROS.

1. Regulation of the intrinsic apoptotic pathway by Bcl-2 family members

Bcl-2 (for B-cell lymphoma 2) family members are proteins that mediate mitochondrial outer membrane permeabilization (MOMP), thereby allowing the release of apoptogenic factors from the intermembranous mitochondrial space. These factors in turn activate a cascade of signals ultimately leading to the activation of effector caspases, proteases with a central role in the execution of cell death. Characteristic of Bcl-2 family proteins is the presence of Bcl-2 homology domains (BH). Functionally, they are divided into anti-apoptotic and pro-apoptotic members. The anti-apoptotic members such as Bcl-2, Bcl-xL and Mcl-1 contain BH1, BH2, BH3 and BH4 domains. The proapoptotic members fall into two subclasses: (i) the ultimate MOMP

effectors Bax and Bak containing BH1, BH2 and BH3 domains, and (ii) the BH3-only class, which carries a single BH3 domain. Upon activation, Bax and Bak insert into the outer mitochondrial membrane and oligomerize to presumably form dynamic lipid pores that release the lethal proteins from the mitochondrial intermembranous space. BH3-only proteins (more than a dozen exist) fall into two subgroups - 'activators' and 'derepressors', according to how they trigger apoptosis. Activators (tBid and Bim) trigger MOMP by direct stimulation of Bax and Bak oligomerization, while derepressors such as Puma, Noxa and Bad inhibit the anti-apoptotic Bcl-2 family members to release pro-apoptotic members from their inhibition (e.g. Bax or tBid from Bcl-xL and Bak from Mcl1) (40).

2. Permeability Transition Pore (PTP)

The protein composition of PTP is not yet fully defined but one of the models suggests that it encompasses proteins from the outer mitochondrial membrane (OMM) (such as Voltage Dependent Anion Channel, VDAC), the inner mitochondrial membrane (IMM) (such as Adenine Nucleotide Translocase, ANT) and the mitochondrial matrix (e.g. Cyclophilin D, CypD) (40). VDAC is a structural component, while ANT and Cyclophilin D are thought to have regulatory functions. VDAC and ANT do not always seem to be essential and may be redundant (41-43), but CypD has a genetically proven crucial regulatory role (44-47). PTP opening causes massive influx of ions that dissipates the IMM potential $\Delta\Psi$, necessary for normal mitochondrial respiration and ATP production, thereby causing a bioenergetic catastrophe. Moreover, rapid influx of water causes swelling of the mitochondrial matrix, rupture of the rigid OMM and importantly, release of all sequestered apoptogenic factors. This sudden increase of inner

membrane permeabilization is called mitochondrial permeability transition (mPT) and plays an important role in necrosis and apoptosis. mPT is triggered by mitochondrial sequestration of high levels of calcium and is regulated by factors such as low ATP levels and high levels of ROS. PTP opening and mPT occur during myocardial infarction and stroke and currently, inhibitors of PTP (and more specifically of CypD) such as non-immunosuppressive Cyclosporine A derivatives are undergoing preclinical evaluations (40).

E. The mitochondrial p53 pathway

Besides being a transcriptional factor, p53 has well-established and important cytoplasmic functions. One of them is the direct mitochondrial p53 pathway. In response to a stress signal, cytoplasmic p53 accumulates and rapidly translocates to mitochondria where it interacts with members of the anti- and pro-apoptotic Bcl-2 family members to either inhibit or activate them. This direct action of p53 results in robust mitochondrial outer membrane permeabilization (MOMP), unleashing the enzymatic apoptotic machinery of caspases and chromatin degradation.

1. p53 translocates to mitochondria upon various stress stimuli

The first hint of a transcription-independent apoptotic activity of p53 dates back to 1994-1995, when it was demonstrated that p53-dependent apoptosis occurred in the presence of transcriptional or translational inhibitors, and that p53 truncation mutants lacking transcriptional activity can still trigger apoptotic function (48, 49). Later studies suggested that direct p53 signaling is participating in regulating caspase activity (50, 51). However, these studies did not

provide any mechanistic explanation and until the beginning of the new century the novel, transcription-independent proapoptotic function of p53 remained enigmatic.

The breakthrough study that first showed a direct role of p53 in mitochondrial apoptosis came from our lab, demonstrating that during p53-dependent apoptosis, a fraction of stress-stabilized wild-type p53 rapidly translocates to the mitochondrial outer membrane. p53 translocation precedes changes of mitochondrial membrane potential, cytochrome c release and caspase activation (52). As definitive proof, a mitochondrially targeted p53 fusion protein that bypasses the nucleus and has no residual transactivation function was able to induce apoptosis and long-term growth suppression nearly as efficiently as conventional p53 when expressed in several p53-null cancer cell lines (6, 52). Subsequent studies from our lab established that mitochondrial translocation of endogenous wtp53 occurs during the full spectrum of p53-activating cellular stress categories (various types of DNA damage, hypoxia, oncogene deregulation, oxidative damage) in different cell types (human and mouse; primary, immortal and malignant; epithelial, mesenchymal and lymphoid/myeloid) (53-55). This translocation occurs during p53-dependent apoptosis but not during p53-induced cell cycle arrest or p53-independent apoptosis (52-55).

2. Direct interaction with Bcl-2 family members

Mitochondrially translocated p53 interacts directly with several members of the Bcl-2 family. In response to stress, wtp53 interacts with and neutralizes the anti-apoptotic members Bcl-xL and Bcl-2. This interaction stimulates MOMP and subsequent apoptosis (6) and is associated with disruption of inhibitory complexes between Bcl-xL or Bcl-2 with MOMP

inducing members (i.e. BH3-only and Bax/Bak) that pre-exist in unstressed cells (6, 56). Indeed, purified p53 is able to displace tBid and Bax from inhibitory complexes formed with Bcl-xL *in vitro* (57). Only the p53 core domain but not its amino-and carboxyterminal regions interact (58). Significantly, despite high levels of stabilized mutant p53 protein constitutively present at mitochondria, missense mutant p53 proteins are defective in forming complexes with Bcl-xL/2 (6, 56).

The core domain of mitochondrial p53 also directly interacts with pro-apoptotic Bak, which constitutively resides in the outer mitochondrial membrane (6, 59). This interaction liberates Bak from pre-existing inhibitory complexes with the anti-apoptotic Mcl-1 protein (59). Similarly to Bcl-xL/2 interactions, conserved residues of the p53 core domain participate in stable Bak interaction (60).

Although a stable p53-Bax interaction was not observed, p53 is able to directly activate Bax in the absence of other proteins (57). Recombinant p53 and Bax proteins together (but neither of them alone) trigger the permeabilization of model liposomes whose lipid composition mimics that of mitochondrial inner/outer membrane contact sites. This is accompanied by Bax insertion into liposomes and Bax oligomerization, and is most likely due to a “hit and run” mechanism, involving a conformational change of Bax but not a stable interaction between Bax and p53 (57).

3. Mono-ubiquitination of cytoplasmic p53 promotes mitochondrial translocation

An important question is how translocation of p53 to mitochondria is regulated. In light of two pertinent negatives, i.e. the absence of a mitochondrial translocation motif within the p53

polypeptide sequence and the fact that N- and C-terminal phosphorylation/acetylation modifications play no major role in mitochondrial targeting of p53 (61), our group went on to show that (multi)mono-ubiquitination of p53 promotes its targeting to mitochondria. (Multi)mono-ubiquitination has been implicated in processes other than proteosomal destruction of important proteins such as Foxo4 and PTEN, in particular as a signal for intracellular trafficking between compartments (62, 63). (Multi)mono-ubiquitinated proteins are stable, since efficient proteasomal degradation minimally requires a multiubiquitin chain that is at least 4 subunits long per individual lysine residue (64). Importantly, the source of mitochondrially translocated p53 is a separate and distinct stress-stabilized p53 pool in the cytoplasm. Cytoplasmic Mdm2 acts as an E3 ligase but not as a physical shuttler of p53. Upon arrival at mitochondria, p53 undergoes rapid de-ubiquitination by mitochondrial HAUSP via a stress-induced mitochondrial p53-HAUSP complex, which generates the apoptotically active non-ubiquitinated p53. Taken together, a distinct cytoplasmic pool of mono-ubiquitinated p53, generated as intermediary in resting cells by basal levels of Mdm2 and similar E3 ligases, is subject to a rapid action binary switch from a fate of inactivation via polyubiquitination and degradation in unstressed cells, to a fate of activation via mitochondrial trafficking ((65) and reviewed in (66)).

4. The mitochondrial p53 pathway in pathophysiology

The relevance of the direct mitochondrial p53 program to the overall p53-mediated stress response *in vivo* is underlined by some recent studies in animals and supports a role in the pathophysiologic response to genotoxic, hypoxic and specific toxic insults.

Acute radiation response

In mice exposed to whole body γ-irradiation (5 or 10 Gy) or a single injection of a clinical dose of etoposide, mitochondrial p53 accumulation occurs in radiosensitive organs such as thymus, spleen and testis, but not in radioresistant organs like liver and kidney. In radiosensitive organs mitochondrial p53 translocation is rapid (detectable at 30 min in thymus and spleen) and triggers a p53-dependent first wave of caspase -3 activation within the first hour, followed by an early wave of apoptosis (detectable at 2 hrs in thymus), which precedes p53 target gene activation. Thus, in radiosensitive organs mitochondrial p53 accumulation *in vivo* triggers a rapid first wave of apoptosis that is transcription-independent, followed by a slower wave that is transcription-dependent and mediated by its target genes (67).

Brain injury

Evidence for an important role of the mitochondrial p53 death pathway in ischemic and oxidative cerebral injury is also emerging: Mitochondrial - rather than nuclear - accumulation of p53 in hypoxia-sensitive hippocampal CA1 neurons strongly correlates with CA1 cytochrome C release and neuronal death within the first 24 hrs in a transient global cerebral ischemia model in rat (68, 69). In C6 glioma cells and primary rat astrocytes exposed to oxidative stress, p53 levels rise and localize primarily at mitochondria, coinciding with caspase-3 activation and apoptosis (70). Conversely, a neuron-protective effect from ischemic pre-conditioning correlates with

suppressed mitochondrial p53 translocation during subsequent ischemia-reperfusion challenge (71). Genetic studies with p53 knockout mice (currently three such studies have been reported) show contradicting and perplexing results. In one study with mice subjected to middle cerebral artery occlusion, attenuation of p53 offer protection against brain injury. However, mice with heterozygous deletion for p53 show better protection than p53 null mice (72). In another study, following transient global cerebral ischemia, hippocampal neuronal death was also dependent on gene dose with p53 null mice showing the highest protection (73). In the third study, after middle cerebral occlusion, brain injury was surprisingly bigger in p53 +/- and p53 -/- mice compared to WT mice, suggesting a protective role for p53 (74). Different factors could explain these seemingly contradicting results, such as mouse strains used, severity of stress etc. At any rate, it is clear that p53 plays a critical role during ischemic brain damage, and further studies are needed to define this role.

Ischemia-reperfusion injury of the kidney

Another pathophysiological setting where the mitochondrial p53 program likely contributes to apoptosis is ischemia-reperfusion injury of the kidney. This injury is modeled by transient bilateral renal artery occlusion and is characterized by death of tubular epithelial cells, mainly in the proximal convoluted portion. It is documented that p53 is a critical mediator of tubular epithelial cells death (75, 76). In injured tubules, p53 stabilization is to a large extent cytoplasmic rather than nuclear, strongly co-localizes with mitochondria and correlates with apoptosis of tubular cells (76). Inhibition of mitochondrial p53 translocation, rather than its

nuclear functions, prevents tubular death and renal function in mice (76). This supports a critical role of mitochondrial p53 during ischemia-reperfusion injury of the kidney.

Liver injury

A study by Leu et al. proved a critical role of mitochondrial p53 during genotoxic stress-induced cell death in the liver. The study showed that activated p53 transcriptionally induces the IGFBP1 prosurvival factor, which in part translocates to mitochondria and binds to Bak. This impairs the mitochondrial p53 activity by preventing its binding to Bak. IGFBP1-/- liver shows spontaneous apoptosis associated with mitochondrial p53-Bak complexes. Conversely, overexpression of IGFBP1 attenuates the apoptotic response to cisplatin and doxorubicin even in non-hepatic cells. Importantly, treatment with PFTμ (which selectively inhibits p53 mitochondrial function without interfering with p53's transcription function) significantly reduces cisplatin-induced liver cell death (77).

Additionally, the often fatal liver 'necrosis' that occurs after αAmanitin poisoning by the mushroom *Amanitis phalloides* is overwhelmingly due to the mitochondrial p53 program. αAmanitin is a potent transcriptional inhibitor by blocking RNA polymerase II, but kills cells by inducing mitochondrial p53 translocation and p53-dependent MOMP in liver and other cells (53, 77). Accordingly, p53-/- or Bak-/- mice are largely protected from αAmanitin-induced liver damage, while WT mice undergo organ destruction (77).

F. p53 based therapies and Nutlin

Strategies to treat cancer by restoring p53 function are a highly promising field. In tumors with loss of p53 function, which is an extremely common clinical situation, sustained inactivation of the p53 tumor suppressor pathway is required for tumor maintenance. This concept was recently proved by several conditional mouse models, where restoration of p53 function led to tumor regression *in vivo*, either via induction of apoptosis or senescence programs, depending on the tumor type (24, 25, 78). Therefore big efforts are focused on developing small molecules that could restore p53 functions in tumors. Small molecules such as CP-31398 (Pfizer) and PRIMA structurally rescue tumor-derived p53 mutant proteins. Alternatively, in tumors retaining wild-type p53, compounds such as Nutlin (Roche) or RITA activate wtp53 by liberating it from its inhibitory MDM2 interaction. Another important venue focuses on supplying 'conventional' wtp53 via adenoviral type 5 delivered gene therapy (79-83).

Nutlin is a potent and highly selective imidazoline-based MDM2 inhibitor. It blocks MDM2-mediated p53 degradation and transcriptional repression, thereby leading to non-genotoxic p53 stabilization and activation of growth arrest and apoptosis (84-86). Nutlin promotes cell death in cultured leukemia cells, select osteosarcoma cells and their xenografts

(87, 88). It is currently undergoing Phase I and II clinical trials for hematologic and some solid malignancies in combination with conventional chemotherapeutics (86, 87). However, its clinical development has been plagued by a major roadblock that became apparent in most solid cancers. Although Nutlin efficiently induces transient cell cycle arrest, pre-clinical and clinical data from a wide array of solid tumors indicates that it is inefficient in inducing definitive apoptosis (89-91). Thus, how to convert Nutlin from a cytostatic to a cytotoxic drug has become an intense research topic. One of the venues into this direction focuses on identifying synthetic lethal partner drugs in order to design combinatorial therapies.

Robust upregulation of Nutlin-induced p21, concomitant with attenuated expression of pro-apoptotic genes, has been thought to be a major reason why many tumors merely undergo reversible growth arrest rather than apoptosis upon Nutlin (89-91). Alternatively, and not mutually exclusive, p53 inhibition by the remaining MDMX was proposed as a cause for apoptosis resistance after Nutlin (92). Although MDMX is highly homologous to MDM2, Nutlin is inefficient in interrupting the transcription repressive MDMX-p53 complex, which prevents p53 transcriptional activity in numerous cancer cell lines (92-95). Indeed, knock-down of MDMX by RNAi renders Nutlin more efficient in promoting apoptosis of cultured tumor cells (94, 96). Therefore, concomitant inhibition of MDMX and MDM2 could prove to be the better therapeutic strategy. Currently, pharmacological inhibitors of MDMX are not available and their development is a necessity.

During my dissertation research I have conducted 3 different projects in the p53 field. The first aimed to determine what if any role the mitochondrial p53 program might play during Nutlin-induced apoptosis. I show that Nutlin causes cytoplasmic p53 accumulation and translocation to mitochondria. Additionally, Nutlin does not interfere with MDM2's ability to

monoubiquitinate p53, due to the fact that MDM2-p53 complexes are only partially disrupted and that Nutlin-stabilized MDM2 retains its E3 ubiquitin ligase activity. Nutlin-induced mitochondrial p53 translocation is rapid and associated with cytochrome C release that precedes induction of p53 target genes. Specific inhibition of mitochondrial p53 translocation by Pifithrin μ reduces the apoptotic Nutlin response, underlining the significance of p53's mitochondrial program in Nutlin-induced apoptosis. Surprisingly, blocking the transcriptional arm of p53, either via αAmanitin or the p53-specific transcriptional inhibitor Pifithrin α, not only fails to inhibit, but greatly potentiates Nutlin-induced apoptosis. Thus, the direct mitochondrial p53 program significantly contributes to Nutlin-induced apoptosis at least in certain cell/tumor types and likely is a therapeutically relevant mechanism in p53-based therapies.

In my second project I show that the apoptotic efficiency of Nutlin for solid tumor cells in vitro and in xenografts is synergistically enhanced when combined with the non-genotoxic Hsp90 inhibitor 17AAG. The Hsp90 chaperone complex is highly upregulated in tumors and cancer cells are addicted to Hsp90 for their survival. I demonstrate that in multiple difficult-to-kill solid tumor cells 17AAG modulates several critical components that synergize with Nutlin-activated p53 signaling to convert Nutlin's transient cytostatic into a permanent cytotoxic killing response. 17AAG destabilizes MDMX, reduces Nutlin-induced MDM2 expression, while it enhances PUMA and inhibits oncogenic survival pathways like PI3K/AKT that counteract p53 signaling at multiple levels. Mechanistically, 17AAG interferes with the repressive MDMX-p53 axis by inducing robust MDMX degradation, thereby markedly increasing p53 transcription compared to Nutlin alone. Finally, the drug combination stabilizes human xenograft tumors in mice, while both of the drugs alone fail to do so. In sum, Nutlin+17AAG represent the first

effective pharmacologic knockdown of MDMX. Thus, my study identifies 17AAG as a promising synthetic lethal partner for a more efficient Nutlin-based therapy.

My third project describes a novel and surprising function of mitochondrial p53. It shows that during oxidative stress mitochondrial p53 regulates the mitochondrial Permeability Transition (mPT) to induce programmed cell necrosis. I find that in contrast to the prototypical MOMP-inducer tBid, purified p53 protein regulates the PTP pore independently of Bax and Bak in isolated mitochondria. Treatment of primary and cancer cell lines with hydrogen peroxide (H_2O_2), the classic oxidant to study cellular responses to oxidative stress, induces rapid translocation of p53 to the mitochondrial matrix, where p53 interacts directly with the obligatory PTP-regulatory protein Cyclophilin D (CypD), but not with VDAC or ANT. Both p53 and CypD-deficient cells show reduced sensitivity to H_2O_2-induced PTP opening and cell death. Blocking p53 transcriptional activity does not prevent mPT, indicating transcription-independent regulation of PTP by p53. Conversely, mitochondrial targeting of p53 increases mPT and cell death caused by H_2O_2, independently of Bax and Bak but in a CypD-dependent manner. Necrotic rather than apoptotic cell death occurs, as measured by viability assays, electron microscopy, HMGB1 release and TUNEL assay. Therefore my results for the first time demonstrate an important additional function of mitochondrial p53: regulation of mitochondria permeability and necrotic cell death during oxidative stress. Intriguingly, mice experiments further implicate this function of p53 during brain ischemia reperfusion injury.

II. Results

A. The transcription-independent mitochondrial p53 program is a major contributor to Nutlin-induced apoptosis in tumor cells

In ML-1 and RKO cells, Nutlin stabilizes p53 protein, induces p53 transcriptional activity and causes significant apoptotic response. Nutlin was previously shown to induce apoptosis in a subset of cancer cell lines that harbor wt p53 (86, 89, 97). The effect of Nutlin in the myeloid leukemia cell line ML-1 and the colorectal cancer cell line RKO was tested. p53 accumulation in crude extracts was detectable by Western blotting as early as 1 hour after Nutlin treatment (Figure 1A). Induction of the p53 transcriptional targets MDM2 and p21 started at 3 hours and peaked at 8 hours after addition of Nutlin (Figure 1A). Results are shown for the ML-1 cell line. To detect the apoptotic response of these cell lines, two approaches were used. First, the cells were treated with 10 μM Nutlin for different time points up to 24 hours. Lysates were prepared and analyzed for PARP cleavage using Western blotting. ML-1 cells exhibited significant PARP cleavage between 6 and 8 hours after Nutlin treatment (Figure 1A). RKO cells had less pronounced apoptotic response and detectable PARP cleavage at 24 hours (data not shown). In addition, the cells were treated with 10 μM Nutlin for 24 hours and processed for TUNEL staining (Figure 1B).

Figure 1B shows that 24 hours after Nutlin treatment of ML-1 cells, 76% of the cells were positive for TUNEL staining, indicating the robust apoptotic response of these cells.

Nutlin causes p53 accumulation in both nucleus and cytoplasm and does not interfere with mono-ubiquitination of cytoplasmic p53. As discussed, our group previously showed that after stress, a pool of cytoplasmic p53 is mono-ubiquitinated by MDM2 and translocates to mitochondria (65) . Once at mitochondria, mono-ubiquitinated p53 is deubiquitinated by local HAUSP to induce outer mitochondria membrane permeabilization by interaction with Bcl-2 family members. Nutlin treatment of ML-1 and RKO cells resulted in significant accumulation of p53 protein in both nucleus and cytoplasm (Figure 2A). As a consequence of p53 transcriptional activity in the nucleus, the protein levels of MDM2 were also elevated in both nucleus and cytoplasm (Figure 2A). Importantly, the levels of mono-ubiquitinated p53 protein in the cytoplasm were not affected by the presence of Nutlin (Figure 2B). A previous study by Vassilev et al showed that Nutlin-induced MDM2 retains its ubiquitin ligase activity and thus facilitates the degradation of MDMX (97). Since the ligase activity of MDM2 is not affected by Nutlin, our results also suggest that MDM2 is still able to mono-ubiquitinate p53 in the presence of Nutlin. Furthermore, co-immunoprecipitation experiments showed that the MDM2-p53 complex was partially disrupted by Nutlin (Figure 2C). Lysates from RKO cells treated with 10 μM Nutlin for 6 hours were used. In the presence of Nutlin, MDM2 co-immunoprecipitated with p53 was readily detected, albeit reduced compared to the MDM2 input (Figure 2C left, compare much higher MDM2 levels in treated versus untreated cells, but the same amount of co-precipitated p53). The same was true for the inverse experiment, where the amount of p53 co-immunoprecipitated with MDM2 was compared to p53 input (Figure 2C right). Together, these results suggest that the remaining low levels of complexes between MDM2 and p53, although

insufficient for mediating p53 poly-ubiquitination and destabilization, are sufficient for mediating p53 mono-ubiquitination which then promotes p53 trafficking to mitochondria.

Nutlin treatment induces accumulation of p53 in mitochondria. Several studies have implied that Nutlin induces mitochondrial functions of p53 (98, 99). However, there has been no clear evidence for mitochondrial translocation of p53 after Nutlin treatment. Nutlin induced significant mitochondria accumulation of p53 in both Ml-1 and RKO cells (Figure 3A). Importantly, this translocation occurred as early as 1 hourr after adding the drug and gradually increased with time (Figure 3B). Release of Cytochrome C from the mitochondrial fraction was observed even 1 hour after treatment, coinciding with p53 translocation. Cytochrome C release is an indication for mitochondrial outer membrane permeabilization and is one of the earliest hallmarks of mitochondria-mediated apoptosis. As seen in Figure 1 and as published by other authors, Nutlin treatment upregulated transcriptional targets of p53 at the earliest at 3 hours. These results indicate that p53 translocation to mitochondria precedes the induction of p53 transcriptional targets during Nutlin- induced apoptosis.

Inhibition of p53 mitochondrial translocation by PFTμ significantly alters Nutlin induced apoptosis. PFTμ is a small molecule inhibitor that inhibits p53 association with mitochondria by reducing the affinity of p53 to the Bcl-2 family members Bcl-2 and BCL-xL or BAK (77, 100). This inhibitor has been shown to rescue cells and mice from lethal doses of irradiation or DNA damaging agents (77, 100). We used this inhibitor to determine the contribution of mitochondrial p53 during Nutlin-induced apoptosis. Cells pretreated with PFTμ showed significant reduction of p53 in mitochondrial fractions (Figure 4A). This reduction of p53 at mitochondria was associated with less Cytochrome C release indicating reduced permeabilization of the outer mitochondrial membrane (Figure 4A). TUNEL staining and visualization of PARP cleavage by Western

blotting confirmed that PFTμ indeed caused significant reduction of Nutlin-induced apoptosis (Figures 4B and 4C). Quantification of the TUNEL results revealed that this reduction was approximately 2.6 fold (34 % apoptosis with Nutlin alone as compared to 13% when PFTμ was first added). These results confirmed the contribution of mitochondrial p53 during Nutlin-induced apoptosis.

Inhibition of general transcription by αAmanitin does not prevent apoptotic response to Nutlin. To further support the direct role of mitochondrial p53 during the apoptotic response to Nutlin we went on to block Nutlin-induced transcriptional activities of p53. This allows determining whether p53 mitochondrial functions alone are sufficient to mediate the apoptotic response upon Nutlin treatment. We used the general transcription inhibitor αAmanitin (Figure 5) and the specific p53 inhibitor PFTα (pifithrin α) (Figure 6).

αAmanitin is an inhibitor of RNA polymerase II (RNA pol II) and is widely used as an inhibitor of general transcription. It is known to cause apoptosis through elevation of p53. After careful screening we found a dose and time of treatment which did not induce significant apoptosis or elevated p53 levels but was sufficient to inhibit Nutlin-induced transcriptional activities of p53. Pretreatment of ML-1 cells with αAmanitin blocked the induction of p21 after Nutlin treatment, indicating blockade of p53 transcriptional functions, while p53 levels remained induced at the same level as Nutlin alone (Figure 5A). Surprisingly, there was significantly more PARP cleavage in the combination αAmanitin + Nutlin compared to Nutlin alone (Figure 5A). This indicated that more pronounced apoptosis was observed when transcription was blocked. The latter was confirmed with TUNEL staining (Figures 5B and 5C). αAmanitin did not interfere with mitochondrial translocation of p53. Instead, in the presence of αAmanitin, more p53 was detected at mitochondria (Figure 5D). Because p21 inhibits cell cycle progression and

overexpression of p21 can cause G1 arrest and escape from apoptosis. The blocked transcription of p21 after Nutlin could account for the higher apoptotic response in the presence of αAmanitin. Another reason could be the transcriptional repression of anti-apoptotic proteins or other transcriptional products that might negatively affect the mitochondrial pro-apoptotic functions of p53.

Inhibition of p53-mediated transcription by PFTα does not prevent apoptotic response to Nutlin. PFTα is a small molecule inhibitor that was isolated as a suppressor of p53-mediated transactivation and capable of rescuing mice from lethal genotoxic stress caused by gamma radiation (101). Similarly to αAmanitin, pretreatment of ML-1 cells with PFTα did not affect stabilization of p53 protein upon Nutlin treatment (Figure 6A) nor did it interfere with p53 mitochondrial translocation (Figure 6C). However, it potentiated Nutlin-induced apoptosis (Figure 6B). Thus, Nutlin is not only able to induce apoptosis in the absence of active p53-mediated transcription, but greatly potentiates it. These results suggest the existence of a negative autoregulatory loop where p53 transcriptional targets might inhibit its transcription-independent pro-apoptotic functions.

B. Blockade of Hsp90 by 17AAG antagonizes MDMX and synergizes with Nutlin to induce p53-mediated apoptosis in solid tumors.

17AAG induces p53, while destabilizes MDMX and MDM2 proteins. Wild type p53, mutant p53 and MDM2 are hsp90 client proteins (102-107). While it is generally accepted that hsp90 mediates the massive stabilization of mutant p53, the role of hsp90 in regulation of wild type p53 protein has not been clearly established. Some reports suggest that hsp90 stabilizes wild type p53 protein during heat shock (104) or by opposing MDM2 function (108). Other studies demonstrate that inhibition of hsp90 induces wt p53 protein levels and p53-dependent cell death in cancer cells (109, 110). Therefore, we first examined how 17AAG affected wild type p53 and its regulators MDM2 and MDMX in a subset of cancer cell lines.

Different tumor cell lines with wild type p53 (RKO- colorectal carcinoma, MCF7- breast adenocarcinoma, U2OS- osteosarcoma and AGS- gastric adenocarcinoma) were treated with 17AAG for different times and the protein levels of p53, MDMX, MDM2 as well as the p53 target gene p21 were assessed (Figure 7). In all cell lines, p53 protein levels were increased upon 17AAG treatment, albeit with some kinetics differences. In RKO, U2OS and AGS p53 protein was accumulated as soon as 4 hours after treatment, while in MCF7 cell line p53 accumulation

was observed after 24 hours of treatment (Figure 7). Interestingly, in all cell lines the levels of MDMX protein were strongly decreased between 12 and 24 hours after 17AAG treatment,. Moreover, downregulation of MDM2 was also observed in RKO and AGS cells (Figure 7). Protein levels of the p53 transcriptional target p21 were induced in all cell lines (Figure 7).

To determine whether these changes in protein expression were due to transcriptional regulation or are an effect on protein stability, we performed qRT-PCR and cycloheximide chase experiments. 17AAG increased both p53 mRNA and protein stability (Figure 8A). Consequently, 17AAG increased gene expression of the classic p53 targets MDM2, p21 and PUMA, validating p53 activation (Figure 8B). MDMX message levels remained unaffected by 17AAG, indicating that downregulation of the MDMX protein seen in Figure 7 occurred mainly at the posttranscriptional level (Figure 8B). These results also indicated that 17AAG modulated posttranscriptionally MDM2 as well, since increased MDM2 mRNA levels did not reflect the increased protein levels seen in Figure 7.

Further, pre-treatment with pan-caspase inhibitor Z-VAD reversed 17AAG-induced MDM2 degradation, while the effect on MDMX protein stability remained unchanged (Figure 9A). Proteasome inhibition by ALLN was able to stabilize both MDM2 and MDMX after 17AAG treatment (Figure 9B). Thus, 17AAG affects MDM2 stability through caspase activation, while MDMX protein stability is decreased in a caspase-independent manner.

17AAG disrupts the interactions between p53, MDMX and MDM2. Since Hsp90 binds to MDM2, while p53, MDM2 and MDMX bind to each other, we determined whether 17AAG could affect these interactions. Co-immunoprecipitation experiments revealed that 17AAG rapidly disrupted the complex between MDMX and p53 within 2 hours of treatment, a time point

when MDMX protein levels were still not affected (Figure 10A and 10C). Furthermore, 17AAG disrupted the MDMX-MDM2 complex (Figure 10A) and also inhibited the Hsp90-MDM2 complex, as previously reported (Figure 10B). The MDM2-p53 complex remained unaffected (Figure 10A). These results demonstrate that besides affecting the stability of the major p53 regulators MDMX and MDM2, 17AAG also affects their interactions. This could also account for the modulation of p53 signaling upon hsp90 inhibition.

17AAG induces apoptosis in a p53 dependent manner. In primary MEFs and murine medulloblastoma models, 17AAG was shown to induce apoptosis in a p53-dependent manner (110). Therefore, we examined whether this would hold true for other cancer cell lines. We compared the response to 17AAG of the isogenic colorectal cancer cell line pair HCT116 p53+/+ and HCT116 p53-/-. Similarly to the other cancer cell lines tested, HCT116 p53+/+ did show an increase of p53 protein levels, decrease of MDMX and increase of p21 and PUMA protein levels (Figure 11A). In contrast, treatment of HCT116 p53 -/- cells with 17AAG did not alter the levels of PUMA and p21 proteins (Figure 11A). Moreover, PARP cleavage upon 17AAG treatment was significantly higher in HCT116 p53+/+ cells, indicating higher apoptosis levels (Figure 11A).

To further confirm the p53 dependence of 17AAG-induced apoptosis, we measured caspase activation in these cells. Caspase activity was about 2-fold higher in 17AAG treated HCT116 p53+/+ cells compared to HCT116 p53-/- cells (Figure 11B). This induction of apoptosis after 17AAG treatment was further confirmed by measuring AnnexinV and Propidium Iodide (PI) by FACS, where double negative populations represent surviving unaffected cells. Survival upon 17AAG treatment was significantly higher in the p53-/- as compared to p53+/+

cells (Figure 11C). Thus, we conclude that 17AAG induces apoptosis in a p53-dependent manner.

17AAG induces transcription of p21, PUMA and MDM2 in p53-dependent manner. In the same isogenic system HCT116 p53+/+ and HCT116 p53-/-, we further compared induction of mRNA levels of the p53 targets MDM2, p21 and PUMA. mRNA levels of all three were induced significantly upon 17AAG treatment in the p53+/+, but not in the p53-/- cells (Figure 12). Thus, 17AAG induces p53-mediated transcription of both apoptotic and cell cycle genes.

Combination of 17AAG with Nutlin synergistically induces apoptotic cell death in a subset of cancer cell lines. Although the precise mechanism of how 17AAG affects p53 signaling remains to be determined, we hypothesized that since 17AAG stabilizes wtp53, induces p53-mediated transcription and causes cell death in a p53-dependent manner, it would likely synergize with other drugs that affect p53 signaling. Nutlin is a small molecule designed to stabilize wtp53 by interfering with its interaction with MDM2. 17AAG did not disrupt the interaction between MDM2 and p53, which indicated that 17AAG stabilizes p53 by a mechanism different from Nutlin. We treated a subset of cancer cell lines with Nutlin alone, 17AAG alone or the combination of Nutlin with 17AAG. Significantly higher PARP cleavage was detected when the two drugs were combined as compared to single drugs treatments (Figure 13A). Similarly, caspase activation (Figure 13B) and the amount of Annexin/PI positive cells (Figure 13C) were much higher when the two drugs where combined. Importantly, this enhancement of cell death was observed only in p53+/+, but not in p53-/- cells (Figures 14A and 14B). To determine if the enhancement of cell death after drug combinations was synergistic, we calculated Combinatorial Indexes (CI) for the cell lines RKO, U2OS, MCF7 and AGS. CI values smaller than 1 indicate synergism, CI equal to 1 indicate additive effect and CI bigger than 1

indicate antagonistic effect (111). In all cell lines tested, CI values were smaller than 1 indicating synergistic interaction between 17AAG and Nutlin (Figure 15).

17AAG destabilizes MDMX protein in Nutlin-treated cancer cells and can potentiate Nutlin-induced p53-mediated transcription of PUMA. To explain the synergistic effect between Nutlin and 17AAG, we next examined whether 17AAG affects Nutlin-induced p53 signaling. It was previously shown that p53 levels can be a determinant of arrest (lower levels) versus apoptosis (higher levels) (112). However, in our cell lines endogenous p53 levels did not further increase with Nutlin+17AAG compared to Nutlin alone (Figure 16A). Thus, increased apoptosis was not simply due to higher p53 levels.

In the presence of Nutlin, 17AAG still decreased MDMX protein level (Figure 16A). MDMX degradation was again primarily a caspase-independent event, as shown by Z-VAD treatment (Figure 16B). This robust MDMX degradation coincided with a further surge of the p53 transcriptional response compared to Nutlin or 17AAG alone, as judged by the representative induction of p21, PUMA and MDM2 targets (Figure 16C).

On the protein level, the addition of 17AAG induced differential regulation of these three Nutlin-induced p53 targets, likely due to Hsp90 influence on their stability, which altogether generated the apoptosis-promoting effects of the drug. PUMA protein was significantly upregulated in RKO, MCF7 and HCT116 cells upon combined treatment compared to Nutlin or 17AAG alone (Figures 16A, 17B). At the same time Nutlin+17AAG significantly downregulated MDM2 protein levels compared to Nutlin alone in all 5 lines tested (Figures 16A, 17A). This was a secondary caspase-mediated effect since it was blocked by Z-VAD (Figure 16B). Nutlin is known to induce p21 protein (89-91), also seen here (Figures 16A, 17A). However, Nutlin-

induced p21 was significantly suppressed down to near basal levels by concomitant 17AAG (Figures 16A, 17A). Because robust p21 induction has been considered a determinant of the Nutlin-associated apoptosis resistance (89-91), the drug combination-induced p21 downregulation that we observed might also contribute to enhanced apoptosis.

Finally, the effect of 17AAG on protein stability and transcription of Nutlin-induced p21, PUMA and MDM2 was p53-dependent, since it was only present in HCT116 p53+/+ but not in p53-/- cells (Figure 17). In contrast, the degradation of MDMX incurred by 17AAG was p53-independent (Figure 17).

The synergistic interaction between Nutlin and 17AAG is in part due to 17AAG-induced MDMX downregulation and inhibition of AKT signaling. Downregulation of MDMX potentiates Nutlin-induced apoptosis. (92-94). Since 17AAG downregulated MDMX in all cancer cell lines tested and also disrupted the complex between p53 and MDMX, we hypothesized that these effects of 17AAG on MDMX could play a role for the observed synergism between 17AAG and Nutlin. Indeed, oxerexpression of MDMX in U2OS cells did inhibit PARP cleavage and caspase activity upon combined treatment (Figures 18A and 18B). Nutlin-induced p21 and PUMA protein levels were also reduced upon MDMX overexpression (Figure 18A, compare samples 2 and 8). Conversely, when MDMX was downregulated by siRNA, the protein levels of p21 and PUMA were higher after Nutlin treatment compared to control siRNA-treated cells (Figure 18C left). Therefore, downregulation of MDMX unlocks the transcriptional activity of p53 at least in some cancer cells lines, an observation also made by others (92). Importantly, downregulation of MDMX also enhanced caspase activity upon Nutlin treatment (Figure 18C), further confirming the idea that inhibition of MDMX by 17AAG contributes to the enhanced pro-apoptotic Nutlin response.

Many hsp90 client proteins are oncogenes that depend on chaperone support for functionality. Therefore 17AAG affects multiple oncogenic signaling pathways (113-115), many of which are known to regulate p53 signaling at various levels. Thus, it is likely that other events besides downregulation of MDMX could also contribute towards the apoptotic synergism between Nutlin and 17AAG. For example, AKT stability and activity are affected by 17AAG (113, 114, 116), while AKT is known to phosphorylate p53, MDM2 and MDMX (38). Some studies have already shown that inhibitors of PI3K/AKT pathway can potentiate Nutlin –induced cell death (117, 118). We observed that 17AAG downregulated both p-AKT and AKT in our cancer cell lines (Figure 19A). We also observed enhanced PARP cleavage and caspase activity when Nutlin was combined with a PI3K inhibitor (Figures 19B and 19C). Interestingly, similarly to 17AAG, the PI3K inhibitor markedly enhanced Nutlin-induced PUMA expression (Figure 19C, compare sample 2 to 3 and 4), suggesting that enhanced expression of Nutlin-activated apoptotic genes by 17AAG might in part also work through its effect on AKT. Overall, these results suggest that the synergism between Nutlin and 17AAG is in part also due to inhibition of the PI3K pathway.

The combination of Nutlin with 17AAG promotes increased tumor cell death in mouse xenografts. To further support our data of functional synergism between Nutlin and 17AAG, we performed in vivo analyses of tumor xenografts in nude mice. Eight mice were injected with $5x10^6$ RKO cells per flank and at day 12 (called Day 0 in Figure 20A), tumors were palpable (200-300 mm^3). The mice were randomized into four treatment groups: Vehicle, Nutlin alone, 17AAG alone, and Nutlin+17AAG.

At Day 11 of treatment, tumors of mice treated with Nutlin alone or 17AAG alone had failed to respond to the drug compared to vehicle-treated controls, and instead had increased

about 5-fold in volume. In contrast, tumors treated with Nutlin+17AAG grew slower and increased only 3-fold (Figure 20A). Moreover, at Day 15 of treatment, tumors of mice treated with Nutlin + 17AAG had reached a plateau and remained stable thereafter, while tumors treated with Vehicle, Nutlin alone or 17AAG alone further accelerated their growth. In fact, two Nutlin-treated mice, one Vehicle-treated mouse and one 17AAG-treated mouse had to be sacrificed at Day 15 since they had reached the allowable limit of tumor burden. In contrast, only one Nutlin+17AAG mouse needed to be sacrificed; however not because of excessive tumor burden but because of a treatment-induced necrotic area in one of the tumors. Moreover, the drug combination was well tolerated. Over the treatment period, mice receiving Nutlin + 17AAG showed no discernable changes in weight or behavior compared to Vehicle controls. To verify that the combination of Nutlin + 17AAG increased tumor cell death in vivo, caspase activation was analyzed in tumor lysates (Figure 20B). Protein was isolated from three randomized tumors per treatment and analyzed by immunoblot. The highest levels of caspase activity (cleaved caspase) were observed in tumors treated with Nutlin+17AAG compared to vehicle control and single drug tumors. These results once again confirmed that Nutlin combined with 17AAG is superior in promoting apoptosis of cancer cells in xenografts compared to single drugs.

C. p53 protein regulates the mitochondrial permeability transition pore during oxidative stress-induced necrosis and ischemic stroke

In addition to Bax/Bak lipid pores, purified p53 also engages PTP to induce mitochondrial membrane permeabilization. We previously showed in isolated mitochondria that purified p53 causes robust Cytochrome C (CytoC) release by inducing Bak oligomerization and MOMP with the same efficiency as tBid (6, 119). Moreover, we showed that p53 is able to release the entire gamut of soluble and non-soluble apoptogenic factors including non-cleaved AIF and Endo G that are tethered to the IMM by severely disrupting both outer and inner mitochondrial membrane integrity. In contrast, tBid is restricted to releasing only soluble components via MOMP (119). This suggests a stronger permeabilizing effect by p53 than by the prototypical activator of the Bax/Bak pore, tBid. Thus, we hypothesized that p53 is capable of recruiting additional BH3-independent pathways of mitochondrial permeabilization.

To this end, we compared the release response of isolated WT and Bax/Bak double knockout (DKO) mitochondria towards highly purified recombinant p53 and tBid (Figure 21A). Bax/Bak DKO cells are deprived of the apoptotic gateway to mediate CytoC release for caspase activation (120). Indeed, p53 was able to rapidly release CytoC, Smac (soluble) and AIF

(membrane tethered) from both WT and Bax/Bak DKO mitochondria, while the tBid-induced release was restricted to WT mitochondria (Figure 21A). The strict Bax/Bak-dependence of tBid-mediated MOMP is completely consistent with the notion of tBid as direct activator of the Bax/Bak lipid pore (121). In contrast, p53 apparently has additional mitochondrial targets to mediate mitochondrial permeabilization.

We reasoned that p53 might also engage the mitochondrial PTP pore. To look for evidence of p53-induced functional alterations of this pore, we used the fluorescent dye calcein, a highly selective indicator of sustained PTP opening *in situ* (40). MOMP and the Bax/Bak lipid pore are completely incompetent for calcein release (122). Adding increasing doses of purified p53 to calcein-prelabeled WT or Bax/Bak DKO mitochondria resulted in a rapid and almost complete loss of signal, indicating PTP opening. In contrast, even the highest dose of tBid lacked any effect (Figure 22A). Moreover, p53 but not tBid induced structural alterations of PTP components. WT mouse liver mitochondria were incubated with increasing amounts of purified p53 prior to chemical cross-linking. VDAC-containing complexes ranging from ~ 60-300 kDa were readily detected in control mitochondria incubated with buffer or BSA, but increasingly disappeared upon addition of p53 in a dose-dependent fashion (Figure 22B). Thus, p53 was able to drive VDAC into high molecular weight complexes that no longer entered the gel. This activity was unique to p53, since tBid had no effect on VDAC oligomerization (Figure 22C). Moreover, p53 but not tBid was able to induce swelling (another classical hallmark of PTP opening) of Bax/Bak DKO and WT mitochondria in a CsA-dependent (Figure 23A) and CypD-dependent (Figures 23B, 23C) manner. Thus, in addition to the Bax/Bak lipid pore, p53 can also engage the PTP pore to induce mitochondrial membrane permeabilization.

p53 protein interacts with the essential regulatory PTP component CypD. Based on the result above, we next asked whether and if so upon which stimulus p53 interacts with components of the PTP complex. Since both p53 and mPT play important roles during oxidative stress (123-125), we looked for an interaction between p53 and the PTP components CypD, ANT and VDAC upon H_2O_2 treatment. Immunoprecipitation detected a prominent oxidative stress-induced endogenous complex between p53 and the essential regulatory PTP component CypD. No interaction was seen between p53 and the proposed structural components VDAC and ANT (Figure 24A). The H_2O_2-inducible specific p53-CypD complex was confirmed with pull down assays of HA-tagged CypD, VDAC and ANT expressed in cells with endogenous p53 (Figure 24B). Moreover, endogenous mitochondrial p53 binds to recombinant GST-CypD in a CsA-dependent manner (Figure 24C). Finally, cell-free pull down experiments with recombinant proteins confirmed the direct CsA-sensitive interaction (Figure 24D). Mapping experiments with a series of p53 deletion mutants identified p53 amino acids 80-220 as the region required for CypD interaction (Figures 25A and 25B). While we failed to identify a single specific subregion, the p53 contact domains that are required for Bcl-xL/Bcl-2 interaction (designated with 'Δ') (6) were not required for CypD binding (Figure 25C), underlining structural differences between the two types of interactions. Tetrameric p53 is the preferred partner for CypD interaction (Figure 25D), while it is debated whether mitochondrial p53 that directly triggers Bcl-2 family-mediated apoptosis at the OMM acts as monomer or tetramer (126, 127).

Rapid stabilization and mitochondrial translocation of p53 upon oxidative stress. Next we asked whether p53 accumulates in mitochondria upon oxidative stress. Treating various wtp53 harboring cell lines and primary MEFs with 0.25 - 0.75 mM H_2O_2 uniformly induced robust cellular p53 stabilization (Figure 26A). This oxidative stress-induced p53 response was fast,

reaching its peak within 1 hour in most cells (Figure 26B). Immunofluorescence staining of C6 rat glioma cells treated with H_2O_2 for 4 hrs showed primarily punctate p53 accumulation in the cytoplasm, confirming earlier findings (70) and suggesting an important mitochondrial function of p53 protein within this window of time during oxidative stress (Figure 27A). p53 accumulated in mitochondria that were free of detectable contamination within 4 hrs of H_2O_2 treatment (Figure 27B). Importantly, submitochondrial fractionation confirmed that during oxidative stress a fraction of p53 accumulated in the matrix where CypD is located, while some also localized to the surface, as expected (Figure 27C). This is consistent with hypoxia-induced endogenous complexes between p53 and the major matrix import proteins mtHsp70 and mtHsp60 we reported earlier (128). The observed p53 fractions in intermembranous space and inner membrane likely represent transport intermediates to the matrix.

Oxidative stress induces mitochondrial Permeability Transition in a p53- dependent manner. CypD-regulated mPT is a crucial event during H_2O_2-induced cell death, definitively established by the CypD knockout mice. Our initial results in isolated mitochondria had shown that purified p53 protein was able to engage PTP in a CypD-dependent manner (Figures 22 and 23). However, an mPT-regulatory role of p53 *in vivo* remained to be established. We therefore asked whether H_2O_2 - induced PTP opening in cells is p53-dependent.

Opening of the PTP pore and subsequent mPT results in dissipation of the mitochondrial membrane potential $\Delta\Psi m$ across the IMM. The cationic fluorescent dye tetramethylrhodamine methyl ester (TMRM) is widely used to assess changes in $\Delta\Psi m$ and mPT. TMRM is readily sequestered by healthy mitochondria, but its fluorescence is rapidly lost when $\Delta\Psi m$ is dissipated. Indeed, in response to H_2O_2 treatment WT MEFs completely lost TMRM fluorescence. This occurred in a CypD-dependent manner, since CypD inhibitor CsA completely blocked this event.

In contrast, p53-/- MEFs remained completely unaffected (Figures 28A-28C). This strong p53-dependent response was also observed in the isogenic HCT116 p53+/+ and p53-/- pair (not shown). These results were further confirmed by direct *in situ* assessment of PTP pore opening via Calcein release, which again showed p53 and CypD dependence (see CsA, Figures 29A and 29B). Of note, while CsA can block other cytosolic cyclophilins besides mitochondrial matrix-specific CypD, none of them play any role in mitochondrial mPT. In sum, the mPT-regulatory activity of p53 in cells is also CypD-dependent.

Oxidative stress induces necrosis that depends on both p53 and CypD. Both necrosis and apoptosis are oxidative stress-induced cell death modes (129). Upon oxidative stress, CypD primarily mediates necrotic death via PTP and mPT (44, 45), and evidence exists that CypD can actively suppress apoptosis (130-132). On the other hand, while p53 protein is a well-established apoptosis regulator, almost nothing is known if and when p53 participates in regulating necrotic cell death. Importantly, primary p53-deficient MEFs were equally well protected from H_2O_2-induced cell death as CypD-deficient MEFs, while 60% of WT MEFs died, as indicated by cell viability assays measuring metabolic activity and membrane integrity (Figure 30A). To determine the nature of this cell death we first measured apoptosis. Notably, only negligible TUNEL positivity was detected in all genotypes and H_2O_2 conditions used (Figure 30B). Thus, upon oxidative stress the protection of primary MEFs bestowed by loss of p53 and CypD, and conversely the death of WT MEFs, is largely unrelated to apoptosis. Instead, electron microscopy of H_2O_2-treated WT MEFs revealed all signatures of necrosis, such as loss of plasma membrane integrity, organelle swelling, massive intracellular vacuoles and lack of nuclear fragmentation (Figure 30C). The same holds true for cancer cells, as shown by the HCT116 p53+/+ and p53 -/- colorectal carcinoma pair (Figure 31A). Lack of p53 or silencing of CypD by

shRNA caused significant resistance to H_2O_2 - induced cell death, while 50% of WT cells were killed. On the other hand, a similar rescue effect was obtained by eliminating/silencing p53 alone or together with CypD, i.e. p53 was epistatic to CypD, further supporting that they act on the same biochemical pathway. Again, apoptosis levels in HCT116 p53+/+ cells were very low (10%), confirmed by the complete absence of cleaved PARP (Figure 31B), and did not account for the observed 50% of cell death (Figure 31A). Instead, H_2O_2-treated cells released large quantities of High Mobility Group Box 1 (HMGB1) protein into the culture medium in a dose-dependent, p53-dependent and CypD-dependent manner (Figure 31C). Released HMGB1 is the classical biochemical hallmark specific for necrosis. In contrast, in apoptotic cells HMGB1 binds irreversibly to the condensed chromatin in the nucleus (133). In sum, this data indicated that the predominant mode of cell death in response to H_2O_2 was p53/CypD-mediated necrotic cell death in both primary and cancer cells.

Targeting of p53 to mitochondria induces mPT and cell death in a CypD dependent manner. We showed that oxidative stress-induced p53 translocation to mitochondria, however it is known that oxidative stress also causes activation of p53 target genes (134). Some of these transcriptional targets might contribute to regulate H_2O_2 response in a CypD-dependent manner. For example many proteins participating in pro- or anti-oxidation and modulation of cellular ROS levels are p53 targets (135-137). Therefore, direct prove is necessary to substantiate the involvement of mitochondrial p53, as opposed to its nuclear action.

In respect with that we first employed direct targeting of p53 to the mitochondrial matrix. Our lab had previously generated various mitochondrially targeted versions of wt p53 protein (6) and one of them, called Lp53wt (wt p53 fused to the mitochondrial import leader sequence of ornithine transcarbamylase) targets p53 specifically to mitochondrial matrix. Importantly, this fusion protein is devoid of transcriptional activities (6). Adenoviral delivery of Lwtp53 into WT MEFs (Figure 32A) caused significant loss of TMRM fluorescence, while in CypD-/- MEFs TMRM fluorescence remained unchanged (Figure 32B), indicating that mitochondrial p53 could indeed regulate PTP in vivo, independently of p53 transcriptional targets.

Lp53 also sensitized MEFs and HCT116 p53-/- cells to H_2O_2 - induced cell death which was dependent on the presence of CypD (Figure 33A). Measurement of HMGB1 release into media (Figure 33A) or lack of significant apoptosis levels (Figure 33B) indicated the necrotic nature of the undergoing cell death.

Oxidative stress – induced PTP opening and cell death are largely transcription independent. Conversely to using direct targeting of p53 to mitochondrial matrix while bypassing p53 mediated transcription we next used general transcription inhibitor αAmanitin or inhibitor of p53 mediated transcription PFTα. Both the inhibitors caused reduction of p21 upon H_2O_2 treatment (Figure 34A), indicating block of p53-mediated transcription. Additionally, both of them did not affect p53 protein levels (Figure 34A) or p53s' mitochondrial localization (Figure 34B). Importantly, none affected significantly PTP opening or cell death when added prior to oxidative stress (Figures 34C and 34D), therefore confirming that oxidative stress-induced PTP opening or cell death could be indeed at least partly and in certain circumstances transcription independent.

Leader p53 sensitizes Bak/Bak DKO cells to oxidative stress in a CypD dependent manner. To further interrogate the role of mitochondrial p53 in necrosis, we used Bax and Bak double-knockout (DKO) cells. These cells are deprived of the apoptotic gateway to mediate Cytochrome C release for caspase activation and are widely used to study non-apoptotic cell death (120, 138, 139).

Adenovirally delivered Lp53 into Bax/Bak DKO cells was readily detectable in mitochondrial fractions and importantly, was able to bind to CypD as revealed by immunoprecipitations (Figure 35A). Further, DKO cells were significantly more sensitive to oxidative stress in the presence of Lwtp53, and this sensitivity was almost completely abolished when CypD protein expression was blocked by RNAi (Figure 35B). Lack of apoptosis was confirmed by the absence of caspase-3 and PARP cleavage, while release of HMGB1 into media confirmed that Lp53 was able to accelerate necrotic cell death only in the presence of CypD (Figure 35C). Therefore we conclude that the interaction between mitochondrial p53 and CypD is an important event for regulation of necrotic cell death during oxidative stress, a function of mitochondrial p53 described for first time.

Pathologic p53-CypD Complex Formation During Ischemic Stroke-Induced Brain Tissue Necrosis. *In vivo*, the parameters required for induction of mPT are fulfilled during stroke (transient ischemia - reperfusion injury of the brain). During brain ischemia, the absence of glucose and oxygen causes mitochondrial dysfunction, intracellular calcium uptake and a sharp decrease in ATP levels. Subsequent brain reperfusion generates the conditions required for mPT as mitochondria repolarize, sequester excess cytosolic calcium accumulated during the ischemic period, and generate ROS and oxidative stress. Cells (mainly neurons but also glia) die largely by necrosis, although in the peripheral penumbra apoptosis also takes place. Importantly, CypD

deficiency confers significant protection against ischemic brain injury in permanent and transient ischemic stroke models in mice (46).

Since our cell culture data identified a physical and functional interaction between mitochondrial p53 and CypD that is critical for oxidative stress-induced necrosis, we investigated the pathophysiologic role of the PTP-regulating function of p53 in transient ischemia/reperfusion stroke. To this end, WT, p53+/-, p53-/- and WT control mice pre-treated with CsA were subjected to carefully controlled unilateral acute middle cerebral artery occlusion (MCAO) for 1 hr, followed by 24 hrs of reperfusion. Infarct size was measured by staining coronal brain slices with triphenyl-tetrazolium chloride (TTC), a dye that is oxidized by intact mitochondrial dehydrogenase to yield the red product formazan. In the infarcted area (white), mitochondria are uncoupled and dysfunctional and no longer stain with TTC. WT brains (n=8) were grossly infarcted. Intriguingly, p53 +/- brains (n=8) were strongly protected from stroke, similar to WT control mice protected by intraperitoneal injection of CsA 15 min prior to MCAO (n=6) (Figures 36A, 36B). Most importantly, a pathologic p53-CypD complex was robustly induced in infarcted WT brains after MCAO, as shown by co-immunoprecipitation with a specific p53 antibody but not with IgG (Figure 36C, 'MCAO'). Intriguingly, the induced p53-CypD complex was undetectable in CsA-pretreated, stroke-protected WT control mice. Moreover, the complex was only barely detectable in p53+/- mice, whose stress-mediated p53 induction did not exceed the baseline p53 levels of WT mice and were also protected from infarction (Figure 36C). Thus, a strong association exists between the formation of the pathologic p53-cypD complex and ischemia-reperfusion brain infarction. These data support the idea that this novel p53-CypD axis is an important pathophysiologic contributor to ischemic stroke.

III. Discussion

The transcription-independent mitochondrial p53 program is a major contributor to Nutlin-induced apoptosis in tumor cells

p53 reactivating compounds such as Nutlin hold great promise as a therapeutic strategy for human tumors retaining wild-type p53. Nutlin is a highly selective competitive inhibitor of the MDM2-p53 interaction that potently stabilizes and activates wild-type but not mutant p53 protein in tumor cells. In contrast to chemotherapeutics, where activation of p53 is result of genotoxicity, Nutlin's ability to activate wild-type p53 in a non-genotoxic manner might render it a viable alternative. In fact, studies have demonstrated Nutlin's potent ability to induce growth inhibition of human tumor cells in culture and tumor xenografts in nude mice (86, 89). As single agent, Nutlin showed most promising results in hematopoietic cancers, where the p53 gene remains mainly WT (98, 140-143). Nutlin is also promising in neuroblastoma, a solid tumor characterized by essentially exclusive wild-type p53 status (144-146). Moreover, since Nutlin does not bind to p53 or induce post-translational modifications, Nutlin can also act in concert with conventional chemotherapeutics, potentially improving the efficacy and lowering the genotoxic burden by enabling dose reduction. For example, synergistic effects with genotoxic drugs were found in studies of cultured and clinical samples of multiple myeloma (147), acute myelogenous leukemia (143) and chronic lymphocytic leukemia (140, 142). Clinical trials of Nutlin in combination with chemotherapy are currently ongoing (148, 149).

As discussed, activating p53 signaling by Nutlin is particularly promising in hematologic malignancies such as leukemias and lymphomas due to several favorable parameters that compound in this disease group: i) p53 mutations are rare, ii) inactivation of wild-type p53 by Mdm2 overexpression are frequent molecular events, e.g. in acute myeloid leukemia, iii) downstream p53 signaling is intact and iv) the cell-intrinsic response to Nutlin-

induced p53 activation tends to be apoptosis rather than cell cycle arrest, favoring the preferred cytotoxic rather than a mere cytostatic outcome.

However, the great majority of wild-type p53 human tumor cells of non-hematopoietic lineages, particularly carcinomas, undergo cell cycle arrest in response to Nutlin rather than apoptosis (86, 89, 141-143). Therefore, clarifying the precise mechanism(s) of Nutlin-mediated apoptosis is critical for designing rational strategies on how to convert Nutlin from a mere cytostatic to a cytotoxic anticancer agent. The apoptotic effects of Nutlin in wtp53 tumor cells are currently ascribed to the activation of transcriptional activities of p53 in the nucleus. Indeed, once freed from MDM2 by Nutlin, p53 accumulates in the nuclei of cancer cells, followed by activation of a broad wild-type p53-dependent transcriptional program that includes induction of the pro-apoptotic Puma, Noxa, Bax and DR5 genes, as well as repression of pro-survival genes (86, 89, 146). Here we show that the transcription-independent mitochondrial p53 program can be a major contributor to Nutlin-induced apoptosis, at least in some tumor cells including leukemia and colon carcinoma. Moreover, in these cells, transcriptional activities of p53 appear to be not only dispensable for the apoptotic Nutlin response, but actively block its mitochondrial p53 death program. In addition to nuclear stabilization, Nutlin treatment of ML-1 and RKO cells also causes significant cytoplasmic accumulation of p53 and rapid mitochondrial translocation associated with early MOMP activity. Induction of early response transcriptional p53 target genes starts at later time points, indicating that mitochondrial p53 translocation is the first event during Nutlin-induced apoptosis. Specific inhibition of mitochondrial p53 translocation by PFTμ, an inhibitor that blocks p53 interaction with Bcl-2 and Bcl-xL, markedly reduces the apoptotic Nutlin response, underlining the significance of mitochondrial p53 program in Nutlin-induced apoptosis. Our group had previously shown that MDM2-mediated monoubiquitination

of p53 greatly promotes p53 mitochondrial translocation (65). Thus, an important concern is whether therapeutic targeting of specific E3 ligases such as MDM2 might also disrupt MDM2's role as p53 monoubiquitinase and thereby blunt the tumor suppression offered by mitochondrial p53 (150). However, our results indicate that Nutlin does not change the monoubiquitination status of cytoplasmic p53, probably due to the fact that MDM2-p53 complexes are only partially disrupted and Nutlin-stabilized MDM2 retains its E3 ubiquitin ligase activity (97).

Three earlier studies had also noted that in addition to the nuclear p53 death pathway, Nutlin can also induce mitochondrial p53 death functions (98, 99, 143). Using immunofluorescence-based mitochondrial co-localization and cycloheximide sensitivity, Kojima et al concluded that in response to Nutlin, a significant fraction of clinical samples of acute myeloid and chronic lymphocytic leukemias co-recruited the mitochondrial p53 apoptotic pathway. Interestingly, samples in the primarily transcription-independent group responded significantly better to Nutlin-induced apoptosis (98, 143). Going beyond this observation, we report here that at least in some human leukemia cells the p53 transcriptome not only is dispensable for the apoptotic Nutlin response, but in net balance appears to actively block the Nutlin-induced mitochondrial death program of p53. This is based on the fact that specific blockade of p53-mediated transcription by PFTα potentiates Nutlin-induced apoptosis of ML-1 cells by several fold. Our result might be of therapeutic significance in future clinical trials of Nutlin or later generation Nutlin-type MDM2 inhibitors.

Very recently a large series of clinical samples of chronic lymphocytic leukemia was also reported to undergo drug-induced apoptosis via the transcription-independent mitochondrial p53 pathway in response to the clinically used chemotherapeutics chlorambucil and fludarabine

plus Nutlin, with PFTα potentiating the death response (99).Our results substantiate and expand these findings.

While other parameters can interfere with Nutlin-induced apoptosis sensitivity of tumor cells (such as overexpression of MDM2, Mdmx, delta Np73 and Notch-1, loss of p14ARF or abrogation of downstream apoptotic effectors (88, 151), our data indicate that p53's transcriptional activity itself could play a counteracting role. Which p53 targets might be responsible for this dampening effect? Likely it is several rather than a single target, but one strong candidate is the p53-induced p21Cip1, a CDK inhibitor causing G1 and G2 cell cycle arrest and known to block apoptosis (152). In support, αAmanitin or PFTα pretreatment blocks p21 induction in ML-1 cells.

In sum, our study further clarifies the mechanism of Nutlin-induced cell death by demonstrating the importance of transcription-independent mitochondrial p53 functions. Moreover, our study suggests that concomitant blockade of p53-mediated transcription might improve Nutlin's therapeutic efficacy by enhancing the intrinsic mitochondrial p53 apoptotic response, at least in leukemia.

Blockade of Hsp90 by 17AAG antagonizes MDMX and synergizes with Nutlin to induce p53-mediated apoptosis in solid tumors.

As discussed above, although Nutlins holds big promise, especially in leukemias, the vast majority of wild-type p53 human tumor cells of non-hematopoietic lineages undergo cell cycle arrest, conferring only cytostatic rather than the desired cytotoxic antitumoral activity (89-91). Little is known about the factors that prevent tumors from undergoing Nutlin-mediated

apoptosis. Although the reasons for this may vary depending on cell or tumor type, several possibilities exist. One possibility could be that in some tumors, pro-apoptotic p53 signaling is inhibited by oncogenic signaling, thus the ability of p53 to induce apoptosis is suppressed. Another possibility could be that additional events such as modifications are necessary in order for p53 to activate its apoptotic machinery. Third, p53 might require cooperation with other signaling pathways, which might be inactivated in tumors. It is therefore not surprising that p53 can contribute to apoptosis during genotoxic chemotherapy when a broad array of pathways become activated or inhibited and closely interact with each other.

In this respect, major academic and pharmaceutical efforts are currently underway to identify factors that contribute to lack of apoptosis during Nutlin treatment. Earlier studies have reported that inhibition of oncogenic signaling pathways enhance apoptosis induction by Nutlin in certain tumor types. For example, inhibition of PI3K/AKT signaling was shown to synergistically promote apoptosis in ALL or CLL cells upon Nutlin (153, 154), and inhibition of ERK signaling synergistically enhance Nutlin-induced apoptosis in AML cells (117, 118). It was also shown that downregulation of MDMX enhances Nutlin-induced apoptosis (92-94, 96).

Our study focused on 17AAG to promote Nutlin-induced apoptosis for the following reasons: *i)* Inhibition of hsp90 was shown to cause wt p53 stabilization (109, 110). *ii)* 17AAG was recently shown to kill cancer and primary cells in p53-dependent manner (110). *iii)* Hsp90 is overexpressed in the vast majority of cancers and has numerous (in part oncogenic) client proteins, many of which can affect the p53 pathway in one way or another. Examples are many kinases, known to directly or indirectly phosphorylate and modulate the functions of p53 and/or of MDM2 and MDMX: AKT/PKB, Chk1, GSK3b, ErbB2 (or mutant EGFR), p38 MAPK, Raf/ERK MAPK pathway and many others (113-116).

We show that in difficult-to-kill solid human cancer cells 17AAG modulates several components and pathways to favorably cooperate in Nutlin-activated p53 signaling and to convert the Nutlin response from cytostatic to cytotoxic. Although likely not a complete list, we identify several factors that contribute to the synergistic interplay between 17AAG and Nutlin. *i)* 17AAG first and foremost destabilizes the MDMX protein and reduces MDM2 protein levels; *ii)* 17AAG induces pro-apoptotic p53 targets such as PUMA; *iii)* 17AAG reduces p21 protein which at high levels might at least in some cancers favor Nutlin-induced cell cycle arrest; and *iv)* 17AAG inhibits oncogenic survival pathways such as PI3K/AKT by destabilizing AKT, which normally can counteract p53 signaling at multiple levels.

When combined, 17AAG enhances Nutlin-activated p53 transcription without changing p53 levels. Mechanistically, 17AAG interferes with the repressive MDMX-p53 axis by disrupting MDMX-p53 complexes and inducing robust MDMX degradation (38). While RNAi-mediated knockdown demonstrates the central importance of MDMX in Nutlin resistance in an experimental setting, an RNAi approach is currently not within clinical reach. Thus, to our knowledge the Nutlin+17AAG combination represents the first effective pharmacological inhibition of MDMX.

The mechanism by which 17AAG induces MDMX degradation remains to be determined. MDMX is not a known HSP90 client and therefore its 17AAG-mediated destabilization is likely indirect, and could for example be through affecting MDMX modifications. Concerning MDM2, it is a known Hsp90 client and Hsp90 inhibition by the 17AAG precursor Geldanamycin stimulates MDM2 degradation (107). Moreover, our co-immunoprecipitations showed that 17AAG disrupts the MDM2-MDMX complex. This could contribute to MDM2 destabilization, since one function of MDMX is to stabilize MDM2 (155).

Likewise, 17AAG could contribute to p53 stabilization since the MDM2-MDMX heterodimer is thought to be a more effective E3 ligase for p53 compared to MDM2 homodimers. The latter could explain also why p53 is stabilized upon 17AAG treatment before MDMX degradation occurs in some of the cell lines. Although we were able to identify some important determinants, further elucidation of the synergistic mechanisms is warranted. 17AAG might also modulate p53 transcription through other mechanisms, e.g. by affecting co-activators and/or p53 modifications.

In sum, the molecular rationale for this drug combination is quite compelling. 17AAG targets different tumor types by destabilizing multiple oncogenic pathways via Hsp90 interference (156). This suggests that the Nutlin+17AAG combination might resurrect Nutlin as a clinically viable uniform platform against a broad spectrum of wtp53 harboring solid tumors. Moreover, 17AAG-type inhibitors specifically target tumor cells (115, 116) for two reasons: Hsp90 upregulation is tumor-specific and ubiquitous in tumors, and 17AAG exhibits a 100-fold higher activity toward tumor cell-derived Hsp90 complexes than against Hsp90 purified from normal cells (157). Thus, 17AAG may also help in improving the therapeutic window by better targeting the Nutlin responses specifically to tumor cells and reduce the bone marrow suppression-based toxicity of Nutlin.

p53 protein regulates the mitochondrial Permeability Transition Pore during oxidative stress-induced necrosis and ischemic stroke

Here we identify a new role of p53 in activating necrotic cell death. In response to oxidative stress and ischemia, p53 protein accumulates in the mitochondrial matrix and triggers PTP opening, mPT and necrosis by physical interaction with the critical PTP regulator CypD. This

p53 action is transcription-independent and inhibited by the specific CypD inhibitor CsA, and by genetic CypD deletion or knockdown. In support, in contrast to the prototypical MOMP-inducer tBid, purified p53 protein has efficacy that goes beyond activating the Bax/Bak lipid pore at the outer membrane. p53 is able to also rapidly open the PTP pore at the inner membrane in healthy Bax-/-Bak-/- mitochondria where tBid fails. Similarly, p53 causes structural alterations of the PTP pore, while tBid does not. Using gene knockout and knockdown in mouse and human cells, we show that oxidative stress induces PTP opening, mPT and necrosis that concomitantly depend on the presence of p53 and CypD. Importantly, WT, Bax/Bak DKO and p53-/- cells are all (further) sensitized to H_2O_2-induced PTP opening and necrotic death upon direct delivery of p53 into the mitochondrial matrix. This sensitivity is reversed by knockdown of CypD, confirming the physiological p53-CypD cross-talk. Most intriguingly, a robust p53-CypD complex is formed during necrosis in brain tissue upon ischemia/reperfusion stroke injury. In contrast, genetic reduction of p53 levels (p53+/- mice) or CsA-pretreatment of WT mice prevents this complex from forming, and is associated with effective stroke protection. This strongly supports a pathophysiologic role of the mitochondrial p53-CypD axis in ischemic stroke.

Aside from p53, very few extramitochondrial proteins are known to bind CypD and trigger pathologic PTP opening. A compelling analogy to p53, albeit acting chronically, is the highly toxic, soluble intracellular form of β amyloid peptide (Aβ), a key protein in Alzheimer's disease (AD) that progressively accumulates in brain mitochondria of AD patients and AD transgenic mice. In AD, Aβ forms a critical complex with CypD that promotes PTP opening, thereby boosting Ca^{2+}-induced mitochondrial damage and neuronal injury. Inhibiting PTP or ablating CypD in AD mice renders their cortical brain mitochondria resistant to PTP opening and improves their cognitive functions (158).

In response to many insults, a continuum of apoptosis and necrosis exists. Such insults induce apoptosis at lower doses and necrosis at higher doses, a scenario that is clearly the case in ischemic brain infarction with an apoptotic penumbra surrounding a necrotic center (159). The long-standing paradigm had been that p53 controls apoptosis but plays no role in necrosis. Only recently the very first link between p53 and necrosis was reported. Upon etoposide-mediated DNA damage Bax/Bak DKO MEFs die via slow necrosis, which is largely controlled by p53-mediated transcription of cathepsin Q in cooperation with DNA damage-induced ROS (160). Interestingly, however, this transcriptional p53-cathepsin Q axis only plays a minor role in the corresponding WT MEF necrosis. In contrast, H_2O_2-induced necrosis in DKO MEFs was found to be completely transcription-independent (160), supporting our finding of direct CypD-mediated necrotic signaling by p53. Thus, in response to oxidative stress our data establish a necrotic mitochondrial p53 program, in addition to the well-characterized mitochondrion-based apoptotic p53 program. The decision whether to engage one and/or the other appears to depend on the type and dose of stress. Clearly though, necrotic signaling also uses p53-independent pathways, depending on the insult. Examples are necrosis induced by DNA alkylating agents which signals through PARP and necrosis signaling via the TNFR/RIP1 pathway (159) .

Our data shows that p53 can control a CypD-mediated necrotic program during oxidative stress in various cell types and in likely in brain tissue *in vivo*. The surprisingly strong brain protection from ischemia/reperfusion injury of p53+/- mice (Figures 36A and 36B) is likely due to two components: The absence of a destructive p53-CypD complex, thereby protecting the PTP pore (Figure 36C), and the presence of weaker p53 apoptosis program such as e.g. Puma and Noxa (Figure 37A). Importantly though, the absence of the p53-CypD complex strongly correlates with stroke protection. This is indicated by CsA-protected WT brains that do not form

the p53-CypD complex, yet concomitantly mount a full-blown p53 apoptosis program including Puma and Noxa (Figure 37A). Parenthetically, the p53 homolog p73, which is robustly expressed in adult mouse and human brain, was not induced in the ischemic brain tissues (Figure 37B). Finally, although low or uninduced levels of p53 can clearly mount a transcriptional anti-oxidant defense by regulating expression of e.g. sestrins, glutathione peroxidase and TIGAR, this is highly tissue-specific. Notably, in brain tissue p53 is constitutively pro-oxidant in both physiologic and pathologic conditions due to transcriptional repression of antioxidant genes (161). Thus, a protective p53 anti-oxidant program is likely not a factor in the observed p53+/- stroke protection. Interestingly, p53-/- brains were not as protected as p53+/- brains (not shown), as observed by others (72). This could be explained by the fact that in ischemic p53-/- brains, lack of p21 induction might trigger abortive reentry of post-mitotic neurons into the cell cycle, leading to cell death. This is supported by the observation that p21 is induced after cerebral ischemia (162) and conversely, CDK inhibitors reduce infarct size after focal cerebral ischemia (163).

CypD-/- mice show strong protection against focal ischemia-reperfusion brain injury (46). Similarly, mice and rats treated with CsA or non-immunosuppressive derivatives that do not bind to calcineurin are also protected from stroke (164-166). Clinically, CsA is chronically given to organ transplant patients as a time-tested immunosuppressant. Our data suggest that acute temporary blockade of the destructive p53-CypD complex by CsA-type inhibitors may be a therapeutic strategy to limit infarct extent in the rising number of ischemic stroke patients where reperfusion of the occluded artery can be reestablished by interventional thrombolysis.

IV. Future Directions

Development of p53 based therapies is emerging and exciting research field. However, we need to gain a lot more knowledge before these therapies can be applied successfully in clinic. Nutlin, a small molecule inhibitor that reactivates wild type p53 by separating it from MDM2, has been a major breakthrough in the field. Unfortunately, it is now clear that Nutlin and similar compounds more often exert cytostatic rather than cytotoxic activities when used to treat tumors. Therefore research needs to focus on understanding the mechanisms of Nutlin-induced cell death and how to convert Nutlin from cytostatic to cytotoxic.

My first project identifies that in the acute myeloid leukemia cell line ML-1 Nutlin causes apoptosis with significant contribution of the direct mitochondrial p53 functions. Thus, the project further clarifies the mechanisms of Nutlin-induced cytotoxicity at least in this cell line. However, several questions remain open. Because we use only one cell line, it is obvious to ask whether this mechanism is cancer/cell type specific. To answer this question, the same approaches should be applied to other Nutlin-sensitive cancer cell lines and possibly cancer models (xenograft or genetic mouse models). This would allow determining whether mitochondrial p53 contributes towards Nutlin-induced toxicity only in certain types of cancers, or it is a uniform mechanism. Additionally, present study does not explore whether mitochondrial p53 functions might be suppressed in cell lines responding with arrest or generally resistant to Nutlin treatment. An approach that could be considered is to compare levels of mitochondrial p53 translocation upon treatment in sensitive versus resistant cell lines. Moreover, one could compare binding of p53 to Bcl-2 family members in Nutlin-sensitive and Nutlin-resistant cell lines. If these studies identify that mitochondrial p53 pathway is suppressed in Nutlin-resistant cell lines and/or mouse cancer models, they would have significant impact towards the improvement of p53 based therapies.

We observe that blocking of p53 mediated transcription by Pifithrin-α potentiates Nutlin-induced apoptosis. These results are very compelling and need further clarification. They suggest the existence of p53 transcriptional targets that might suppress its own mitochondrial functions. Future studies should determine whether one could sensitize Nutlin-resistant cell lines by using Pifithrin-α. If so, further identifying of the particular p53 transcriptional targets responsible for this negative auto-regulation would also have great contribution towards improving Nutlin response and understanding p53 signaling.

My second project identifies synergistic interaction between Nutlin and the Hsp90 inhibitor 17AAG. We show that 17AAG destabilizes p53 and MDMX proteins as well as separates MDMX form p53. Mechanistically, MDMX destabilization and/or AKT pathway suppression contribute towards the synergism. The finding that inhibition of Hsp90 affects MDMX protein stability is described here for first time and suggests that MDMX might be Hsp90 client protein. Nevertheless, the mechanism by which 17AAG destabilizes MDMX remains unclear and future studies need to establish that. One possibility is that Hsp90 binds directly to MDMX. This could be tested by immunoprecipitations and pull-down experiments. Second, Hsp90 could affect MDMX stability indirectly. For example, Hsp90 binds to and affects MDM2 functions, while MDM2 regulates MDMX stability. Therefore, 17AAG could regulate MDMX stability indirectly, through regulation of MDM2 ubiquitin ligase activity. Several kinases, known to phosphorylate MDMX are Hsp90 client proteins, such as AKT, CHK1, CDK1, c-Abl. Thus, it should be determined whether Hsp90 regulates MDMX stability or binding to p53 through affecting MDMX phosphorylation status. Another possibility is the involvement of 17AAG-induced ribosomal stress. It is known that MDMX binds to ribosomal proteins such as L11, and that ribosomal stress causes separation and MDMX protein

degradation. Inhibition of Hsp90 induces ribosomal stress; consequently, the interaction between L11 and MDMX could be disrupted by 17AAG treatment and result in MDMX destabilization. Several Hsp90 client proteins (such as ErbB2) undergo proteasomal degradation after Hsp90 inhibition, mediated by the ubiquitin ligase CHIP. Involvement of CHIP in regulating MDMX stability after 17AAG treatment could also be explored in future.

Because Hsp90 has numerous client proteins, it is very likely that other client proteins, besides MDMX and AKT could be involved in the synergistic interaction between Nutlin and 17AAG. It has been shown that inhibition of ERK MAPK can potentiate Nutlin-induced cytotoxic response, while Raf (ustreatm of ERK) is a client protein of Hsp90. Therefore, involvement of Raf/ERK MAPK pathway in the synergism between 17AAG and Nutlin could be explored. Other potential candidates are GSK-3β, p38 MAPK pathways, CHK1 checkpoint kinase as all of these are known to be Hsp90 client proteins, and as well have been implicated in the regulation of p53 signaling.

The diversity of Hsp90 targets also suggests a possibility that the mechanisms for the synergism between Nutlin and 17AAG might differ among different cancer types. Furthermore, some types of cancers could be more sensitive to the combination than others. For example, MDMX overexpressing cancers or cancers with hyperactive PI3K pathway could be more responsive. Clarifying these questions would be important for the therapeutic development of this drug combination.

In the xenograft assay with RKO cell line, tumors treated with the drug combination are stabilized over time, but do not regress. It is important to find conditions in which tumor regression would be observed. This can be accomplished by evaluating the administration of

different doses of the drugs or different administration schedules. For example, 17AAG could be administered more in advance since in cell culture, destabilization of MDMX and AKT occur at later time points. Furthermore, the drug combination could be evaluated in more advanced cancer models such as genetic mouse models, which would prove it to be more therapeutically relevant.

My third project elucidates a novel function of mitochondrial p53: it shows regulation of mitochondrial Permeability Transition Pore by p53 during oxidative stress-induced necrosis, and implicates this function in brain ischemia-reperfusion injury. For the first time, we demonstrate direct interaction between p53 and the mitochondrial matrix protein CypD, which plays a central role in regulation of PTP. Although, the study identifies minimal region of p53 protein required for the interaction with CypD, it is still not clear how this interaction occurs, and mutant p53 that does not bind to CypD is not identified. Identifying such a mutant is important to further validate the functional relationship between the two proteins. In mice ischemia-reperfusion brain injury, the complex formation between p53 and CypD correlates with level of injury, however, these results remain correlative and do not prove a role of the interaction in ischemic stroke. This can be tested by generating mutant p53 transgenic mice lacking binding to CypD, and compare the levels of brain injury upon MCAO with WT mice. If p53 mutant mice show reduced brain injury, such an experiment would be direct proof that the interaction between p53 and CypD has a role in stroke. Crystallography or computer modeling with minimal p53 and CypD interaction regions can be applied to discover such a p53 mutant protein. The knowledge for the interaction would be also very useful for potential development of an inhibitor.

Central function of p53 upon stress is considered the regulation of apoptosis or cell cycle arrest. We show that in the case of oxidative stress caused by H_2O_2 in MEFs and cancer cell

lines, p53 plays a role in regulating PTP and necrotic, rather than apoptotic cell death. These results seem surprising considering that oxidative stress leads to DNA damage which triggers p53 dependent apoptosis or cell cycle arrest. Additionally, in our isolated mitochondria assays purified p53 protein causes release of apoptogenic factors independently of Bax/Bak lipid pores presumably through PTP regulation. mPT causes mitochondrial swelling, rupture of outer mitochondrial membrane and release of apoptogenic factors. Therefore one would expect more pronounced apoptotic response upon oxidative stress. These observations could be explained by the fact that apoptosis is energy dependent process and although initial activation of apoptotic cascade might occur, quick accumulation of ROS causes PTP opening, ATP loss and therefore lack of energy necessary for apoptotic cell death to progress. Conversely, one might question why mainly p53 dependent apoptosis occurs during DNA damage since DNA damage causes accumulation of ROS. It is possible that activation of DNA damage kinases occurs faster than accumulation of ROS and the levels of ROS generated by DNA damage might not be significant to cause enough PTP opening, loss of energy and block of apoptosis. Additionally, several redox dependent kinases activated by ROS are known to regulate p53 activity and their spatio-temporal activation upon H_2O_2 or DNA damage might differ. Moreover, ROS can affect the redox state and oxidation of p53 itself. Exploring these possibilities in future could explain the differences in p53 activity upon DNA damage and exogenous oxidative stress.

V. Materials and Methods

The transcription-independent mitochondrial p53 program is a major contributor to nutlin-induced apoptosis in tumor cells

Cell culture and drugs. The human myeloid leukemia cell line ML-1 and the colorectal cancer cell line RKO were used. Both were cultured in RPMI medium (Gibco, Invitrogen), supplemented with 10% FBS (Gibco. Nutlin 3a was a gift from Dr. L. Vassilev, Roche Pharmaceuticals. PFTμ was a gift from Andrei Gudkov, Lerner Research Institute, OH. α-Amanitin and PFTα were purchased from Sigma (St.Lous, MO).

Immunoblotting and immunoprecipitation. Exponentially growing cells were treated as indicated, lysed with 0.5% Triton X-100 in phosphate-buffered saline supplemented with protease inhibitor cocktail (Roche) and 50 ng/ml ubiquitine aldehyde (Sigma) and sonicated. Standard ECL immunoblotting was performed. For immunoprecipitation, cells were lysed in the same buffer as above. One milligram of total protein was incubated overnight at 4°C with 1 μg of primary antibody and protein A/G agarose beads (Roche). In some instances, p53-specific FL393 antibody conjugated to agarose beads was used. Beads were washed 3 times in buffer (0.5% Triton X-100 in PBS) and proteins were solubilized by boiling in 50 μl of sample buffer prior to SDS-PAGE. The following antibodies were used: monoclonal DO1 and polyclonal FL393 against p53 (Santa Cruz), monoclonals Ab-1 (Calbiochem) and 2A10 (Santa Cruz) against MDM2, polyclonal anti-PARP (Cell Signaling), monoclonal anti-p21 Clone 187 (Santa Cruz). For loading controls antibodies against β-Actin (Ab-5, NeoMarkers), HDAC, mt hsp70 and hsp90 were used.

Nucler/Cytoplasmic fractionations. Exponentially growing RKO or ML-1 cells were treated as indicated. Cells were washed with ice-cold TD buffer (135 mM NaCl, 5 mM KCl, 25 mM Tris-

HCl, pH 7.6) and resuspended in 100 µl CaRSB buffer (10mM NaCl, 1.5mM $CaCl_2$, 10mM Tris-HCl, pH 7.5) supplemented with 2x protease inhibitor cocktail and ubiquitinaldehyde. Then 100 µl 1% Triton X-100 in PBS was added, the suspension was gently mixed and nuclei were spun down at 700 rcf for 5 min at 4^{o}C. The cytosolic fraction was transferred to a new tube and nuclei were lysed with 50 µl 0.5% Triton X-100 in PBS and sonicated. In immunoblots, monoclonal anti-HDAC1 (Affinity BioReagents) and monoclonal anti-Heat Shock Protein 90 (Calbiochem) were used as nuclear and cytoplasmic markers, respectively.

Mitochondrial purification. Cells were washed with TD buffer, resuspended in CaRSB buffer and incubated for 10 min to allow swelling. Cells were then homogenized with a loose-fit Dounce homogenizer and addition of 2.5x MS buffer (210 mM mannitol, 70 mM sucrose, 5 mM EDTA, 5 mM Tris, pH 7.6). The homogenate was cleared from nuclei by centrifugation at 1000 g for 5 min at 4^{o}C. The nucleus-free homogenate was subjected to discontinous sucrose gradient ultracentrifugation. Mitochondria fraction was carefully collected at the 1M/1.5M interface of the gradient.

TUNEL staining. Treated and untreated ML-1 and RKO cells were washed with PBS and $5x10^5$ cells were cytospun onto glass slides and processed for TUNEL staining as recommended by the manufacturer (Roche). Staining was quantitated by measuring total pixels per field from 3 random fields (Zeiss Axiovision software).

Blockade of Hsp90 by 17AAG antagonizes MDMX and synergizes with Nutlin to induce p53-mediated apoptosis in solid tumors

Cell culture and drugs. The wtp53 harboring human cancer cell lines U2OS, RKO, HCT116 p53 +/+ (and its isogenic match HCT116 p53 -/-), MCF7 and SJSA and RPMI were maintained in DMEM or RPMI 1640 (for AGS and RPMI-1788) with 10% FBS at 37^{o}C in 5% CO2. Stable U2OS cells expressing doxocyclin-inducible MDMX were generously provided by Geoffrey Wahl and maintained in DMEM supplemented with 10% FBS. The following drugs were used: Nutlin-3a (Sigma), 17AAG (17-allylamino-17-demethoxygeldanamycin, LC Laboratories), Cycloheximide (Sigma), Z-VAD-FMK (R&D Systems), ALLN (Calbiochem) and LY294002 (Roche). The human MDMX siRNA and scrambled siRNA were purchased from Qiagen.

Co-immunoprecipitations and immunoblots. Cells were treated, lysed with 0.5% Triton X-100 in PBS supplemented with protease inhibitor cocktail (Roche) and sonicated. Whole cell extracts (5 - 30 μg) were resolved on 10% SDS-PAGE gels and processed for ECL immunoblotting. For immunoprecipitation cells were lysed in the same buffer. Total protein (1 mg) was incubated overnight at 4°C with 1 μg of primary antibody and protein A/G agarose beads (Roche). Beads were washed 3 times in buffer (0.5% Triton X-100 in PBS) and proteins solubilized by boiling in 50 μl sample buffer prior to SDS-PAGE. The following antibodies were used: monoclonal p53 (DO1, Santa Cruz), monoclonal MDM2 (Ab-1, Calbiochem), rabbit Hdmx/Mdm4 (Bethyl Labs), rabbit cleaved PARP (D214, Cell Signaling), monoclonal p21 (BD Biosciences), rabbit Puma, Akt and phospho-AKT S473 (all Cell Signaling), and rabbit cleaved caspase-3 (Asp175, Cell Signaling). Monoclonal PCNA (PC10, (Santa Cruz)) was used as loading control. All antibodies were diluted 1:1000 to 1:5000.

Realtime qRT-PCR. Total RNA was isolated with Trizol and 10 μg reverse transcribed with random primers and SuperScript II Reverse Transcriptase (Invitrogen). Realtime qRT-PCR was performed in triplicate in a MJ Research DNA Engine Opticon 2 with Qiagen QuantiTect SyBr Green Mix. Cycling conditions were 94^{o}C 30 sec, 55^{o}C 30 sec, 72^{o}C 1 min, and 68^{o}C 10 sec for 35 cycles. Human primer sequences used: MDMX- F:GCCTTGAGGAAGGATTGGTA, R:TCGACAATCAGGGACATCAT;PUMA(BBC3)F:ACGACCTCAACGCACAGTACG,R:TCCCATGATGAGATTGTACAGGAC;P21(CDK1N1A)F:CTGGAGACTCTCAGGGTCGAAA, R:GATTAGGGCTTCCTCTTGGAGAA; MDM2-F:GGCGATTGGAGGGTAGACCT, R:CACATTTGCCTGGATCAGCA. Relative expression of all target genes was normalized to actin expression as internal efficiency control.

Cell death assays. Caspase assays were performed in triplicate with the fluorimetric Homogeneous Caspases Assay (Roche). Briefly, 4 x 10^4 cells plated per well in a 96 well plate were treated with 100 μl of media containing 2 -10 μM 17AAG and/or Nutlin for 8 - 48 hours. Substrate working solution was added and the plate was incubated at 37^{o}C for 2 - 8 hours or room temperature overnight in the dark. Plates were read on a Spectramax M2 ROM with an excitation of 485 nm and emission of 520 nm. Annexin/PI assays were performed with FITC Annexin V (BD Pharmingen) and Propidium Iodide (Sigma) following the protocol from BD Biosciences. After drug treatment, cells were trypsinized and diluted to 1x10^6 cells/mL in 1X Binding Buffer (0.01M Hepes pH 7.4, 0.14M NaCl, 2.5mM $CaCl_2$). Annexin (7.5 μl) and PI (10 μl of 50 μg/ml) were added to 150 μl cell suspension. After 15 min incubation in the dark at room temperature, cell suspensions were adjusted to 500 μl with 1X Binding Buffer and counted in a FacScan analyzer (Argon laser, Becton Dickinson).

To evaluate the combinatorial synergy between the two drugs, the percentage of dead cells was determined by Trypan Blue exclusion assay. IC50 were determined and the isobologram and combination index (CI) analyses were performed with CalcuSyn software as described(111).

Xenograft assays. Six to seven week old athymic male nude mice (nu/nu) were purchased from Harlan Laboratories. All animal experiments were approved by the Stony Brook University Internal Review Board. RKO cells ($5x10^6$ per flank) suspended in 50% Matrigel (BD Biosciences) were injected subcutaneously into the four flanks of mice. Tumors were measured by a caliper and volume (V) was calculated using the formula V = length (L) x width$(W)^2/2$, where width was the smaller dimension of the tumor. When tumors had reached between 200-300 mm^3, treatment was started. The change in tumor volume was calculated by comparing the tumor size during treatment to the original tumor size before treatment began (= Day 0). Tumors were measured 3-4 times per week. Mice were randomized into four treatment groups: vehicle, Nutlin, 17AAG, and Nutlin+17AAG. Student's two-tailed T-test with equal variance was used to determine statistical significance of the relative tumor size changes between vehicle-treated versus drug-treated tumors.

Racemic Nutlin-3 (Cayman Chemical Cat # 10004372) was injected at 35mg/kg per mouse in 10% DMSO. 17AAG (NSC 330507) and the egg phospholipid diluent (EPL) vehicle (NSC 704057) were generously supplied by the Pharmaceutical Management Branch, Cancer Therapy Evaluation Program of The National Cancer Institute. 17AAG was injected at 80mg/kg in 10% DMSO plus 90% EPL. Vehicle mice were injected with the vehicles for both Nutlin and 17AAG.

On Days 0-10 treatment was done by intraperitoneal injection (IP). Nutlin was injected by IP every other day. 17AAG was injected was injected on days 0-2, 4-8. IP injection of vehicle followed the same schedule as Nutlin and 17AAG. On Days 11-18, doses were split between IP and IT (intratumoral injection). Nutlin, 17AAG or vehicle were injected on days 12-13, 15, and 17-18. Mice were sacrificed on Day 21. Tumors were isolated and sonicated in 0.5% Triton X-100 /PBS with protease inhibitor cocktail (Roche) and analyzed by immunoblot.

p53 protein regulates the mitochondrial permeability transition pore during oxidative stress-induced necrosis and ischemic stroke

Cell culture and drugs. Primary WT and p53-/- mouse embryo fibroblasts MEF) were established from E13.5 embryos. Primary CypD-/- MEFs were purchased (ArtisOptimus). Bax/Bak DKO and corresponding WT MEFs were a gift of Dr. Weixing Zong, Stony Brook Univ. MEFs (all SV40 immortalized) and cancer cell lines were maintained in DMEM/10% FBS. Cyclosporine A, αAmanitin, Pifithrin-α, ionomycin and FCCP were purchased from Sigma.

Plasmids and recombinant proteins. pGEX-CypD were a gift from Dr. Dario Altieri, Univ. of Massachusetts (167). Human cypD, ANT-2 and VDAC-1 cDNAs in pHA vectors were gifts from Dr. Stefan Grimm, Max-Planck-Institute, Germany (168). Baculovirally expressed human wt and mutant p53 were purchased (Origene). Recombinant adenovirus (Ad5-GFP) was generated as described previously (169) under the control of a CMV promoter. Luc shRNA and CypD shRNA plasmids were purchased (Dharmacon).

Mitochondrial isolation and assays. Mitochondria from cultured cells and mouse liver were isolated by sucrose gradients as we described (Mihara et al., 2003). Mitochondria (35 μg) were

subjected to chemical crosslinking with BMH (1,6-bis-maleimidohexane, Pierce, 10 mM in DMSO for 10 min) or mock-treated (DMSO only). Submitochondrial fractionation was performed by phosphate swelling-shrinking as described (167) and detailed in supplemental material. Equal protein from whole cell lysates or subcellular/submitochondrial fractions was immunoblotted. Antibodies are listed in supplemental material. Release assays for apoptotic activators were performed on freshly isolated mitochondria (350 μg/ml) incubated with baculoviral human wtp53, tBid proteins (R&D Systems), Type V BSA (Sigma) or buffer for 30 min at 30°C and promptly centrifuged at 4°C (Mihara et al., 2003). The resulting supernatants and washed mitochondrial pellets were analyzed by immunoblots. For swelling assays, resuspended mitochondria (in 120 mM KCl, 10 mM Tris pH 7.6, 5 mM KH2PO4) were incubated with purified proteins or buffer for 30 min at 30 °C. Swelling was promptly monitored by the decrease of 90° light scatter at 540 nm in a spectrophotometer (SpectraMax M2, Molecular Devices) or visualized by Transmission Electron Microscopy detailed in supplemental materials. The mitochondrial membrane potential ΔΨm was assessed by measuring the ΔΨm - dependent uptake of the potentiometric dye TMRM (tetramethylrhodamine methyl ester; 200 nM added to the media) and visualized by a Zeiss Axioskope or quantified by FACS. To directly measure PTP opening in isolated mitochondria or cultured cells, the calcein-AM release assay (MitoProbe Transition Pore Assay, Molecular Probes) was used.

Submitochondrial fractionation. Briefly, purified mitochondrial pellets isolated by sucrose step gradient were resuspended in swelling buffer (10 mM KH2PO4, pH 7.4, and protease inhibitor) and incubated for 15 minutes at 4°C with gentle mixing. Then mitochondria were mixed with equal volume of shrinking buffer (10 mM KH2PO4, pH 7.4, 32% sucrose, 30% glycerol, 10 mM MgCl2, and protease inhibitor) for another 15 minutes at 4°C. After centrifugation at 10,000 × g

for 10 min, the supernatant was collected as containing outer membrane and intermembrane space fractions (OM&IMS). Pellets were washed three times with 1:1 mixture of swelling-shrinking buffer, resuspended in swelling buffer, and sonicated to disrupt the inner membrane (IM & MA). OM & IMS and IM & MA were further fractionated by centrifugation at 120,000 × g for 1 hr at 4°C. The pellets were collected as OM and IM fractions, respectively. Supernatants were concentrated using Centricon 10K and Microcon 10K centrifugal filters (Millipore) and collected as IMS and MA fractions, respectively. Equal protein from whole cell lysates or subcellular/submitochondrial fractions was immunoblotted.

Antibodies used. p53 (DO-1, FL393 (Santa Cruz Biotechn), CM5, CM1 (Novocastra)) , PCNA, AIF (clone E-1) (Santa Cruz Biotechn), mthsp70 (ABR), Cyclophilin D (Calbiochem and Abcam), COX IV (Molecular Probes), HMGB1(Abcam), cleaved caspase 3 and cleaved PARP(Cell Signaling), cytochrome C (Clone 7H8.2C12, Pharmingen), Smac (Clone FKE02, R&D), Endo G (ProSci), Bax (N-20, Santa Cruz), Bak (Bak-NT, Upstate Biotechn), VDAC (Calbiochem)

Transmission Electron Microscopy (TEM). Isolated mitochondria were fixed for 1 hr at 25°C using EM grade glutaraldehyde dissolved in 120 mM KCl, 10 mM Tris pH 7.6 and 5 mM KH2PO4 at a final concentration of 1.25 %. Cells plated on Aclar embedding film precoated with 0.1 % gelatin were fixed with 2.5 % EM grade glutaraldehyde and 2 % paraformaldehyde in 0.1 M phosphate buffer saline (PBS), pH7.4. Samples were placed in 1% osmium tetroxide in 0.1 M PBS pH 7.4, dehydrated in a graded series of ethyl alcohol and embedded in Durcupan resin. Ultrathin sections of 80 nm were cut with a Reichert-Jung UltracutE ultramicrotome and placed on formvar-coated slot copper grids. Sections were counterstained with uranyl acetate and lead

citrate and viewed with a FEI Tecnai12 BioTwinG^2 electron microscope. Digital images were acquired with an AMT XR-60 CCD Digital Camera system at identical settings.

Biochemical assays. For immunoprecipitation, isolated mitochondria or cells were lysed in PBS containing 1% Triton X-100 and protease inhibitors (Roche). After centrifugation at 13,000x g for 10 min at 4ºC, the supernatant was precleared with Protein G-agarose beads (Roche) for 2h at 4ºC, and 500 µg of precleared protein extracts were incubated with antibody to p53 or cypD for 16 h at 4ºC. Precipitated complexes were washed in lysis buffer and bound proteins analyzed by immunoblots. For GST-pull down experiments, bead -bound GST-CypD was blocked with H-buffer (20 mM Hepes pH 7.7, 75 mM KCl, 0.1 mM EDTA, 2.5 mM $MgCl_2$, 0.05% NP40, 1 mM DTT, 1 mg/ml BSA). Blocked beads were incubated with cell/mitochondria lysates or recombinant proteins for 16 h at 4°C in the presence of 5 µM CsA or vehicle. Pelleted beads were washed in H-buffer and bound proteins analyzed by immunoblots. For HA-pull down assays, HA-antibody (Abcam) was used to precipitate protein complexes from cells expressing HA-tagged CypD, VDAC or ANT.

Cell death assays. Cell viability was assessed by Cell Titer Blue (CTB) assay and Trypan Blue Exclusion assays (Sigma). Apoptosis was measured by the TUNEL Detection Kit TMR Red (Roche). Nuclei were counterstained with 1 mg/ml Hoechst 33342. Apoptosis was quantified as the proportion of red/blue areas from 3 representative images (Zeiss Axioskope, Automatic Measurement Program of AxioVision v4.3).

HMGB1 release assay. Medium from treated cells was harvested, spun at 800x g for 5 min and supernatant filtered (0.45 µm). Proteins were precipitated with trichloroacetic acid. Proteins from cell lysates and cell-free supernatant were analyzed by HMGB1 immunoblots.

Transient Focal Cerebral Ischemia (MCAO). Male 6-8 week old littermate WT, and p53+/- (Sv129) were used for all experiments. Focal cerebral ischemia was induced in anesthetized mice by inserting an intraluminal filament in the middle cerebral artery for 60 min, followed by 24 hrs of reperfusion. During the course of the experiment blood flow and body temperature of the animals were monitored by an experienced investigator (KJ) who was naive to the genetic identity of individual mice. Mock injured animals were kept under the same conditions. Where indicated, Cyclosporine A (1mg/kg) was administered 15 mins prior to MCAO by intraperitoneal injection. All animal work was done in accordance with Stony Brook University IACUC.

References

1. Gu W, Shi XL, Roeder RG. Synergistic activation of transcription by CBP and p53. *Nature* 1997 Jun 19; 387 (6635): 819-823.

2. Lu H, Levine AJ. Human TAFII31 protein is a transcriptional coactivator of the p53 protein. *Proc Natl Acad Sci U S A* 1995 May 23; 92 (11): 5154-5158.

3. Kussie PH, Gorina S, Marechal V, Elenbaas B, Moreau J, Levine AJ, *et al.* Structure of the MDM2 oncoprotein bound to the p53 tumor suppressor transactivation domain. *Science* 1996 Nov 8; 274 (5289): 948-953.

4. Toledo F, Wahl GM. Regulating the p53 pathway: in vitro hypotheses, in vivo veritas. *Nat Rev Cancer* 2006 Dec; 6 (12): 909-923.

5. Toledo F, Lee CJ, Krummel KA, Rodewald LW, Liu CW, Wahl GM. Mouse mutants reveal that putative protein interaction sites in the p53 proline-rich domain are dispensable for tumor suppression. *Mol Cell Biol* 2007 Feb; 27 (4): 1425-1432.

6. Mihara M, Erster S, Zaika A, Petrenko O, Chittenden T, Pancoska P, *et al.* p53 has a direct apoptogenic role at the mitochondria. *Mol Cell* 2003; 11: 577-590.

7. Symonds H, Krall L, Remington L, Saenz-Robles M, Lowe S, Jacks T, *et al.* p53-dependent apoptosis suppresses tumor growth and progression in vivo. *Cell* 1994 Aug 26; 78 (4): 703-711.

8. Schmitt CA, Fridman JS, Yang M, Baranov E, Hoffman RM, Lowe SW. Dissecting p53 tumor suppressor functions in vivo. *Cancer Cell* 2002 Apr; 1 (3): 289-298.

9. Miyashita T, Reed JC. Tumor suppressor p53 is a direct transcriptional activator of the human bax gene. *Cell* 1995 Jan 27; 80 (2): 293-299.

10. Yin C, Knudson CM, Korsmeyer SJ, Van Dyke T. Bax suppresses tumorigenesis and stimulates apoptosis in vivo. *Nature* 1997 Feb 13; 385 (6617): 637-640.

11. Zhang L, Yu J, Park BH, Kinzler KW, Vogelstein B. Role of BAX in the apoptotic response to anticancer agents. *Science* 2000 Nov 3; 290 (5493): 989-992.

12. Knudson CM, Tung KS, Tourtellotte WG, Brown GA, Korsmeyer SJ. Bax-deficient mice with lymphoid hyperplasia and male germ cell death. *Science* 1995 Oct 6; 270 (5233): 96-99.

13. Yu J, Zhang L, Hwang PM, Kinzler KW, Vogelstein B. PUMA induces the rapid apoptosis of colorectal cancer cells. *Mol Cell* 2001 Mar; 7 (3): 673-682.

14. Han J, Flemington C, Houghton AB, Gu Z, Zambetti GP, Lutz RJ, *et al.* Expression of bbc3, a pro-apoptotic BH3-only gene, is regulated by diverse cell death and survival signals. *Proc Natl Acad Sci U S A* 2001 Sep 25; 98 (20): 11318-11323.

15. Oda E, Ohki R, Murasawa H, Nemoto J, Shibue T, Yamashita T, *et al.* Noxa, a BH3-only member of the Bcl-2 family and candidate mediator of p53-induced apoptosis. *Science* 2000 May 12; 288 (5468): 1053-1058.

16. Yu J, Zhang L. No PUMA, no death: implications for p53-dependent apoptosis. *Cancer Cell* 2003 Oct; 4 (4): 248-249.

17. Jeffers JR, Parganas E, Lee Y, Yang C, Wang J, Brennan J, *et al.* Puma is an essential mediator of p53-dependent and -independent apoptotic pathways. *Cancer Cell* 2003 Oct; 4 (4): 321-328.

18. Villunger A ME, Coultas L, Mullauer F, Bock G, Ausserlechner MJ, Adams JM, Strasser A. p53- and Drug-Induced Apoptotic Responses Mediated by BH3-Only Proteins Puma and Noxa. *Science* 2003 Aug; 4(8):717.

19. Michalak E, Villunger A, Erlacher M, Strasser A. Death squads enlisted by the tumour suppressor p53. *Biochem Biophys Res Commun* 2005 Jun 10; 331 (3): 786-798.

20. Liu G, Parant JM, Lang G, Chau P, Chavez-Reyes A, El-Naggar AK, *et al.* Chromosome stability, in the absence of apoptosis, is critical for suppression of tumorigenesis in Trp53 mutant mice. *Nat Genet* 2004 Jan; 36 (1): 63-68.

21. Barboza JA, Liu G, Ju Z, El-Naggar AK, Lozano G. p21 delays tumor onset by preservation of chromosomal stability. *Proc Natl Acad Sci U S A* 2006 Dec 26; 103 (52): 19842-19847.

22. Waldman T, Kinzler KW, Vogelstein B. p21 is necessary for the p53-mediated G1 arrest in human cancer cells. *Cancer Res* 1995 Nov 15; 55 (22): 5187-5190.

23. el-Deiry WS. Regulation of p53 downstream genes. *Semin Cancer Biol* 1998; 8 (5): 345-357.

24. Xue W, Zender L, Miething C, Dickins RA, Hernando E, Krizhanovsky V, *et al.* Senescence and tumour clearance is triggered by p53 restoration in murine liver carcinomas. *Nature* 2007 Feb 8; 445 (7128): 656-660.

25. Ventura A, Kirsch DG, McLaughlin ME, Tuveson DA, Grimm J, Lintault L, *et al.* Restoration of p53 function leads to tumour regression in vivo. *Nature* 2007 Feb 8; 445 (7128): 661-665.

26. Leal JF, Fominaya J, Cascon A, Guijarro MV, Blanco-Aparicio C, Lleonart M, *et al.* Cellular senescence bypass screen identifies new putative tumor suppressor genes. *Oncogene* 2008 Mar 27; 27 (14): 1961-1970.

27. Brown JP, Wei W, Sedivy JM. Bypass of senescence after disruption of p21CIP1/WAF1 gene in normal diploid human fibroblasts. *Science* 1997 Aug 8; 277 (5327): 831-834.

28. Budanov AV. Stress-Responsive Sestrins Link p53 with Redox Regulation and Mammalian Target of Rapamycin Signaling. *Antioxid Redox Signal* 2011 Sep 15; 15 (6): 1679-1690.

29. Crighton D, Wilkinson S, O'Prey J, Syed N, Smith P, Harrison PR, *et al.* DRAM, a p53-induced modulator of autophagy, is critical for apoptosis. *Cell* 2006 Jul 14; 126 (1): 121-134.

30. Vousden KH, Ryan KM. p53 and metabolism. *Nat Rev Cancer* 2009 Oct; 9 (10): 691-700.

31. Kawauchi K, Araki K, Tobiume K, Tanaka N. p53 regulates glucose metabolism through an IKK-NF-kappaB pathway and inhibits cell transformation. *Nat Cell Biol* 2008 May; 10 (5): 611-618.

32. Teodoro JG, Evans SK, Green MR. Inhibition of tumor angiogenesis by p53: a new role for the guardian of the genome. *J Mol Med (Berl)* 2007 Nov; 85 (11): 1175-1186.

33. Tanaka H, Arakawa H, Yamaguchi T, Shiraishi K, Fukuda S, Matsui K, *et al.* A ribonucleotide reductase gene involved in a p53-dependent cell-cycle checkpoint for DNA damage. *Nature* 2000 Mar 2; 404 (6773): 42-49.

34. Meletis K, Wirta V, Hede SM, Nister M, Lundeberg J, Frisen J. p53 suppresses the self-renewal of adult neural stem cells. *Development* 2006 Jan; 133 (2): 363-369.

35. Liu Y, Elf SE, Miyata Y, Sashida G, Huang G, Di Giandomenico S, *et al.* p53 regulates hematopoietic stem cell quiescence. *Cell Stem Cell* 2009 Jan 9; 4 (1): 37-48.

36. Godar S, Ince TA, Bell GW, Feldser D, Donaher JL, Bergh J, *et al.* Growth-inhibitory and tumor- suppressive functions of p53 depend on its repression of CD44 expression. *Cell* 2008 Jul 11; 134 (1): 62-73.

37. Hu W, Feng Z, Teresky AK, Levine AJ. p53 regulates maternal reproduction through LIF. *Nature* 2007 Nov 29; 450 (7170): 721-724.

38. Wade M, Wang YV, Wahl GM. The p53 orchestra: Mdm2 and Mdmx set the tone. *Trends Cell Biol* 2010 May; 20 (5): 299-309.

39. Levine AJ, Hu W, Feng Z. The P53 pathway: what questions remain to be explored? *Cell Death Differ* 2006 Jun; 13 (6): 1027-1036.

40. Kroemer G, Galluzzi L, Brenner C. Mitochondrial membrane permeabilization in cell death. *Physiol Rev* 2007 Jan; 87 (1): 99-163.

41. Kokoszka JE, Waymire KG, Levy SE, Sligh JE, Cai J, Jones DP, *et al.* The ADP/ATP translocator is not essential for the mitochondrial permeability transition pore. *Nature* 2004 Jan 29; 427 (6973): 461-465.

42. Halestrap AP. Mitochondrial permeability: dual role for the ADP/ATP translocator? *Nature* 2004 Aug 26; 430 (7003): 1 p following 983.

43. Baines CP, Kaiser RA, Sheiko T, Craigen WJ, Molkentin JD. Voltage-dependent anion channels are dispensable for mitochondrial-dependent cell death. *Nat Cell Biol* 2007 May; 9 (5): 550-555.

44. Baines CP, Kaiser RA, Purcell NH, Blair NS, Osinska H, Hambleton MA, *et al.* Loss of cyclophilin D reveals a critical role for mitochondrial permeability transition in cell death. *Nature* 2005 Mar 31; 434 (7033): 658-662.

45. Nakagawa T, Shimizu S, Watanabe T, Yamaguchi O, Otsu K, Yamagata H, *et al.* Cyclophilin D-dependent mitochondrial permeability transition regulates some necrotic but not apoptotic cell death. *Nature* 2005 Mar 31; 434 (7033): 652-658.

46. Schinzel AC, Takeuchi O, Huang Z, Fisher JK, Zhou Z, Rubens J, *et al.* Cyclophilin D is a component of mitochondrial permeability transition and mediates neuronal cell death after focal cerebral ischemia. *Proc Natl Acad Sci U S A* 2005 Aug 23; 102 (34): 12005-12010.

47. Basso E, Fante L, Fowlkes J, Petronilli V, Forte MA, Bernardi P. Properties of the permeability transition pore in mitochondria devoid of Cyclophilin D. *J Biol Chem* 2005 May 13; 280 (19): 18558-18561.

48. Caelles C, Helmberg A, Karin M. p53-dependent apoptosis in the absence of transcriptional activation of p53-target genes. *Nature* 1994 Jul 21; 370 (6486): 220-223.

49. Haupt Y, Rowan S, Shaulian E, Vousden KH, Oren M. Induction of apoptosis in HeLa cells by trans-activation-deficient p53. *Genes Dev* 1995 Sep 1; 9: 2170-2183.

50. Ding HF, McGill G, Rowan S, Schmaltz C, Shimamura A, Fisher DE. Oncogene-dependent regulation of caspase activation by p53 protein in a cell-free system. *J Biol Chem* 1998 Oct 23; 273 (43): 28378-28383.

51. Gottlieb E, Oren M. p53 facilitates pRb cleavage in IL-3-deprived cells: novel pro-apoptotic activity of p53. *Embo J* 1998 Jul 1; 17 (13): 3587-3596.

52. Marchenko ND, Zaika A, Moll UM. Death signal-induced localization of p53 protein to mitochondria. A potential role in apoptotic signaling. *J Biol Chem* 2000 May 26; 275: 16202-16212.

53. Arima Y, Nitta M, Kuninaka S, Zhang D, Fujiwara T, Taya Y, *et al.* Transcriptional blockade induces p53-dependent apoptosis associated with translocation of p53 to mitochondria. *J Biol Chem* 2005 May 13; 280 (19): 19166-19176.

54. Moll UM, Marchenko N, Zhang XK. p53 and Nur77/TR3 - transcription factors that directly target mitochondria for cell death induction. *Oncogene* 2006 Aug 7; 25 (34): 4725-4743.

55. Sansome C, Zaika A, Marchenko ND, Moll UM. Hypoxia death stimulus induces translocation of p53 protein to mitochondria. Detection by immunofluorescence on whole cells. *FEBS Lett* 2001 Jan 19; 488: 110-115.

56. Tomita Y, Marchenko N, Erster S, Nemajerova A, Dehner A, Klein C, *et al.* WT p53, but not tumor-derived mutants, bind to Bcl2 via the DNA binding domain and induce mitochondrial permeabilization. *J Biol Chem* 2006 Mar 31; 281 (13): 8600-8606.

57. Chipuk JE, Kuwana T, Bouchier-Hayes L, Droin NM, Newmeyer DD, Schuler M, *et al.* Direct activation of Bax by p53 mediates mitochondrial membrane permeabilization and apoptosis. *Science* 2004 Feb 13; 303 (5660): 1010-1014.

58. Sot B, Freund SM, Fersht AR. Comparative biophysical characterization of p53 with the pro-apoptotic bak and the anti-apoptotic BCL-XL. *J Biol Chem* 2007 Oct 5;282(40):29193-200

59. Leu JI, Dumont P, Hafey M, Murphy ME, George DL. Mitochondrial p53 activates Bak and causes disruption of a Bak-Mcl1 complex. *Nat Cell Biol* 2004 May; 6 (5): 443-450.

60. Pietsch EC, Perchiniak E, Canutescu AA, Wang G, Dunbrack RL, Murphy ME. Oligomerization of BAK by p53 utilizes conserved residues of the p53 DNA binding domain. *J Biol Chem* 2008 Jul 25; 283 (30): 21294-21304.

61. Nemajerova A, Erster S, Moll UM. The post-translational phosphorylation and acetylation modification profile is not the determining factor in targeting endogenous stress-induced p53 to mitochondria. *Cell Death Differ* 2005 Feb; 12 (2): 197-200.

62. Haglund K, Di Fiore PP, Dikic I. Distinct monoubiquitin signals in receptor endocytosis. *Trends Biochem Sci* 2003 Nov; 28 (11): 598-603.

63. Sigismund S, Polo S, Di Fiore PP. Signaling through monoubiquitination. *Curr Top Microbiol Immunol* 2004; 286: 149-185.

64. Thrower JS, Hoffman L, Rechsteiner M, Pickart CM. Recognition of the polyubiquitin proteolytic signal. *Embo J* 2000 Jan 4; 19 (1): 94-102.

65. Marchenko ND, Wolff S, Erster S, Becker K, Moll UM. Monoubiquitylation promotes mitochondrial p53 translocation. *Embo J* 2007 Feb 21; 26 (4): 923-934.

66. Marchenko ND, Moll UM. The role of ubiquitination in the direct mitochondrial death program of p53. *Cell Cycle* 2007 May; 6 (14): 1718-1723.

67. Erster S, Mihara M, Kim RH, Petrenko O, Moll UM. In vivo mitochondrial p53 translocation triggers a rapid first wave of cell death in response to DNA damage that can precede p53 target gene activation. *Mol Cell Biol* 2004 Aug; 24 (15): 6728-6741.

68. Endo H, Kamada H, Nito C, Nishi T, Chan PH. Mitochondrial translocation of p53 mediates release of cytochrome c and hippocampal CA1 neuronal death after transient global cerebral ischemia in rats. *J Neurosci* 2006 Jul 26; 26 (30): 7974-7983.

69. Endo H, Saito A, Chan PH. Mitochondrial translocation of p53 underlies the selective death of hippocampal CA1 neurons after global cerebral ischaemia. *Biochem Soc Trans* 2006 Dec; 34 (Pt 6): 1283-1286.

70. Bonini P, Cicconi S, Cardinale A, Vitale C, Serafino AL, Ciotti MT, *et al.* Oxidative stress induces p53-mediated apoptosis in glia: p53 transcription-independent way to die. *J Neurosci Res* 2004 Jan 1; 75 (1): 83-95.

71. Racay P, Tatarkova Z, Drgova A, Kaplan P, Dobrota D. Effect of ischemic preconditioning on mitochondrial dysfunction and mitochondrial p53 translocation after transient global cerebral ischemia in rats. *Neurochem Res* 2007 Nov; 32 (11): 1823-1832.

72. Crumrine RC, Thomas AL, Morgan PF. Attenuation of p53 expression protects against focal ischemic damage in transgenic mice. *J Cereb Blood Flow Metab* 1994 Nov; 14 (6): 887-891.

73. Yonekura I, Takai K, Asai A, Kawahara N, Kirino T. p53 potentiates hippocampal neuronal death caused by global ischemia. *J Cereb Blood Flow Metab* 2006 Oct; 26 (10): 1332-1340.

74. Maeda K, Hata R, Gillardon F, Hossmann KA. Aggravation of brain injury after transient focal ischemia in p53-deficient mice. *Brain Res Mol Brain Res* 2001 Mar 31; 88 (1-2): 54-61.

75. Dagher PC. Apoptosis in ischemic renal injury: roles of GTP depletion and p53. *Kidney Int* 2004 Aug; 66 (2): 506-509.

76. Kelly KJ, Plotkin Z, Vulgamott SL, Dagher PC. P53 mediates the apoptotic response to GTP depletion after renal ischemia-reperfusion: protective role of a p53 inhibitor. *J Am Soc Nephrol* 2003 Jan; 14 (1): 128-138.

77. Leu JI, George DL. Hepatic IGFBP1 is a prosurvival factor that binds to BAK, protects the liver from apoptosis, and antagonizes the proapoptotic actions of p53 at mitochondria. *Genes Dev* 2007 Dec 1; 21 (23): 3095-3109.

78. Martins CP, Brown-Swigart L, Evan GI. Modeling the therapeutic efficacy of p53 restoration in tumors. *Cell* 2006 Dec 29; 127 (7): 1323-1334.

79. Lim DS, Bae SM, Kwak SY, Park EK, Kim JK, Han SJ, *et al.* Adenovirus-Mediated p53 Treatment Enhances Photodynamic Antitumor Response. *Hum Gene Ther* 2006 Mar; 17(3):347-52

80. Peng Z. Current status of gendicine in China: recombinant human Ad-p53 agent for treatment of cancers. *Hum Gene Ther* 2005 Sep; 16 (9): 1016-1027.

81. Roth JA. Adenovirus p53 gene therapy. *Expert Opin Biol Ther* 2006 Jan; 6 (1): 55-61.

82. Sauthoff H, Pipiya T, Chen S, Heitner S, Cheng J, Huang YQ, *et al.* Modification of the p53 transgene of a replication-competent adenovirus prevents mdm2- and E1b-55kD-mediated degradation of p53. *Cancer Gene Ther* 2006 Jul;13(7):686-95

83. Yin S, Goodrich DW. Combination gene therapy with p53 and Thoc1/p84 is more effective than either single agent in an animal model of human pancreatic adenocarcinoma. *Int J Oncol* 2006 Mar; 28 (3): 781-785.

84. Carvajal D, Tovar C, Yang H, Vu BT, Heimbrook DC, Vassilev LT. Activation of p53 by MDM2 antagonists can protect proliferating cells from mitotic inhibitors. *Cancer Res* 2005 Mar 1; 65 (5): 1918-1924.

85. Vassilev LT. Small-molecule antagonists of p53-MDM2 binding: research tools and potential therapeutics. *Cell Cycle* 2004 Apr; 3 (4): 419-421.

86. Vassilev LT, Vu BT, Graves B, Carvajal D, Podlaski F, Filipovic Z, *et al.* In vivo activation of the p53 pathway by small-molecule antagonists of MDM2. *Science* 2004 Feb 6; 303 (5659): 844-848.

87. Saha MN, Micallef J, Qiu L, Chang H. Pharmacological activation of the p53 pathway in haematological malignancies. *J Clin Pathol* 2010 Mar; 63 (3): 204-209.

88. Vassilev LT. MDM2 inhibitors for cancer therapy. *Trends Mol Med* 2007 Jan; 13 (1): 23-31.

89. Tovar C, Rosinski J, Filipovic Z, Higgins B, Kolinsky K, Hilton H, *et al.* Small-molecule MDM2 antagonists reveal aberrant p53 signaling in cancer: implications for therapy. *Proc Natl Acad Sci U S A* 2006 Feb 7; 103 (6): 1888-1893.

90. Huang B, Deo D, Xia M, Vassilev LT. Pharmacologic p53 activation blocks cell cycle progression but fails to induce senescence in epithelial cancer cells. *Mol Cancer Res* 2009 Sep; 7 (9): 1497-1509.

91. Demidenko ZN, Korotchkina LG, Gudkov AV, Blagosklonny MV. Paradoxical suppression of cellular senescence by p53. *Proc Natl Acad Sci U S A* 2010 May 25; 107 (21): 9660-9664.

92. Wade M, Wong ET, Tang M, Stommel JM, Wahl GM. Hdmx modulates the outcome of p53 activation in human tumor cells. *J Biol Chem* 2006 Nov 3; 281 (44): 33036-33044.

93. Hu B, Gilkes DM, Farooqi B, Sebti SM, Chen J. MDMX overexpression prevents p53 activation by the MDM2 inhibitor Nutlin. *J Biol Chem* 2006 Nov 3; 281 (44): 33030-33035.

94. Patton JT, Mayo LD, Singhi AD, Gudkov AV, Stark GR, Jackson MW. Levels of HdmX expression dictate the sensitivity of normal and transformed cells to Nutlin-3. *Cancer Res* 2006 Mar 15; 66 (6): 3169-3176.

95. Laurie NA, Shih CS, Dyer MA. Targeting MDM2 and MDMX in retinoblastoma. *Curr Cancer Drug Targets* 2007 Nov; 7 (7): 689-695.

96. Hu B, Gilkes DM, Chen J. Efficient p53 activation and apoptosis by simultaneous disruption of binding to MDM2 and MDMX. *Cancer Res* 2007 Sep 15; 67 (18): 8810-8817.

97. Xia M, Knezevic D, Tovar C, Huang B, Heimbrook DC, Vassilev LT. Elevated MDM2 boosts the apoptotic activity of p53-MDM2 binding inhibitors by facilitating MDMX degradation. *Cell Cycle* 2008 Jun 1; 7 (11): 1604-1612.

98. Kojima K, Konopleva M, McQueen T, O'Brien S, Plunkett W, Andreeff M. Mdm2 inhibitor Nutlin-3a induces p53-mediated apoptosis by transcription-dependent and transcription-independent mechanisms and may overcome Atm-mediated resistance to fludarabine in chronic lymphocytic leukemia. *Blood* 2006 Aug 1; 108 (3): 993-1000.

99. Steele AJ, Prentice AG, Hoffbrand AV, Yogashangary BC, Hart SM, Nacheva EP, *et al.* p53-mediated apoptosis of CLL cells: evidence for a transcription-independent mechanism. *Blood* 2008 Nov 1; 112 (9): 3827-3834.

100. Strom E, Sathe S, Komarov PG, Chernova OB, Pavlovska I, Shyshynova I, *et al.* Small-molecule inhibitor of p53 binding to mitochondria protects mice from gamma radiation. *Nat Chem Biol* 2006 Sep; 2 (9): 474-479.

101. Komarov PG, Komarova EA, Kondratov RV, Christov-Tselkov K, Coon JS, Chernov MV, *et al.* A chemical inhibitor of p53 that protects mice from the side effects of cancer therapy. *Science* 1999 Sep 10; 285 (5434): 1733-1737.

102. Whitesell L, Sutphin PD, Pulcini EJ, Martinez JD, Cook PH. The physical association of multiple molecular chaperone proteins with mutant p53 is altered by geldanamycin, an hsp90-binding agent. *Mol Cell Biol* 1998 Mar; 18 (3): 1517-1524.

103. Walerych D, Kudla G, Gutkowska M, Wawrzynow B, Muller L, King FW, *et al.* Hsp90 chaperones wild-type p53 tumor suppressor protein. *J Biol Chem* 2004 Nov 19; 279 (47): 48836-48845.

104. Wang C, Chen J. Phosphorylation and hsp90 binding mediate heat shock stabilization of p53. *J Biol Chem* 2003 Jan 17; 278 (3): 2066-2071.

105. Muller L, Schaupp A, Walerych D, Wegele H, Buchner J. Hsp90 regulates the activity of wild type p53 under physiological and elevated temperatures. *J Biol Chem* 2004 Nov 19; 279 (47): 48846-48854.

106. Blagosklonny MV, Toretsky J, Bohen S, Neckers L. Mutant conformation of p53 translated in vitro or in vivo requires functional HSP90. *Proc Natl Acad Sci U S A* 1996 Aug 6; 93 (16): 8379-8383.

107. Peng Y, Chen L, Li C, Lu W, Chen J. Inhibition of MDM2 by hsp90 contributes to mutant p53 stabilization. *J Biol Chem* 2001 Nov 2; 276 (44): 40583-40590.

108. Sasaki M, Nie L, Maki CG. MDM2 binding induces a conformational change in p53 that is opposed by heat-shock protein 90 and precedes p53 proteasomal degradation. *J Biol Chem* 2007 May 11; 282 (19): 14626-14634.

109. Lin K, Rockliffe N, Johnson GG, Sherrington PD, Pettitt AR. Hsp90 inhibition has opposing effects on wild-type and mutant p53 and induces p21 expression and cytotoxicity irrespective of p53/ATM status in chronic lymphocytic leukaemia cells. *Oncogene* 2008 Apr 10; 27 (17): 2445-2455.

110. Ayrault O, Godeny MD, Dillon C, Zindy F, Fitzgerald P, Roussel MF, *et al.* Inhibition of Hsp90 via 17-DMAG induces apoptosis in a p53-dependent manner to prevent medulloblastoma. *Proc Natl Acad Sci U S A* 2009 Oct 6; 106 (40): 17037-17042.

111. Chou TC. Drug combination studies and their synergy quantification using the Chou-Talalay method. *Cancer Res* 2010 Jan 15; 70 (2): 440-446.

112. Chen X, Ko LJ, Jayaraman L, Prives C. p53 levels, functional domains, and DNA damage determine the extent of the apoptotic response of tumor cells. *Genes Dev* 1996 Oct 1; 10 (19): 2438-2451.

113. Whitesell L, Lindquist SL. HSP90 and the chaperoning of cancer. *Nat Rev Cancer* 2005 Oct; 5 (10): 761-772.

114. Neckers L. Hsp90 inhibitors as novel cancer chemotherapeutic agents. *Trends Mol Med* 2002; 8 (4 Suppl): S55-61.

115. Kamal A, Boehm MF, Burrows FJ. Therapeutic and diagnostic implications of Hsp90 activation. *Trends Mol Med* 2004 Jun; 10 (6): 283-290.

116. Kamal A, Burrows FJ. Hsp90 inhibitors as selective anticancer drugs. *Discov Med* 2004 Oct; 4 (23): 277-280.

117. Kojima K, Konopleva M, Samudio IJ, Ruvolo V, Andreeff M. Mitogen-activated protein kinase kinase inhibition enhances nuclear proapoptotic function of p53 in acute myelogenous leukemia cells. *Cancer Res* 2007 Apr 1; 67 (7): 3210-3219.

118. Zhang W, Konopleva M, Burks JK, Dywer KC, Schober WD, Yang JY, *et al.* Blockade of mitogen-activated protein kinase/extracellular signal-regulated kinase kinase and murine double minute synergistically induces Apoptosis in acute myeloid leukemia via BH3-only proteins Puma and Bim. *Cancer Res* 2010 Mar 15; 70 (6): 2424-2434.

119. Wolff S, Erster S, Palacios G, Moll UM. p53's mitochondrial translocation and MOMP action is independent of Puma and Bax and severely disrupts mitochondrial membrane integrity. *Cell Res* 2008 Jul; 18 (7): 733-744.

120. Kim H, Rafiuddin-Shah M, Tu HC, Jeffers JR, Zambetti GP, Hsieh JJ, *et al.* Hierarchical regulation of mitochondrion-dependent apoptosis by BCL-2 subfamilies. *Nat Cell Biol* 2006 Dec; 8 (12): 1348-1358.

121. Kuwana T, Bouchier-Hayes L, Chipuk JE, Bonzon C, Sullivan BA, Green DR, *et al.* BH3 domains of BH3-only proteins differentially regulate Bax-mediated mitochondrial membrane permeabilization both directly and indirectly. *Mol Cell* 2005 Feb 18; 17 (4): 525-535.

122. Petronilli V, Miotto G, Canton M, Colonna R, Bernardi P, Di Lisa F. Imaging the mitochondrial permeability transition pore in intact cells. *Biofactors* 1998; 8 (3-4): 263-272.

123. Vaseva AV, Moll UM. The mitochondrial p53 pathway. *Biochim Biophys Acta* 2009 May; 1787 (5): 414-420.

124. Halestrap AP. Calcium, mitochondria and reperfusion injury: a pore way to die. *Biochem Soc Trans* 2006 Apr; 34 (Pt 2): 232-237.

125. Gudkov AV, Komarova EA. Pathologies associated with the p53 response. *Cold Spring Harb Perspect Biol* 2010 Jul; 2 (7): a001180.

126. Pietsch EC, Leu JI, Frank A, Dumont P, George DL, Murphy ME. The tetramerization domain of p53 is required for efficient BAK oligomerization. *Cancer Biol Ther* 2007 Oct; 6 (10): 1576-1583.

127. Heyne K, Schmitt K, Mueller D, Armbruester V, Mestres P, Roemer K. Resistance of mitochondrial p53 to dominant inhibition. *Mol Cancer* 2008 Jun 12; 7: 54.

128. Sansome C, Zaika A, Marchenko ND, Moll UM. Hypoxia death stimulus induces translocation of p53 protein to mitochondria. Detection by immunofluorescence on whole cells. *FEBS Lett* 2001 Jan 19; 488 (3): 110-115.

129. Javadov S, Karmazyn M. Mitochondrial permeability transition pore opening as an endpoint to initiate cell death and as a putative target for cardioprotection. *Cell Physiol Biochem* 2007; 20 (1-4): 1-22.

130. Machida K, Ohta Y, Osada H. Suppression of apoptosis by cyclophilin D via stabilization of hexokinase II mitochondrial binding in cancer cells. *J Biol Chem* 2006 May 19; 281 (20): 14314-14320.

131. Li Y, Johnson N, Capano M, Edwards M, Crompton M. Cyclophilin-D promotes the mitochondrial permeability transition but has opposite effects on apoptosis and necrosis. *Biochem J* 2004 Oct 1; 383 (Pt 1): 101-109.

132. Eliseev RA, Malecki J, Lester T, Zhang Y, Humphrey J, Gunter TE. Cyclophilin D interacts with Bcl2 and exerts an anti-apoptotic effect. *J Biol Chem* 2009 Apr 10; 284 (15): 9692-9699.

133. Bianchi ME, Manfredi A. Chromatin and cell death. *Biochim Biophys Acta* 2004 Mar 15; 1677 (1-3): 181-186.

134. Gomez Sarosi LA, Rieber MS, Rieber M. Hydrogen peroxide increases a 55-kDa tyrosinase concomitantly with induction of p53-dependent p21 waf1 expression and a greater Bax/Bcl-2 ratio in pigmented melanoma. *Biochem Biophys Res Commun* 2003 Dec 12; 312 (2): 355-359.

135. Sablina AA, Budanov AV, Ilyinskaya GV, Agapova LS, Kravchenko JE, Chumakov PM. The antioxidant function of the p53 tumor suppressor. *Nat Med* 2005 Dec; 11 (12): 1306-1313.

136. Macip S, Igarashi M, Berggren P, Yu J, Lee SW, Aaronson SA. Influence of induced reactive oxygen species in p53-mediated cell fate decisions. *Mol Cell Biol* 2003 Dec; 23 (23): 8576-8585.

137. Hussain SP, Amstad P, He P, Robles A, Lupold S, Kaneko I, *et al.* p53-induced up-regulation of MnSOD and GPx but not catalase increases oxidative stress and apoptosis. *Cancer Res* 2004 Apr 1; 64 (7): 2350-2356.

138. Wei MC, Zong WX, Cheng EH, Lindsten T, Panoutsakopoulou V, Ross AJ, *et al.* Proapoptotic BAX and BAK: a requisite gateway to mitochondrial dysfunction and death. *Science* 2001 Apr 27; 292 (5517): 727-730.

139. Ruiz-Vela A, Opferman JT, Cheng EH, Korsmeyer SJ. Proapoptotic BAX and BAK control multiple initiator caspases. *EMBO Rep* 2005 Apr; 6 (4): 379-385.

140. Secchiero P, Barbarotto E, Tiribelli M, Zerbinati C, di Iasio MG, Gonelli A, *et al.* Functional integrity of the p53-mediated apoptotic pathway induced by the nongenotoxic agent nutlin-3 in B-cell chronic lymphocytic leukemia (B-CLL). *Blood* 2006 May 15; 107 (10): 4122-4129.

141. Gu L, Zhu N, Findley HW, Zhou M. MDM2 antagonist nutlin-3 is a potent inducer of apoptosis in pediatric acute lymphoblastic leukemia cells with wild-type p53 and overexpression of MDM2. *Leukemia* 2008 Apr; 22 (4): 730-739.

142. Coll-Mulet L, Iglesias-Serret D, Santidrian AF, Cosialls AM, de Frias M, Castano E, *et al.* MDM2 antagonists activate p53 and synergize with genotoxic drugs in B-cell chronic lymphocytic leukemia cells. *Blood* 2006 May 15; 107 (10): 4109-4114.

143. Kojima K, Konopleva M, Samudio IJ, Shikami M, Cabreira-Hansen M, McQueen T, *et al.* MDM2 antagonists induce p53-dependent apoptosis in AML: implications for leukemia therapy. *Blood* 2005 Nov 1; 106 (9): 3150-3159.

144. Becker K, Marchenko ND, Maurice M, Moll UM. Hyperubiquitylation of wild-type p53 contributes to cytoplasmic sequestration in neuroblastoma. *Cell Death Differ* 2007 Jul; 14 (7): 1350-1360.

145. Barbieri E, Mehta P, Chen Z, Zhang L, Slack A, Berg S, *et al.* MDM2 inhibition sensitizes neuroblastoma to chemotherapy-induced apoptotic cell death. *Mol Cancer Ther* 2006 Sep; 5 (9): 2358-2365.

146. Van Maerken T, Speleman F, Vermeulen J, Lambertz I, De Clercq S, De Smet E, *et al.* Small-molecule MDM2 antagonists as a new therapy concept for neuroblastoma. *Cancer Res* 2006 Oct 1; 66 (19): 9646-9655.

147. Stuhmer T, Chatterjee M, Hildebrandt M, Herrmann P, Gollasch H, Gerecke C, *et al.* Nongenotoxic activation of the p53 pathway as a therapeutic strategy for multiple myeloma. *Blood* 2005 Nov 15; 106 (10): 3609-3617.

148. Shangary S, Wang S. Small-Molecule Inhibitors of the MDM2-p53 Protein-Protein Interaction to Reactivate p53 Function: A Novel Approach for Cancer Therapy. *Annu Rev Pharmacol Toxicol* 2009;49:223-41.

149. Shangary S, Wang S. Targeting the MDM2-p53 interaction for cancer therapy. *Clin Cancer Res* 2008 Sep 1; 14 (17): 5318-5324.

150. Salmena L, Pandolfi PP. Changing venues for tumour suppression: balancing destruction and localization by monoubiquitylation. *Nat Rev Cancer* 2007 Jun; 7 (6): 409-413.

151. Secchiero P, Melloni E, di Iasio MG, Tiribelli M, Rimondi E, Corallini F, *et al.* Nutlin-3 upregulates the expression of Notch1 in both myeloid and lymphoid leukemic cells, as part of a negative feed-back anti-apoptotic mechanism. *Blood* 2009 Apr 30;113(18):4300-8.

152. Polyak K, Waldman T, He TC, Kinzler KW, Vogelstein B. Genetic determinants of p53-induced apoptosis and growth arrest. *Genes Dev* 1996 Aug 1; 10 (15): 1945-1952.

153. Zhu N, Gu L, Li F, Zhou M. Inhibition of the Akt/survivin pathway synergizes the antileukemia effect of nutlin-3 in acute lymphoblastic leukemia cells. *Mol Cancer Ther* 2008 May; 7 (5): 1101-1109.

154. Zauli G, Voltan R, Bosco R, Melloni E, Marmiroli S, Rigolin GM, *et al.* Dasatinib plus Nutlin-3 shows synergistic anti-leukemic activity in both p53wild-type and p53mutated B chronic lymphocytic leukemias by inhibiting the Akt pathway. *Clin Cancer Res* 2011 Feb 15;17(4):762-70.

155. Stad R, Little NA, Xirodimas DP, Frenk R, van der Eb AJ, Lane DP, *et al.* Mdmx stabilizes p53 and Mdm2 via two distinct mechanisms. *EMBO Rep* 2001 Nov; 2 (11): 1029-1034.

156. Isaacs JS, Xu W, Neckers L. Heat shock protein 90 as a molecular target for cancer therapeutics. *Cancer Cell* 2003 Mar; 3 (3): 213-217.

157. Kamal A, Thao L, Sensintaffar J, Zhang L, Boehm MF, Fritz LC, *et al.* A high-affinity conformation of Hsp90 confers tumour selectivity on Hsp90 inhibitors. *Nature* 2003 Sep 25; 425 (6956): 407-410.

158. Du H, Guo L, Fang F, Chen D, Sosunov AA, McKhann GM, *et al.* Cyclophilin D deficiency attenuates mitochondrial and neuronal perturbation and ameliorates learning and memory in Alzheimer's disease. *Nat Med* 2008 Oct; 14 (10): 1097-1105.

159. Zong WX, Thompson CB. Necrotic death as a cell fate. *Genes Dev* 2006 Jan 1; 20 (1): 1-15.

160. Tu HC, Ren D, Wang GX, Chen DY, Westergard TD, Kim H, *et al.* The p53-cathepsin axis cooperates with ROS to activate programmed necrotic death upon DNA damage. *Proc Natl Acad Sci U S A* 2009 Jan 27; 106 (4): 1093-1098.

161. Chatoo W, Abdouh M, David J, Champagne MP, Ferreira J, Rodier F, *et al.* The polycomb group gene Bmi1 regulates antioxidant defenses in neurons by repressing p53 pro-oxidant activity. *J Neurosci* 2009 Jan 14; 29 (2): 529-542.

162. Tomasevic G, Shamloo M, Israeli D, Wieloch T. Activation of p53 and its target genes p21(WAF1/Cip1) and PAG608/Wig-1 in ischemic preconditioning. *Brain Res Mol Brain Res* 1999 Jul 5; 70 (2): 304-313.

163. Osuga H, Osuga S, Wang F, Fetni R, Hogan MJ, Slack RS, *et al.* Cyclin-dependent kinases as a therapeutic target for stroke. *Proc Natl Acad Sci U S A* 2000 Aug 29; 97 (18): 10254-10259.

164. Korde AS, Pettigrew LC, Craddock SD, Pocernich CB, Waldmeier PC, Maragos WF. Protective effects of NIM811 in transient focal cerebral ischemia suggest involvement of the mitochondrial permeability transition. *J Neurotrauma* 2007 May; 24 (5): 895-908.

165. Khaspekov L, Friberg H, Halestrap A, Viktorov I, Wieloch T. Cyclosporin A and its nonimmunosuppressive analogue N-Me-Val-4-cyclosporin A mitigate glucose/oxygen deprivation-induced damage to rat cultured hippocampal neurons. *Eur J Neurosci* 1999 Sep; 11 (9): 3194-3198.

166. Matsumoto S, Friberg H, Ferrand-Drake M, Wieloch T. Blockade of the mitochondrial permeability transition pore diminishes infarct size in the rat after transient middle cerebral artery occlusion. *J Cereb Blood Flow Metab* 1999 Jul; 19 (7): 736-741.

167. Kang BH, Plescia J, Dohi T, Rosa J, Doxsey SJ, Altieri DC. Regulation of tumor cell mitochondrial homeostasis by an organelle-specific Hsp90 chaperone network. *Cell* 2007 Oct 19; 131 (2): 257-270.

168. Bauer MK, Schubert A, Rocks O, Grimm S. Adenine nucleotide translocase-1, a component of the permeability transition pore, can dominantly induce apoptosis. *J Cell Biol* 1999 Dec 27; 147 (7): 1493-1502.

169. Palacios G, Crawford HC, Vaseva A, Moll UM. Mitochondrially targeted wild-type p53 induces apoptosis in a solid human tumor xenograft model. *Cell Cycle* 2008 Aug 7; 7 (16).

Appendix

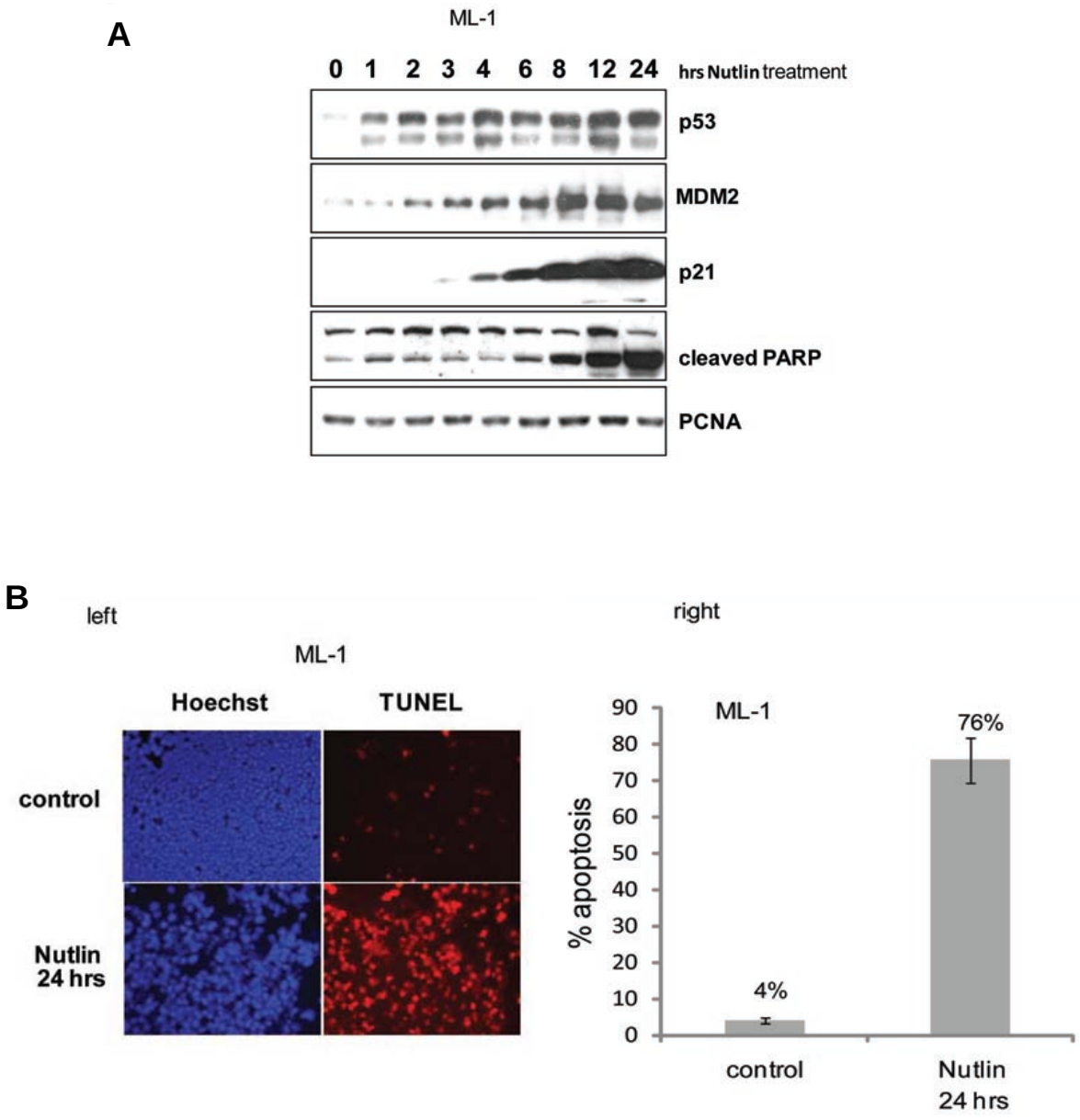

Figure 1. Nutlin stabilizes p53, resulting in induced p53 transcriptional activity and apoptosis in ML-1 cells. (A) ML-1 cells were treated with 10μM Nutlin for the indicated times. Cell lysates were prepared and analyzed by Western blotting using specific antibodies for p53, MDM2, p21, PARP. PCNA was used as a loading control. **(B)** ML-1 cells were treated with 10μM Nutlin for 24 hours and processed for TUNEL staining. *Left*, example of TUNEL staining results of ML-1 cells treated as above. *Right*, chart showing percentage apoptosis obtained from the TUNEL assays above; error bars represent the average of 3 different fields from one TUNEL assay.

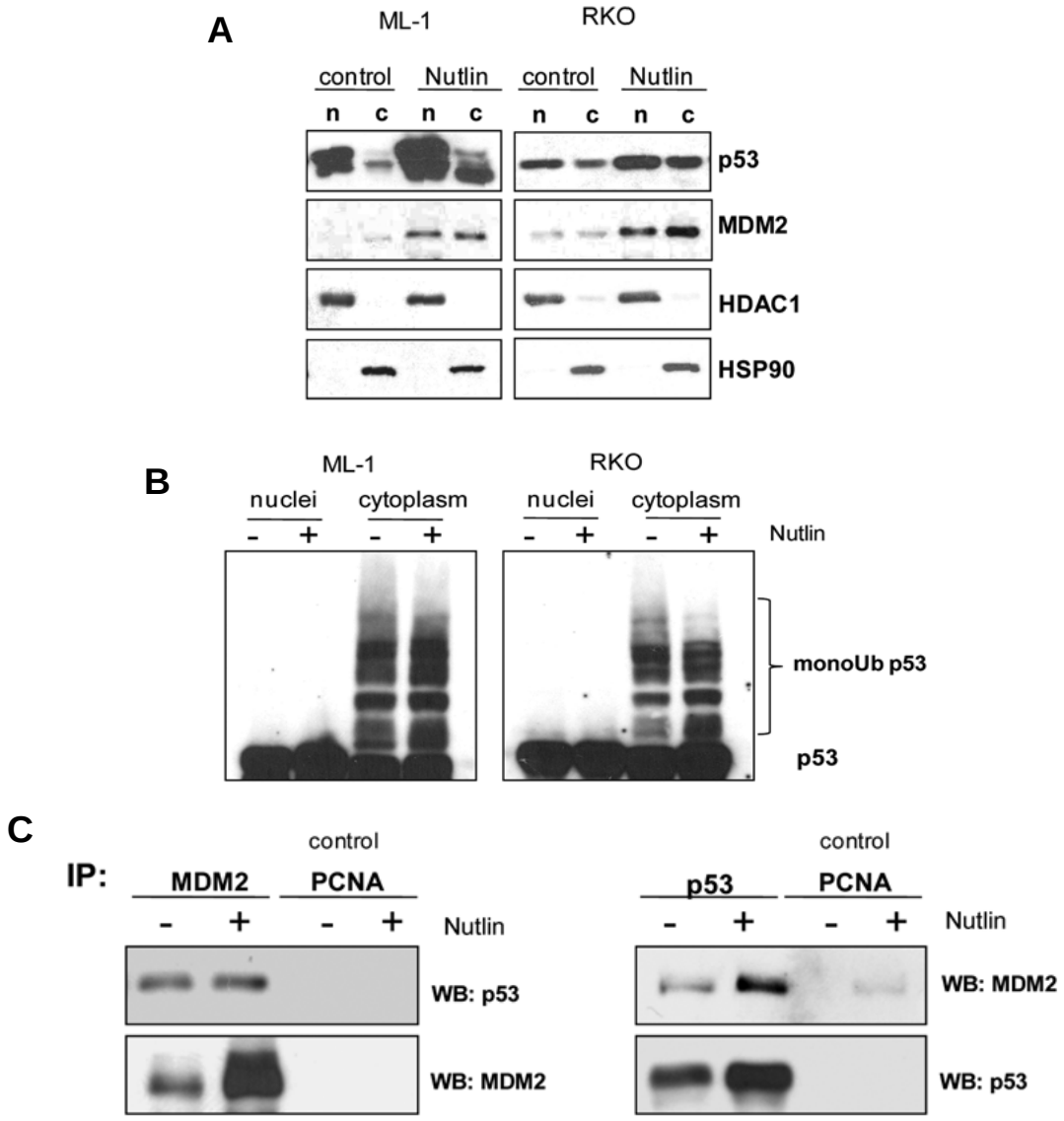

Figure 2. Nutlin stabilizes p53 protein levels in both nucleus and cytoplasm, does not prevent mono-ubiquitination of p53 and disrupts partially the p53-MDM2 complex formation. (A) Stabilization of p53 protein levels and induction of MDM2 in both nucleus and cytoplasm in ML-1 and RKO cell lines upon Nutlin treatment. 6 hours after 10μM Nutlin treatment nuclear (n) and cytoplasmic (c) fractions were prepared as described in materials and methods and analyzed by Western blotting. HDAC1 serves as a nuclear marker, Hsp90 serves as a cytoplasmic marker. **(B)** Nutlin does not prevent mono-ubiquitination of p53. From the experiment described in (A) equal amounts of p53 protein were loaded for Western blotting. The multiple bands above p53 protein band represent mono-ubiquitinated species of p53**. (C)** Nutlin disrupts partially the formation of p53-MDM2 complexes. p53-MDM2 or MDM2-p53 co - immunoprecipitations were performed as described in materials and methods. Lysates were prepared from RKO cells treated or not with 10 μM Nutlin for 6 hours.

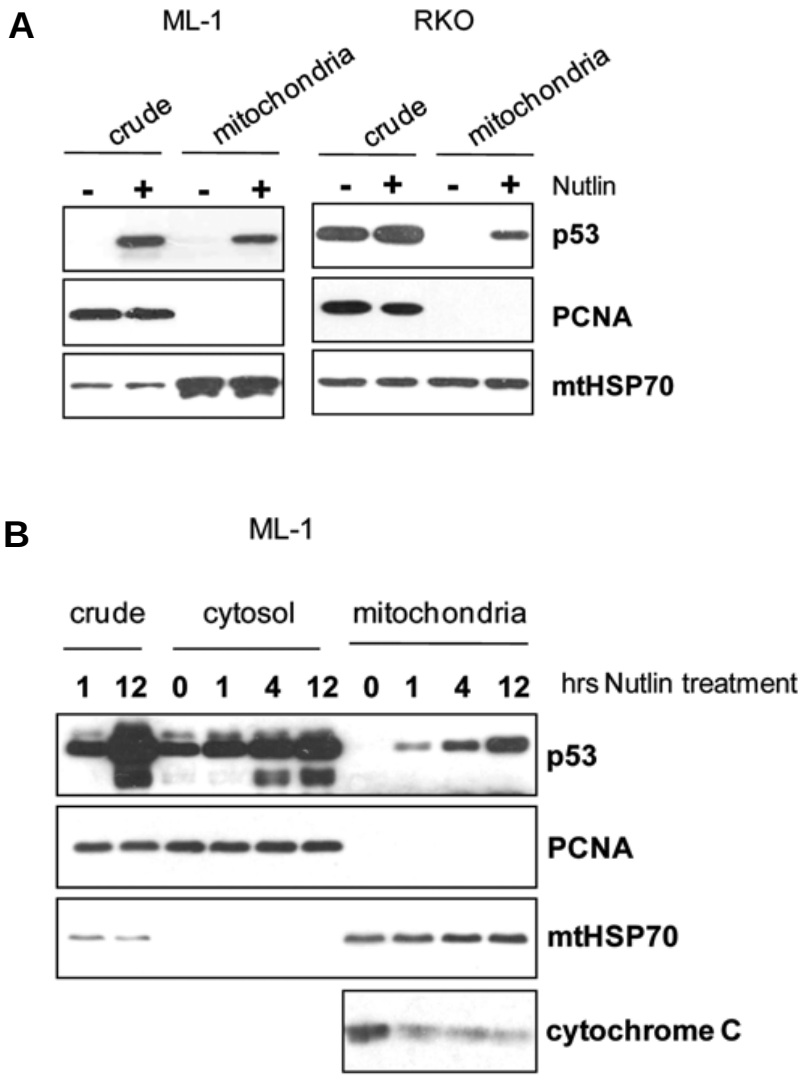

Figure 3. Nutlin promotes mitochondrial translocation of p53. (A) Nutlin induces p53 translocation to mitochondria in both ML-1 and RKO cell lines. Mitochondria fractions from RKO and ML-1 cells treated or not with 10μM Nutlin were prepared as described in materials and methods. Fractions were analysed by Western blotting. PCNA serves as crude extract control, mtHSP70 is a mitochondrial marker. **(B)** Time course of p53 translocation to mitochondria after Nutlin treatment. ML-1 cells were treated with 10μM Nutlin for the indicated times and mitochondria fractions were prepared and analyzed as described in (A).

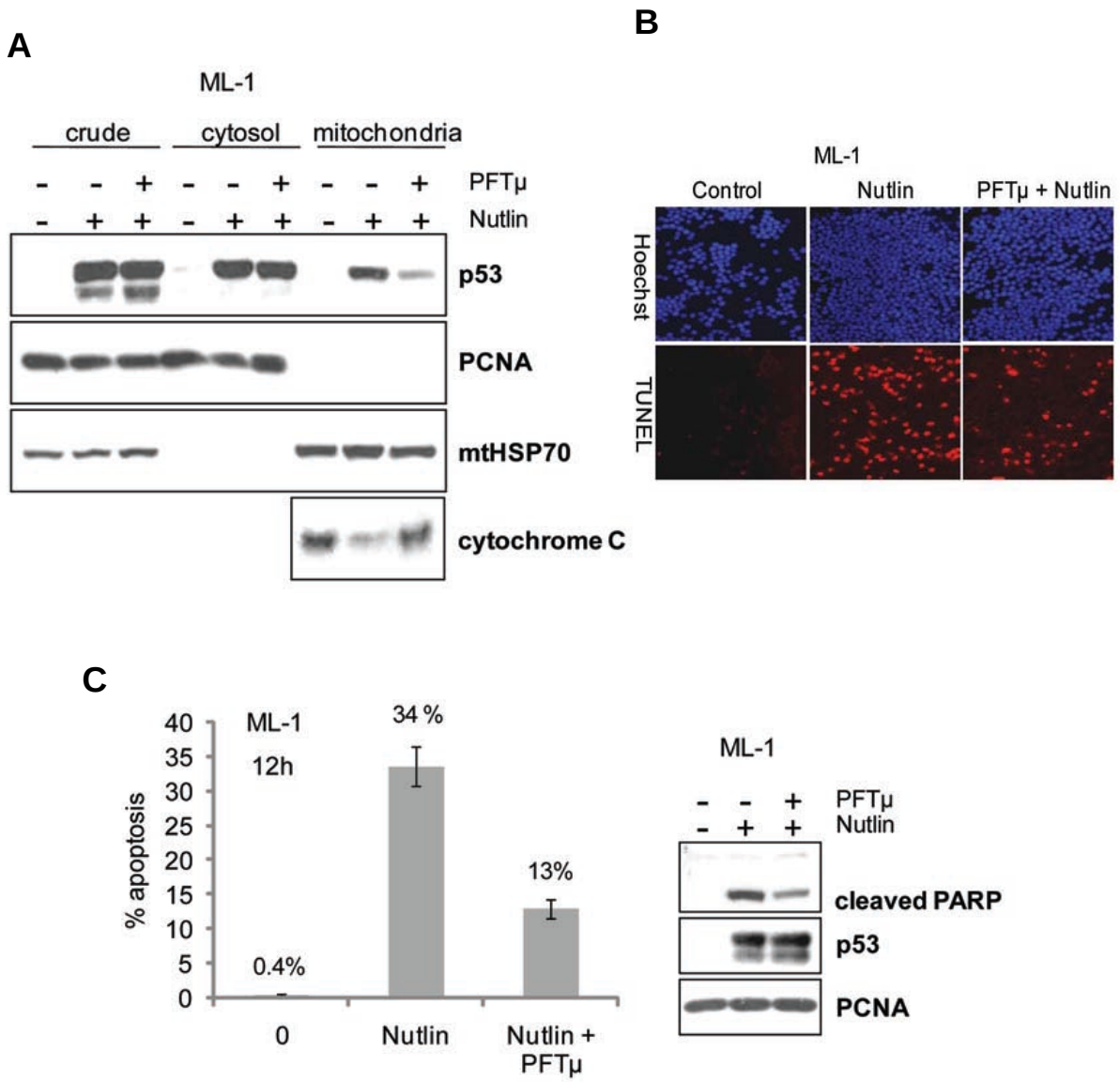

Figure 4. Specific blocking of mitochondrial p53 significantly reduces the apoptotic response to Nutlin. (A) Treatment of ML-1 cells with PFTμ results in reduced p53 levels at mitochondria upon Nutlin treatment and reduced cytochrome C release. ML-1 cells were pre-treated with 25μM PFTμ 2hrs before adding 10μM Nutlin. 12hrs after later mitochondria fractions were prepared as described in materials and methods. **(B, C)** Pretreatment of ML-1 cells with PFTμ reduces apoptotic response to Nutlin. ML-1 cells were pre-treated with 25μM PFTμ for 2 hours followed by treatment with Nutlin for another 12 hours. Cells were processed for TUNEL staining or lysed for Western blotting. **(B)** Example of TUNEL experiment. **(C)** Chart showing percentage apoptosis obtained from the TUNEL experiments described above; and Western blotting showing levels of PARP cleavage and p53. PCNA used as a loading control.

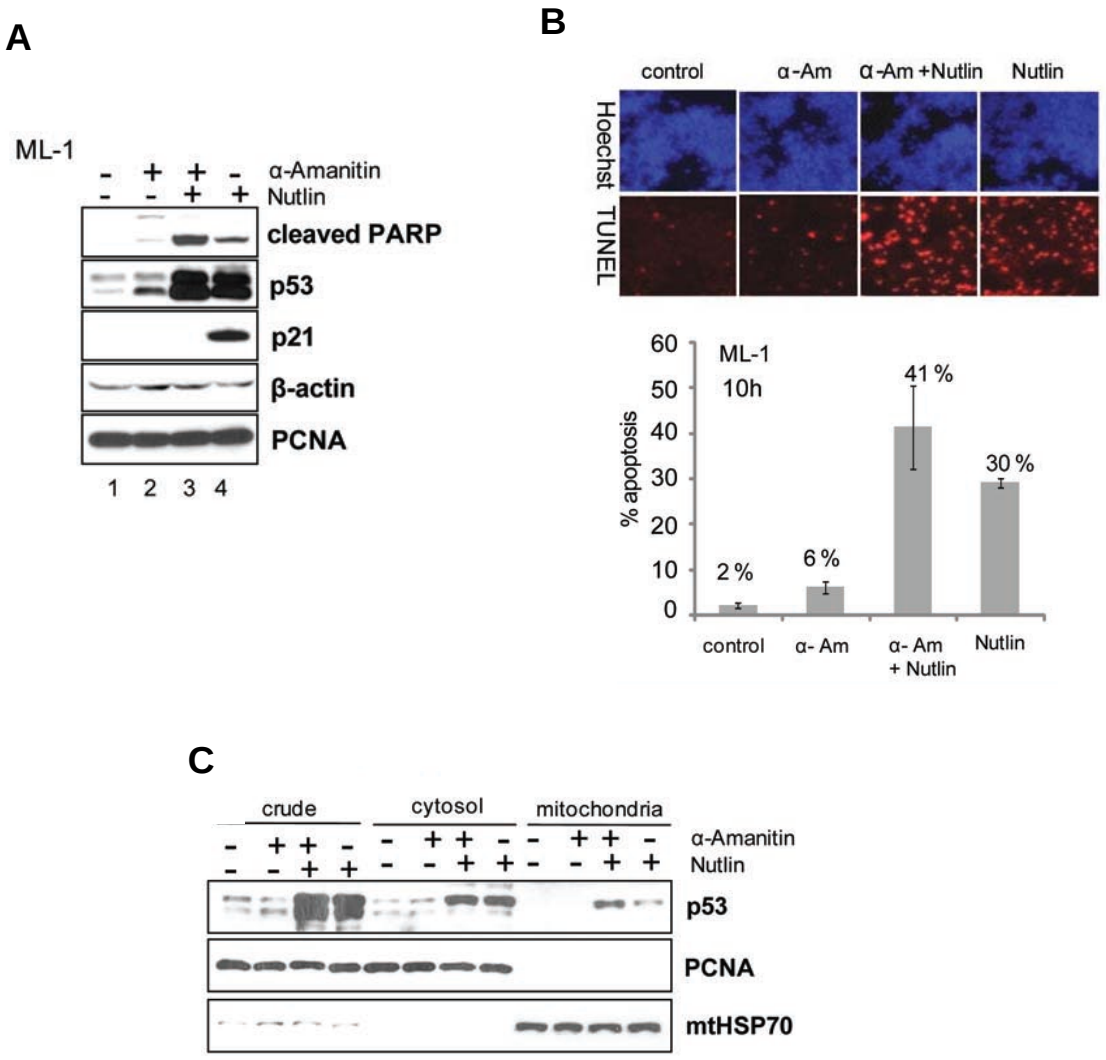

Figure 5. Blocking of Nutlin-induced transcription with αAmanitin does not block apoptotic response to Nutlin. ML-1 cells were pretreated with 10μM αAmanitin for 16 hours, then 10μM Nutlin was added for additional 10 hours. **(A)** Cell lysates from ML-1 cells treated as described above were prepared for Western blotting. Levels of p21 were measured as indication for p53 transcriptional activity, cleaved PARP as a measure for apoptotic response. β-Actin and PCNA serve as loading controls. **(B)** TUNEL assay performed with ML-1 cells treated as described above. *Top*, representative images from TUNEL assay, *Bottom*, chart summarizing percentage apoptosis obtained from TUNEL assay described above. Error bars represent the average of 3 fields from 1 TUNEL assay. **(C)** αAmanitin does not interfere with mitochondria translocation of p53 upon Nutlin treatment. Mitochondria fractions were prepared from cells treated as described in (A) and analyzed by Western blotting. PCNA used as control for crude and cytosolic extracts. mtHSP70 used as mitochondria marker.

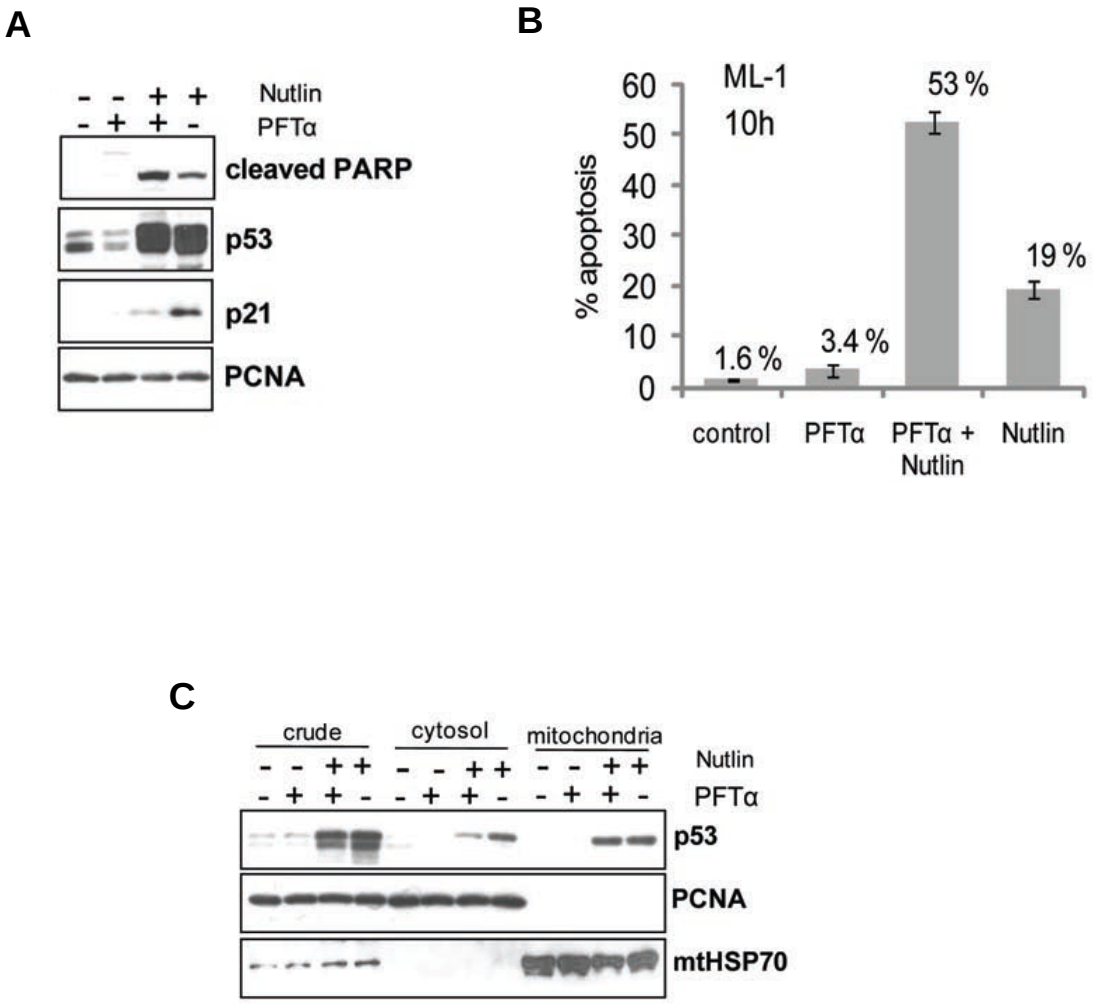

Figure 6. Specific blocking of p53-mediated transcription with PFTα does not block apoptotic response to Nutlin. Pretreatment of ML-1 cells with PFTα does not block Nutlin induced apoptosis. ML-1 cells were pretreated with 20μM PFTα for 4 hours followed by 10μM Nutlin treatment for additional 10 hours. (**A)** Western blot showing that pretreatment of ML-1 cells with PFTα retains PARP cleavage after Nutlin treatment, while does not affect p53 levels. p21 levels are indication for inhibited p53 mediated transcription. **(B)** Graph summarizing TUNEL results from ML-1 cells pretreated with PFTα. **(C)** PFTα does not interfere with Nutlin induced p53 translocation to mitochondria

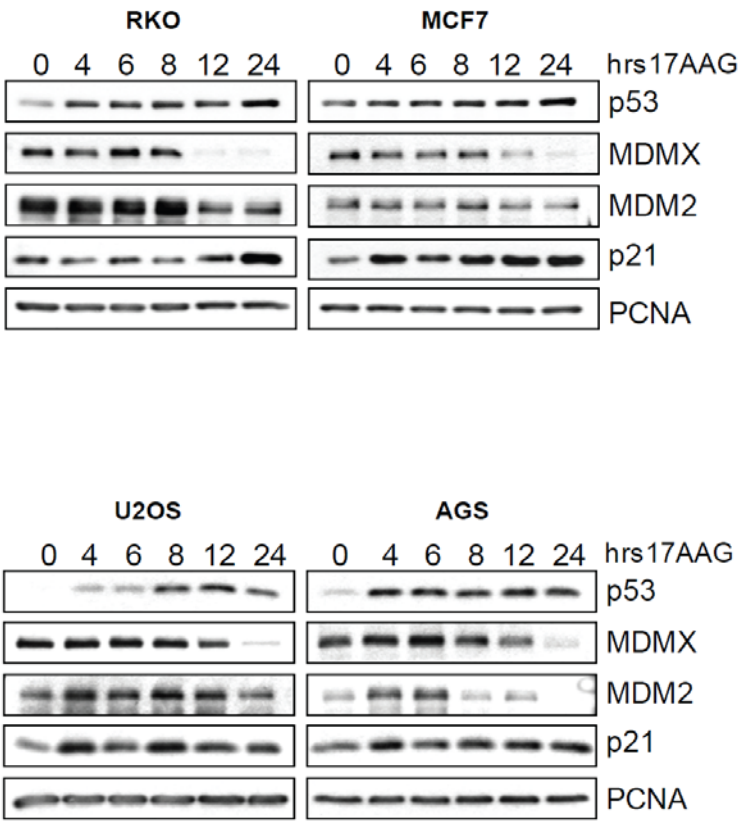

Figure 7. 17AAG increases wtp53 and p21, but decreases MDMX and MDM2 protein levels. Indicated human cancers cell lines (RKO- colorectal carcinoma, MCF7- breast adenocarcinoma, U2OS- osteosarcoma and AGS- gastric adenocarcinoma) were treated with 2 μM of 17AAG for the indicated time points. The protein levels of p53, MDMX, MDM2 and p21 proteins were analyzed by immunoblots**.** PCNA is a loading control**.**

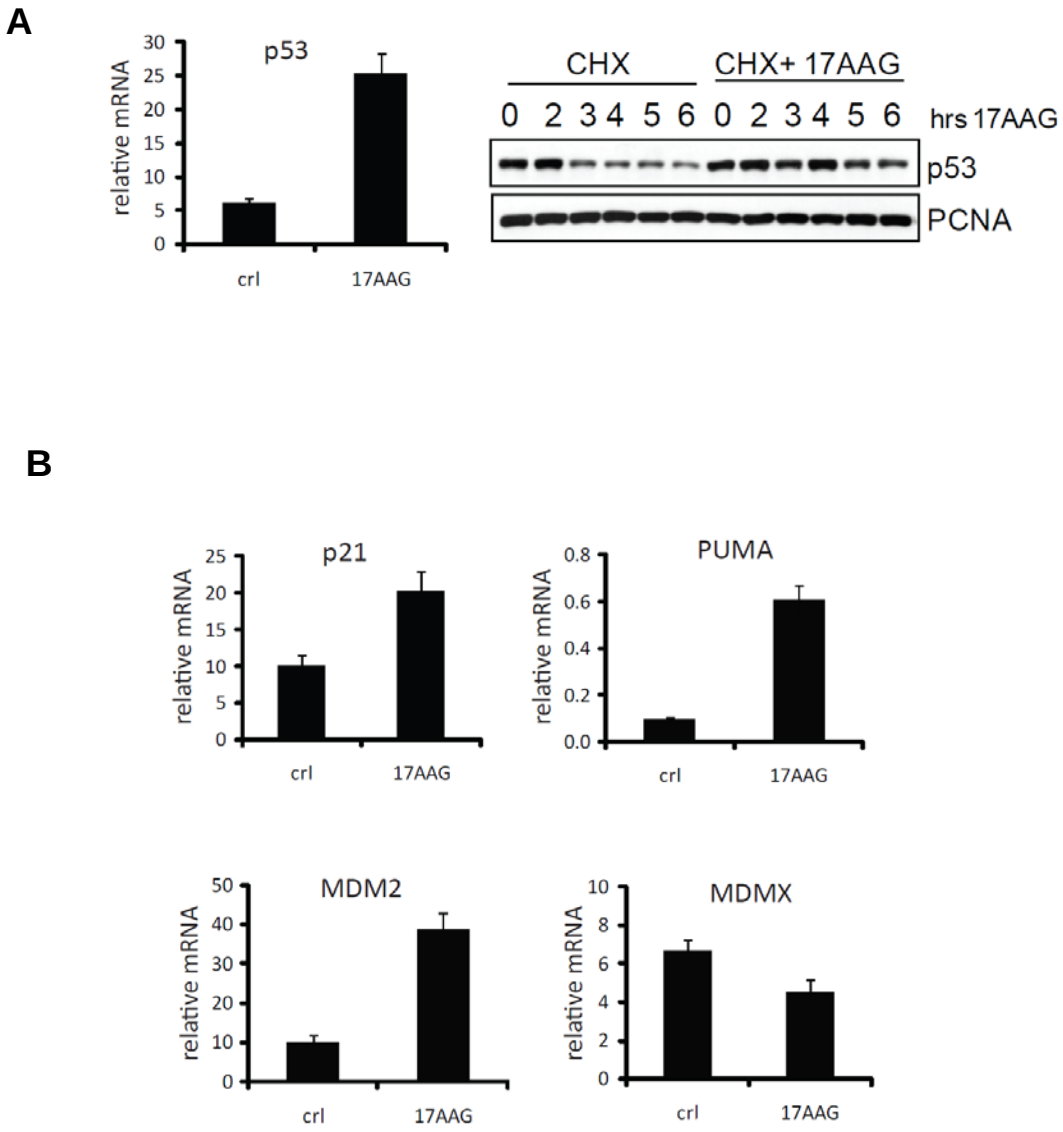

Figure 8. 17AAG stabilizes p53 protein and induces transcription of p53 targets. (A) 17AAG increases both mRNA levels and protein stability of p53. Left, p53 mRNA levels in RKO cells treated with 17AAG or DMSO for 24 hours. qRT-PCR, mRNA levels were normalized to actin. Error bars represent standard errors from 2 independent experiments, each done in triplicate. Right, Cycloheximide (CHX) chase of RKO cells treated as indicated. PCNA is a loading control. **(B)** 17AAG increases transcription of the p53 target genes p21, PUMA and MDM2. RKO cells were treated as in B. mRNA levels of MDMX, p21, PUMA and MDM2 were evaluated by qRT-PCR as in B.

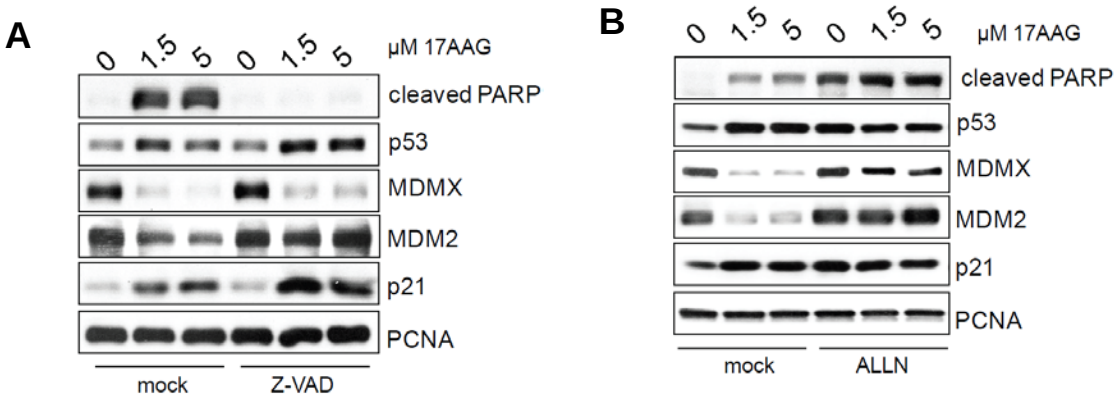

Figure 9. Destabilization of MDMX by 17AAG is caspase-independent and proteasome-dependent, while destabilization of MDM2 is a caspase-dependent event. RKO cells were pretreated with pan-caspase inhibitor Z-VAD-FMK **(A)** or proteasome inhibitor ALLN **(B)** 1 hour before adding 17AAG for an additional 24 hours

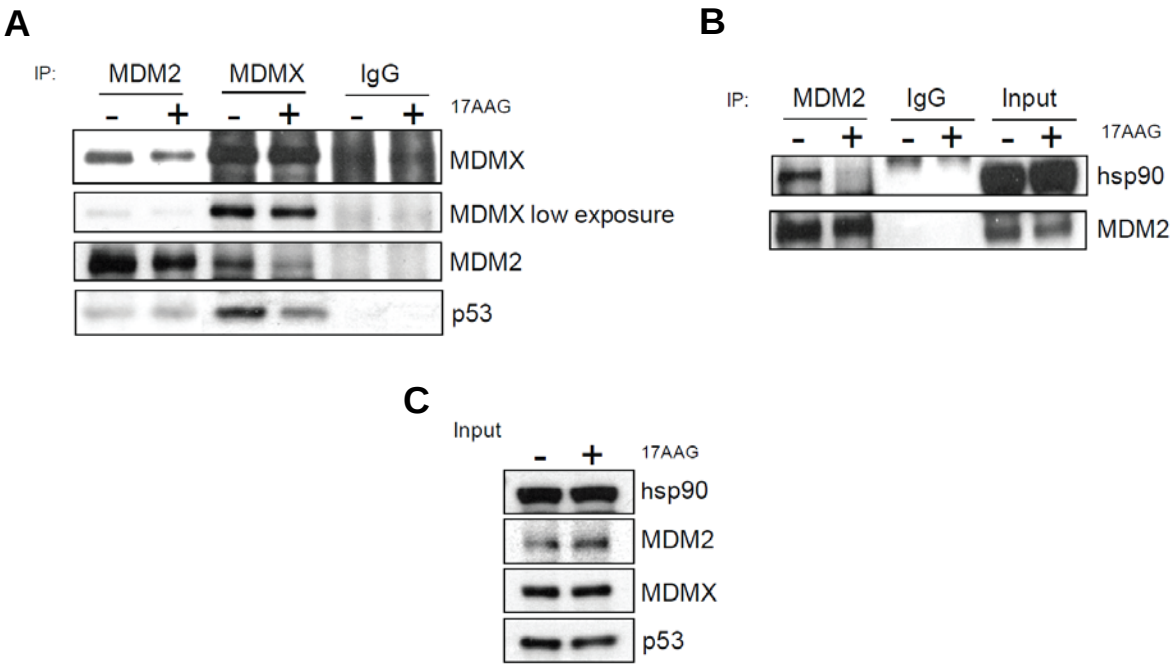

Figure 10. 17AAG disrupts the p53-MDMX and MDMX-MDM2 interactions. (A) 17AAG disrupts the p53-MDMX and the MDM2-MDMX complexes. RKO cells were treated with 1.5 μM of 17AAG for 2 hours followed by immunoprecipitation with MDMX or MDM2 antibodies. MDMX-p53, MDM2-MDMX and MDM2-p53 complexes were detected by immunoblots. Isotype-matched IgGs serve as controls. **(B)** 17AAG separates MDM2 and hsp90. RKO cells were treated as in A followed by immunoprecipitation with MDM2 antibody. Isotype-matched IgG serves as control. **(C)** Immunoblot indicating the relative input of proteins used in left.

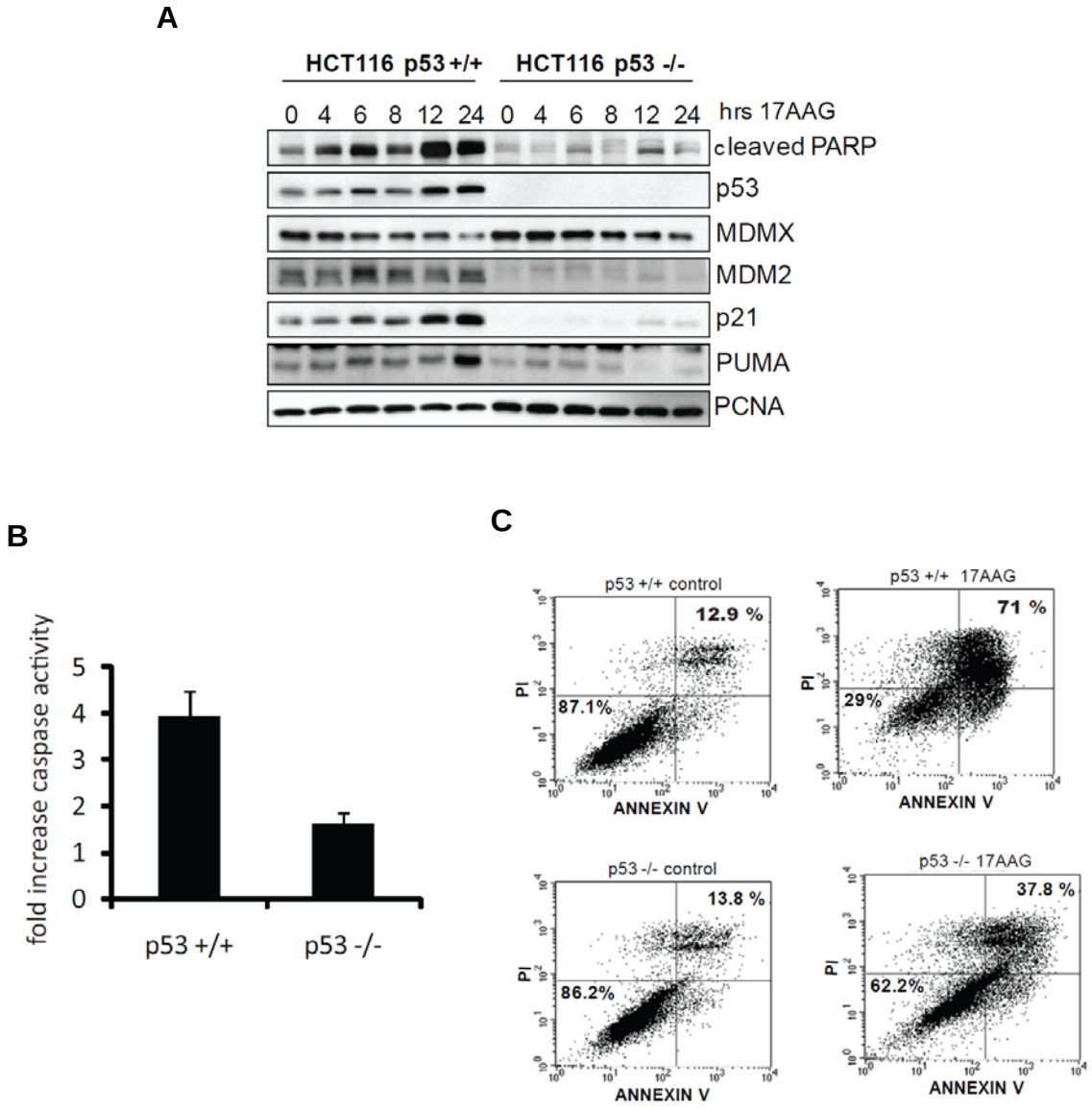

Figure 11. 17AAG kills cancer cells in a p53 dependent manner. (A) p53-/- cells display lower PARP cleavage and lack p21 and PUMA proteins induction upon 17AAG treatment. HCT116 p53+/+ and HCT116 p53-/- cells were treated with 1.5μM 17AAG for the indicated time points and protein levels of cleaved PARP, p53, MDMX, MDM2, p21 and PUMA examined by Western blotting. (**B)** p53-/- cells are less sensitive to 17AAG-induced caspase activation. HCT116 p53+/+ and HCT116 p53-/- cells were treated with 17AAG for 48 hours and caspase activity measured as described in materials and methods. Error bars represent standard errors obtained from four replicates. **(C)** p53-/- cells are more resistant to 17AAG. HCT116 p53+/+ and HCT116 p53-/- cells were treated with 17AAG for 72 hours and processed for Annexin V and PI staining. Indicated percentage of Annexin V/ PI negative population (% survival) was measured by FASC.

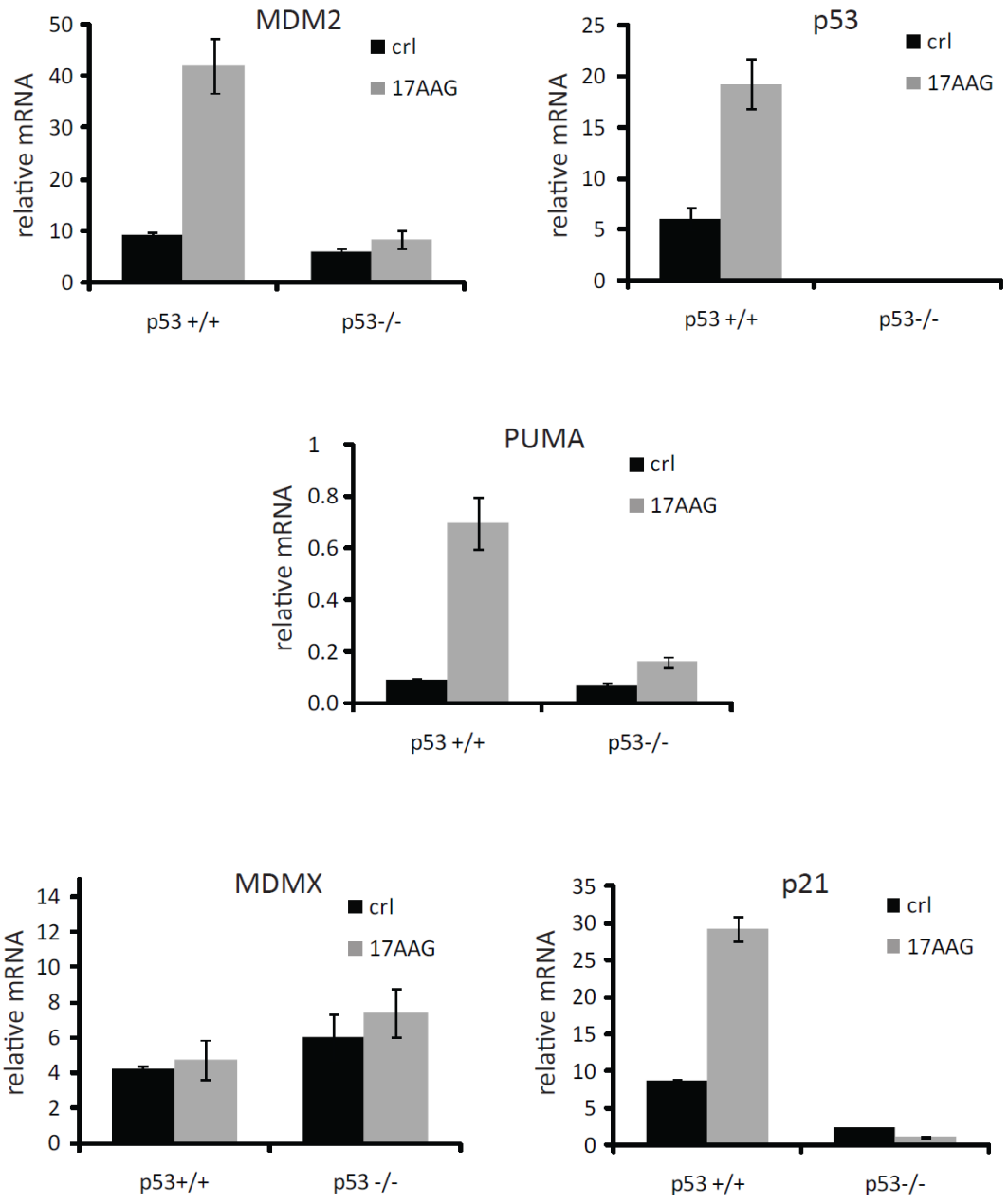

Figure 12. 17AAG induces transcription of p53 targets p21, PUMA and MDM2 in p53+/+ but not in p53-/- cells. HCT116 p53+/+ and HCT116 p53 -/- cells were treated with 1.5μM 17AAG for 24 hours and mRNA levels of the indicated genes were measured by qPCR. . Error bars represent standard errors obtained form 2 independent experiments, each done in triplicates.

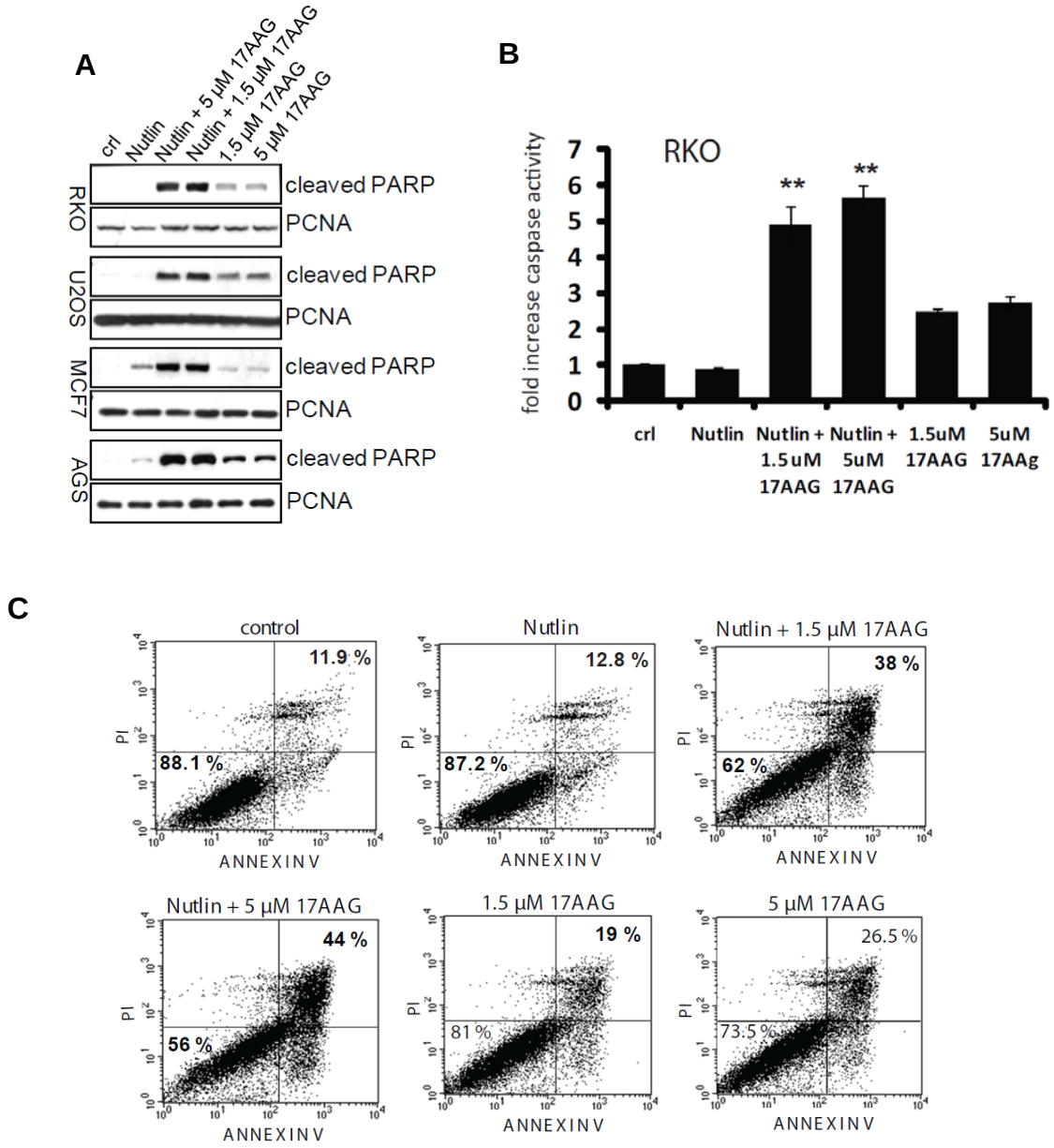

Figure 13. Combining Nutlin and 17AAG significantly increases cell death as compared to single treatments. (A) Increased PARP cleavage upon drug combination. RKO, U2OS, MCF7 and AGS cell lines were treated with 17AAG for 1 hour, before adding Nutlin for additional 24 hours where indicated. Cleavage of PARP was assessed by Western blotting. **(B)** Increased caspase activity upon drug combination. Cells were treated as in A and caspase activity measured as described in materials and methods. Error bars represent standard errors obtained from four replicates. Results are shown for RKO cells only, similar results were seen in U2OS, MCF7 and AGS cells. **(C)** Decreased cell survival upon drug combination. Cells were treated with 17AAG for 1 hour before adding Nutlin for additional 48 hours, then processed for Annexin V and Propidium Iodide (PI) staining. Percentage of Annexin V/PI negative population (% survival- bottom left quadrant) was measured by FACS.

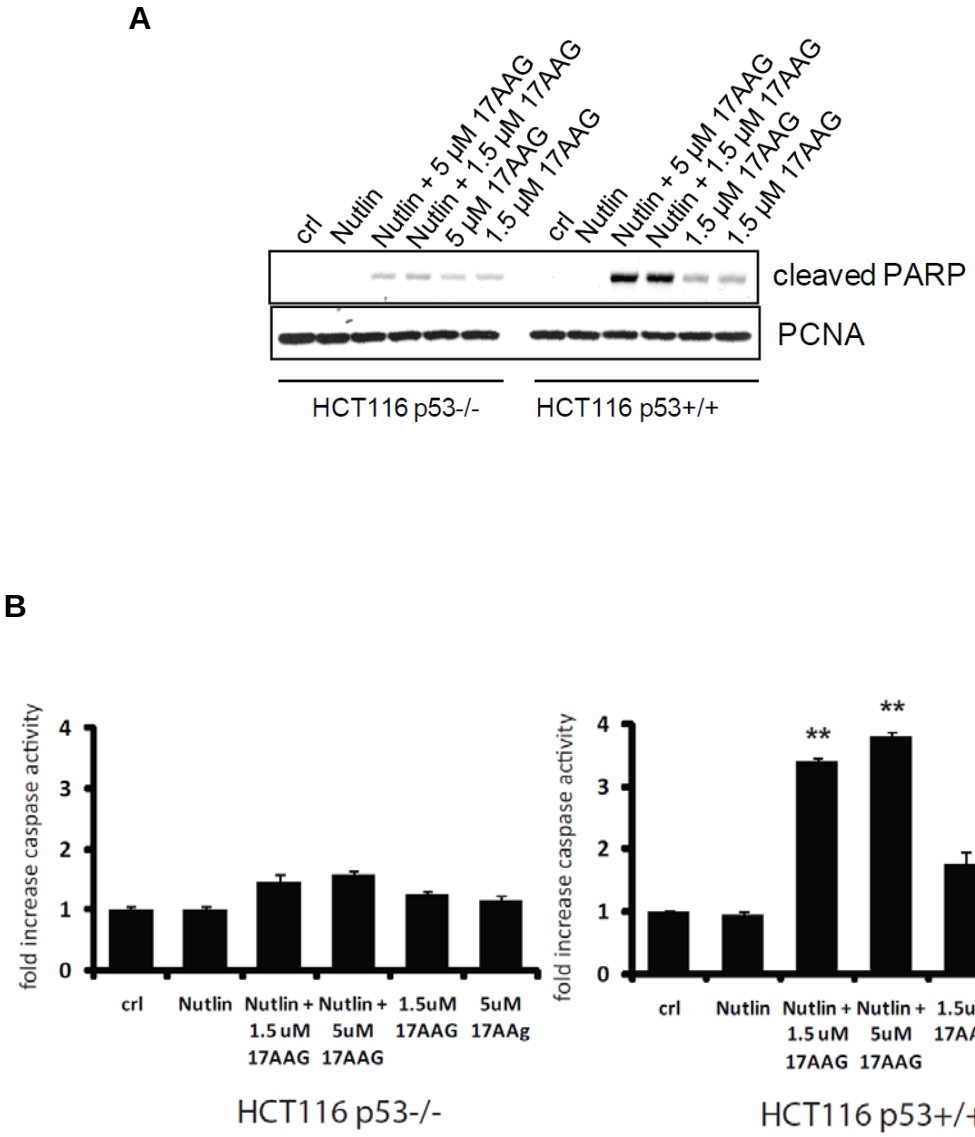

Figure 14. Combination of Nutlin and 17AAG dramatically increases cell death in p53+/+ but not in p53-/- cells. HCT116 p53+/+ or p53-/- cells were treated with 17AAG for 1 hour before adding Nutlin for additional 24 hours and **(A)** cleavage of PARP was assessed by Western blotting or **(B)** caspase activity measured as described in materials and methods. Error bars represent standard errors obtained from four replicates.

.

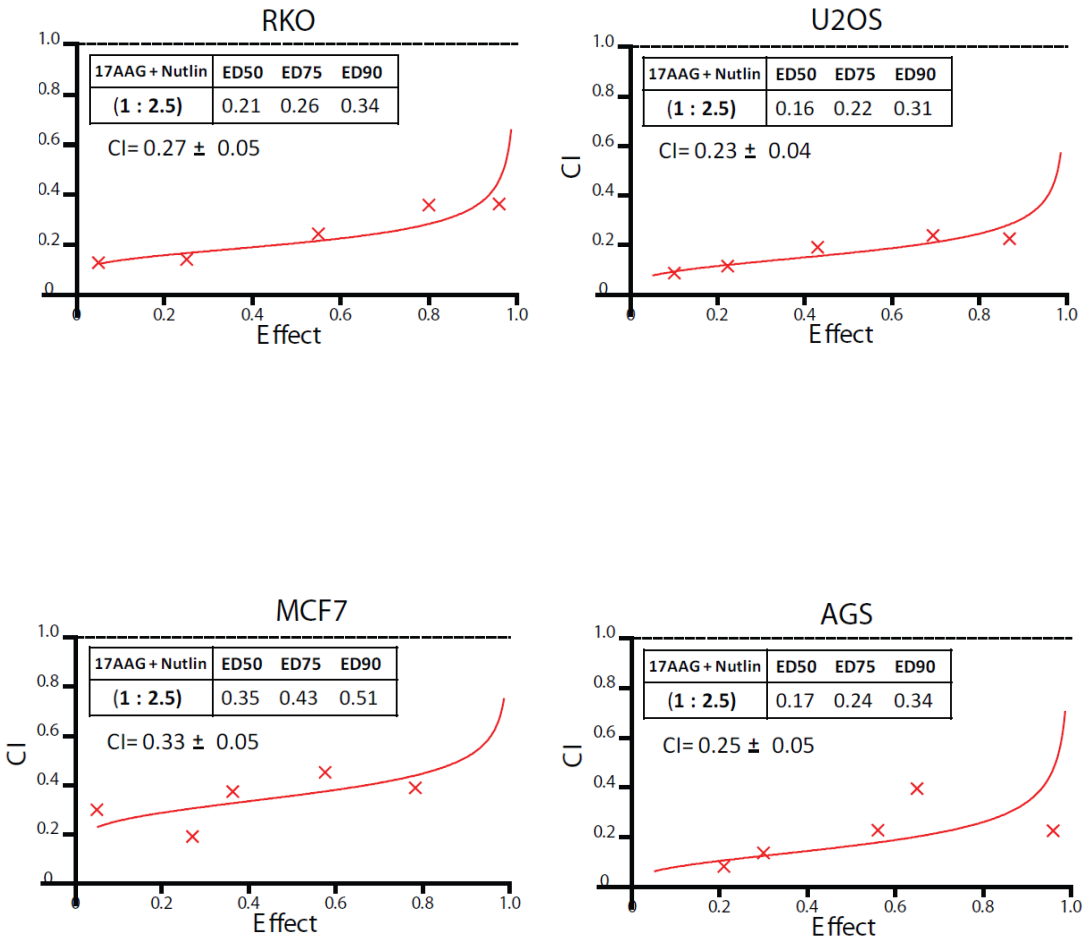

Figure 15. Synergistic induction of cell death upon combination of Nutlin and 17AAG. The indicated cell lines were treated with different doses of 17AAG or Nutlin, or combinations using a fixed ratio for 72 hours. Percentage of dead cells was calculated by trypan blue exclusion assay. Combinatorial indexes were calculated by the isobologram analysis using the CalcuSyn program.

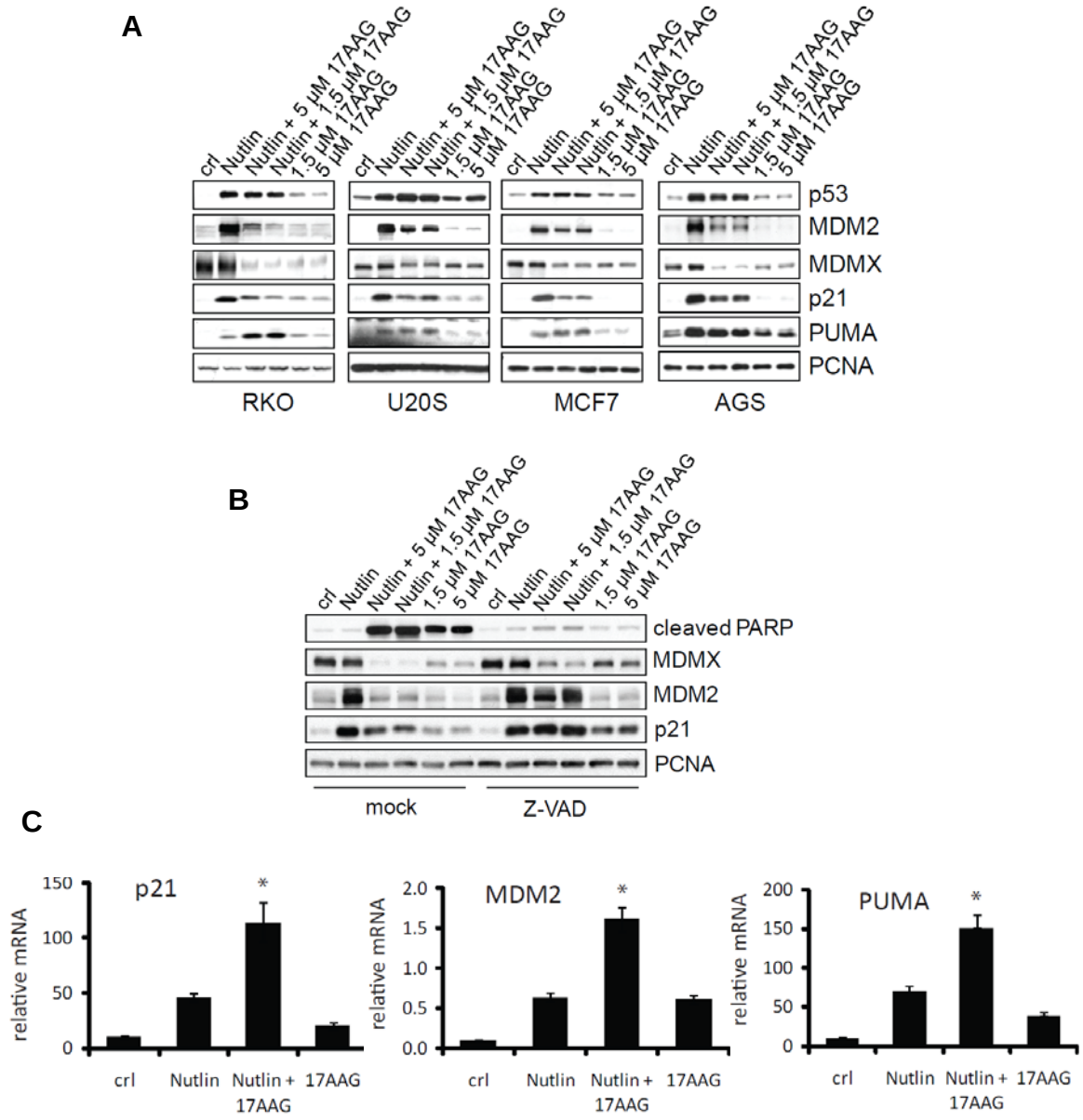

Figure 16. 17AAG modulates Nutlin-induced signaling. (A) 17AAG decreases Nutlin-induced MDM2 and p21 protein levels, while increases Nutlin-induced PUMA protein levels. Indicated cell lines were treated with17AAG for 1 hour before adding Nutlin where indicated. **(B)** 17AAG-induced MDM2 and p21 downregulation upon Nutlin treatment is caspase dependent. RKO cells were pre-treated with 20μM pan caspase inhibitor Z-VAD-FMK or mock for 1 hour pririor to adding Nutlin and/or 17AAG as indicated. **(C)** 17AAG potentiates Nutlin-induced transcription of MDM2, p21 and PUMA. RKO cells were treated as in A and mRNA levels of the indicated genes assessed by qPCR. Data is normalized to actin mRNA levels. Error bars represent standard errors obtained form 2 independent experiments, each done in triplicates.

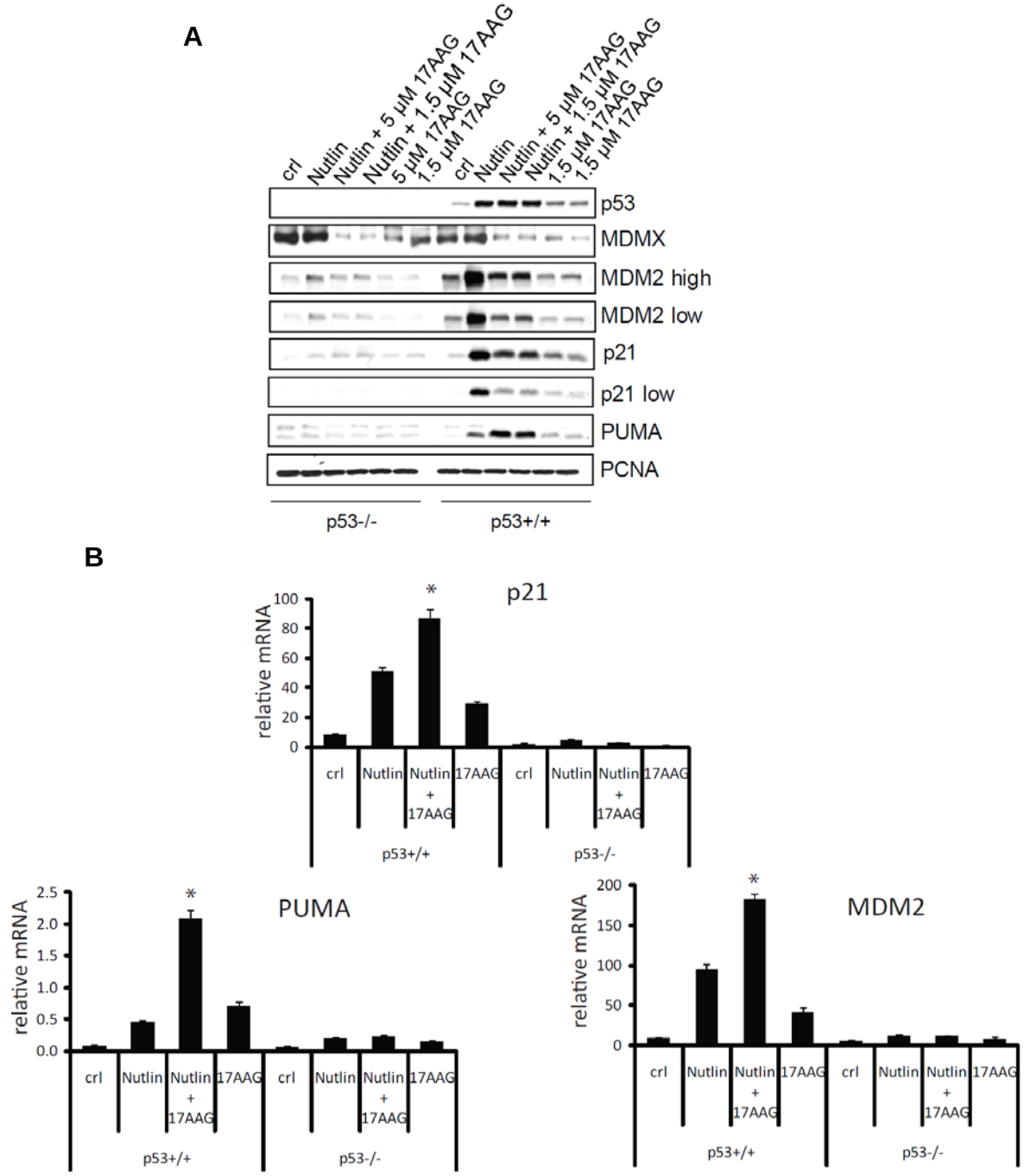

Figure 17. The effect of 17AAG on Nutlin-induced signaling is p53 dependent. (A) Effect of 17AAG on Nutlin-induced p21, PUMA and MDM2 protein levels in p53+/+ and p53-/- cells. HCT116 p53+/+ and HCT116 p53-/- cells were treated and analyzed as in figure 16A. **(B)** Effect of 17AAG on Nutlin-induced transcription of p21, PUMA and MDM2 genes in p53+/+ and p53-/- cells. p53+/+ and HCT116 p53-/- cells were treated and analyzed as in figure 16A.

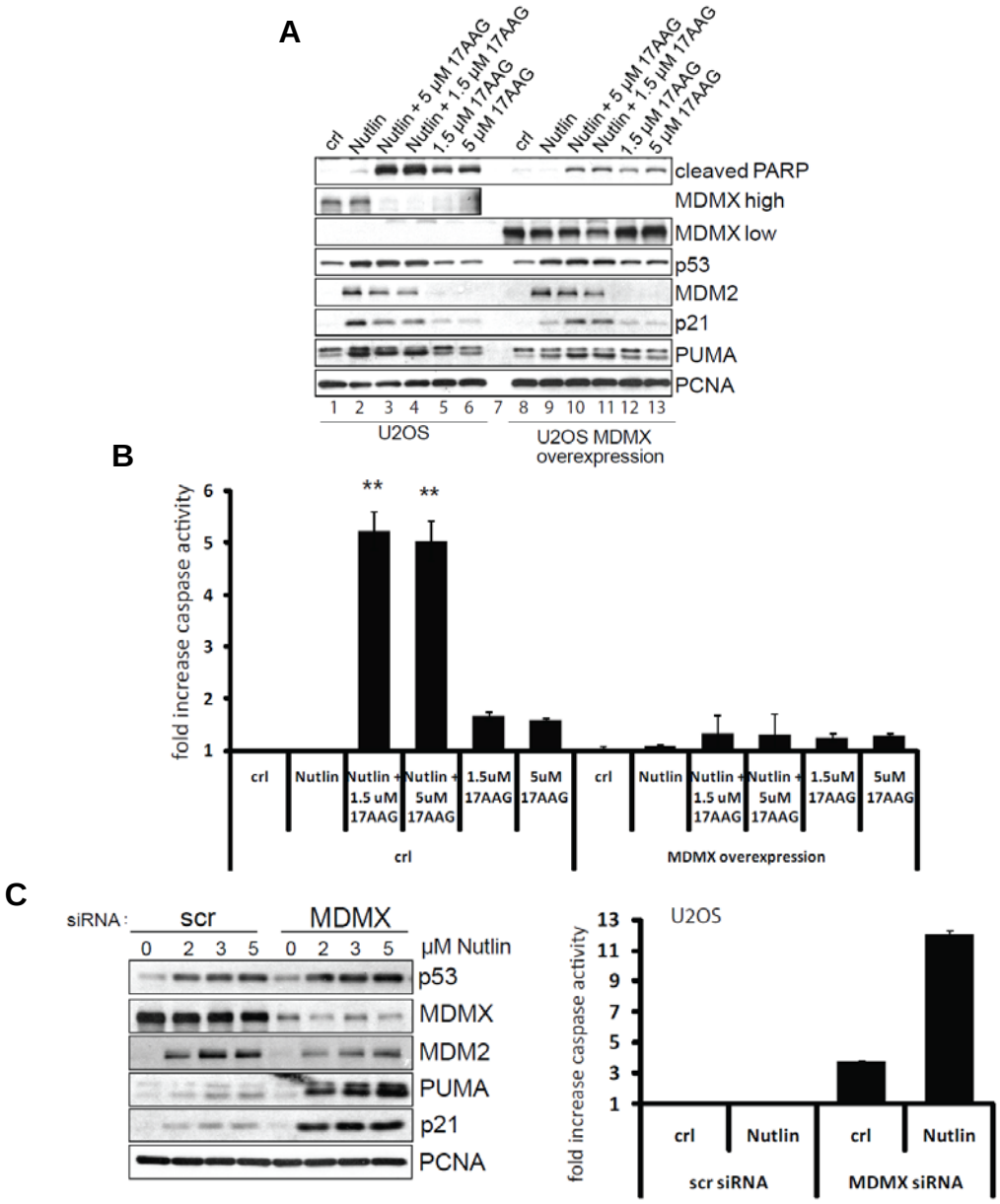

Figure 18. 17AAG enhances Nutlin-induced apoptosis through inhibition of MDMX. (A) Overexpression of MDMX inhibits cleavage of PARP and affects Nutlin-induced p21 and PUMA expression. U2OS cells, stably expressing doxycycline-inducible MDMX construct were treated with doxycyline overnight. Then treatment with 17AAG and/or Nutlin was initiated for additional 24 hours as indicated**. (B)** Overexpression of MDMX inhibits caspase activation caused by the combination 17AAG and Nutlin. U2OS parental cells and U2OS expressing MDMX were treated as in A and caspase activity measured as described in materials and methods. Error bars represent standard errors obtained from four replicates. **(C)** Downregulation of MDMX enhances Nutlin-induced p21 and PUMA proteins and enhances nutlin-induced apoptosis. U2OS and RKO cells were transfected with scrambled or MDMX siRNA for 24 hours, then treated with Nutlin for additional 24 hours. Protein levels were assessed by Western blotting (left) and caspase activity (right) was measured as described in materials and methods.

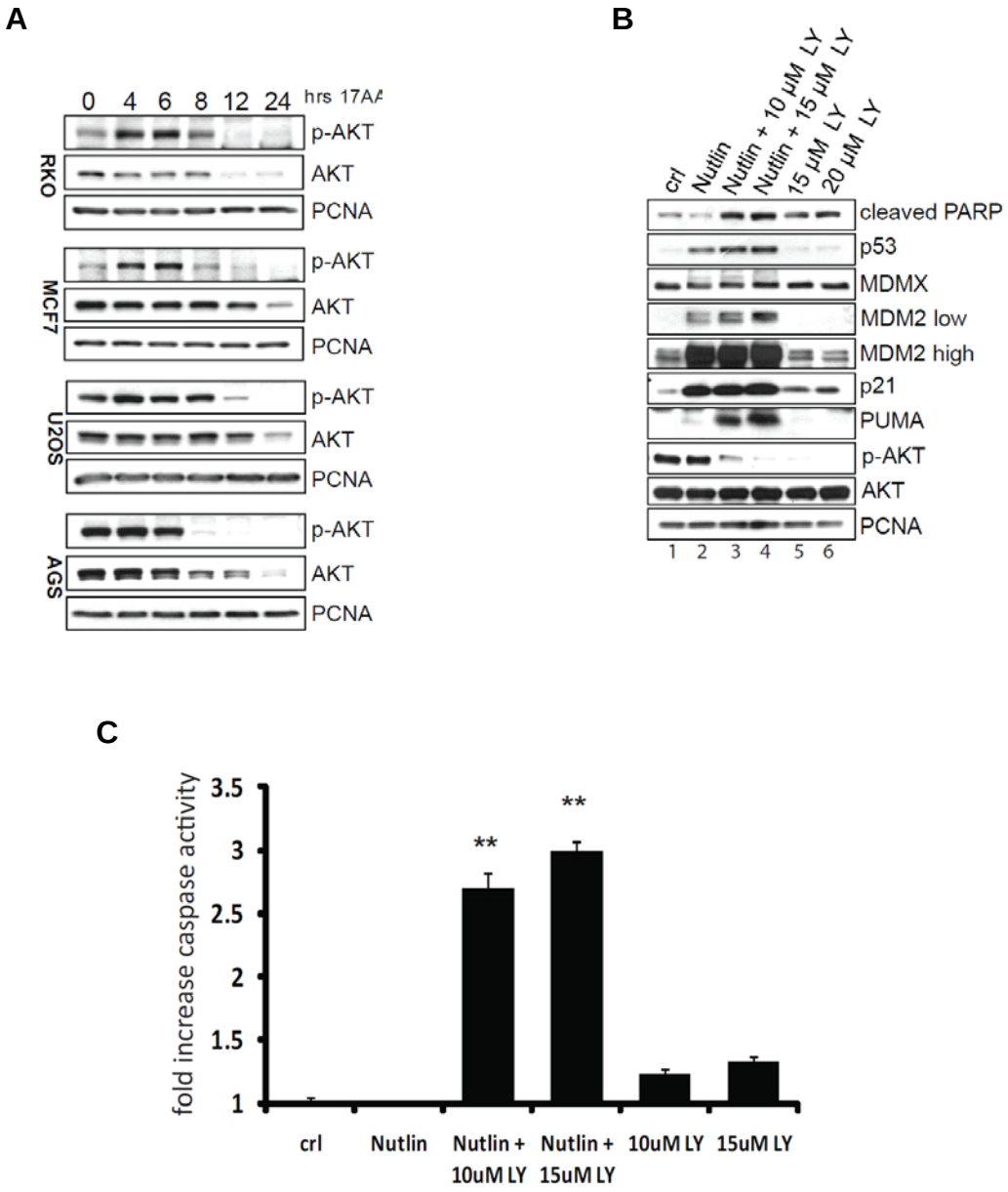

Figure 19. 17AAG enhances Nutlin-induced apoptosis through inhibition of PI3K pathway. **(A)** 17AAG inhibits AKT. Cells were treated with 17AAG for the indicated times and AKT and p-AKT protein levels assessed by Western blotting**. (B)** Inhibition of AKT phosphorylation potentiates Nutlin-induced PARP cleavage and PUMA protein**.** RKO cells were treated with PI3K inhibitor LY294002 1 hour before adding Nutlin for additional 24 hours, then lysed and indicated proteins assessed by Western blotting. **(C)** Inhibition of AKT phosphorylation potentiates Nutlin-induced caspase activation. RKO cells were treated as in B and caspase activity measured as described in materials and methods.

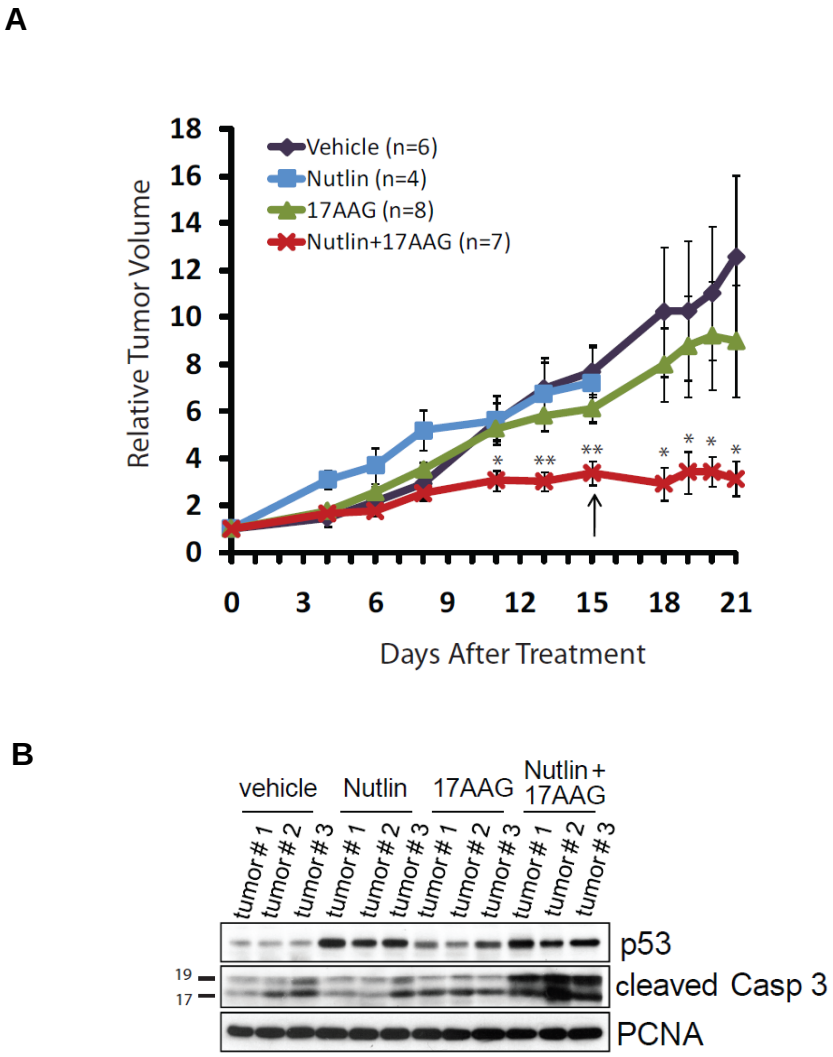

Figure 20. **In vivo activity of the Nutlin and 17AAG drug combination on established RKO tumor xenografts in nude mice. (A)** Relative change of tumor volumes compared to the initial tumor size prior to drug treatments. Tumor volumes were normalized to the initial tumor size measured at Day 0 and the change of volume was averaged among the tumors receiving the same treatment (Vehicle in blue, Nutlin in red, 17AAG in green, and Nutlin+17AAG in purple). Tumor volumes were calculated three or four days during the week. At day 15 (arrow), both Nutlin mice, one Vehicle mouse, and one 17AAG mouse were sacrificed due to tumor burden and one Nutlin+17AAG mouse was sacrificed due to extensive necrosis. The rest of the mice were sacrificed on day 22. The error bars indicate standard error calculated from seven tumors per condition and after day 15 error bars were calculated from three tumors per condition. **(B)** PARP cleavage and caspase activity are increased in tumors treated with Nutlin and 17AAG versus the individual and vehicle treatments. The levels of cleaved Caspase 3 and p53 were assessed by Western. PCNA was used as an internal control.

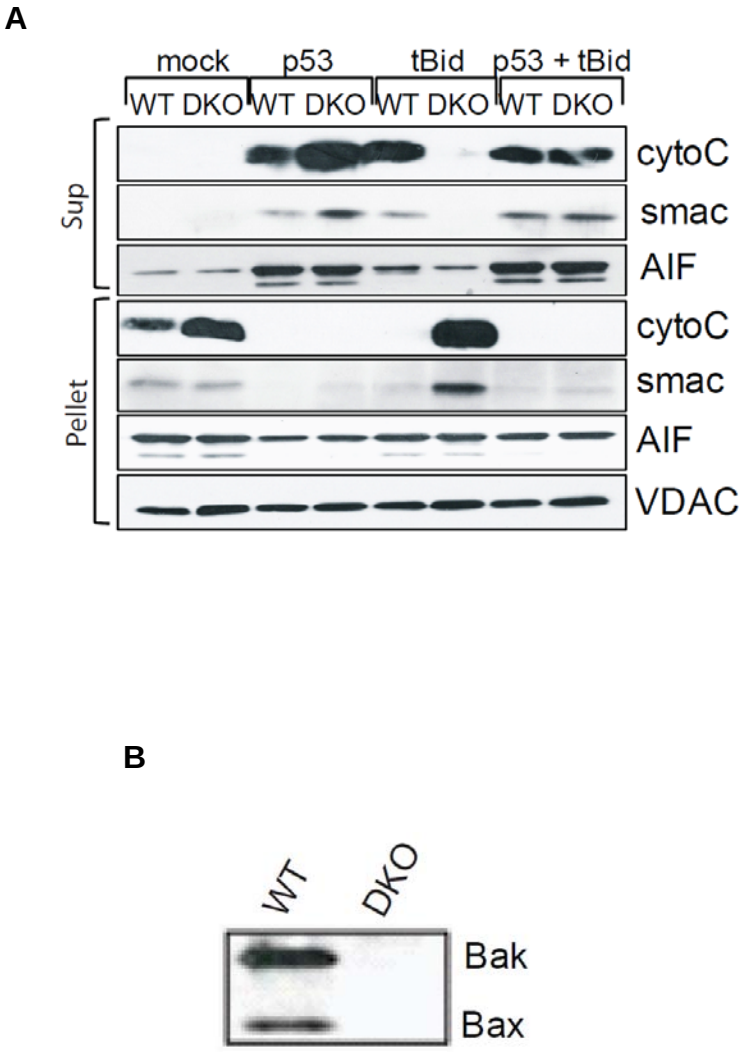

Figure 21. In contrast to tBid, p53's MOMP activity can be independent of Bax and Bak. **(A)** Isolated mitochondria from WT or Bax-/-Bak-/- (DKO) MEFs were incubated with buffer (mock), purified p53 (100 nM) or tBid (100 nM). MOMP was determined by release of CytoC, Smac and AIF into the supernatant (Sup) or their retention in pellet via immunoblotting, VDAC, loading control. **(B)** Verification of Bax/Bak DKO MEF by Western blotting

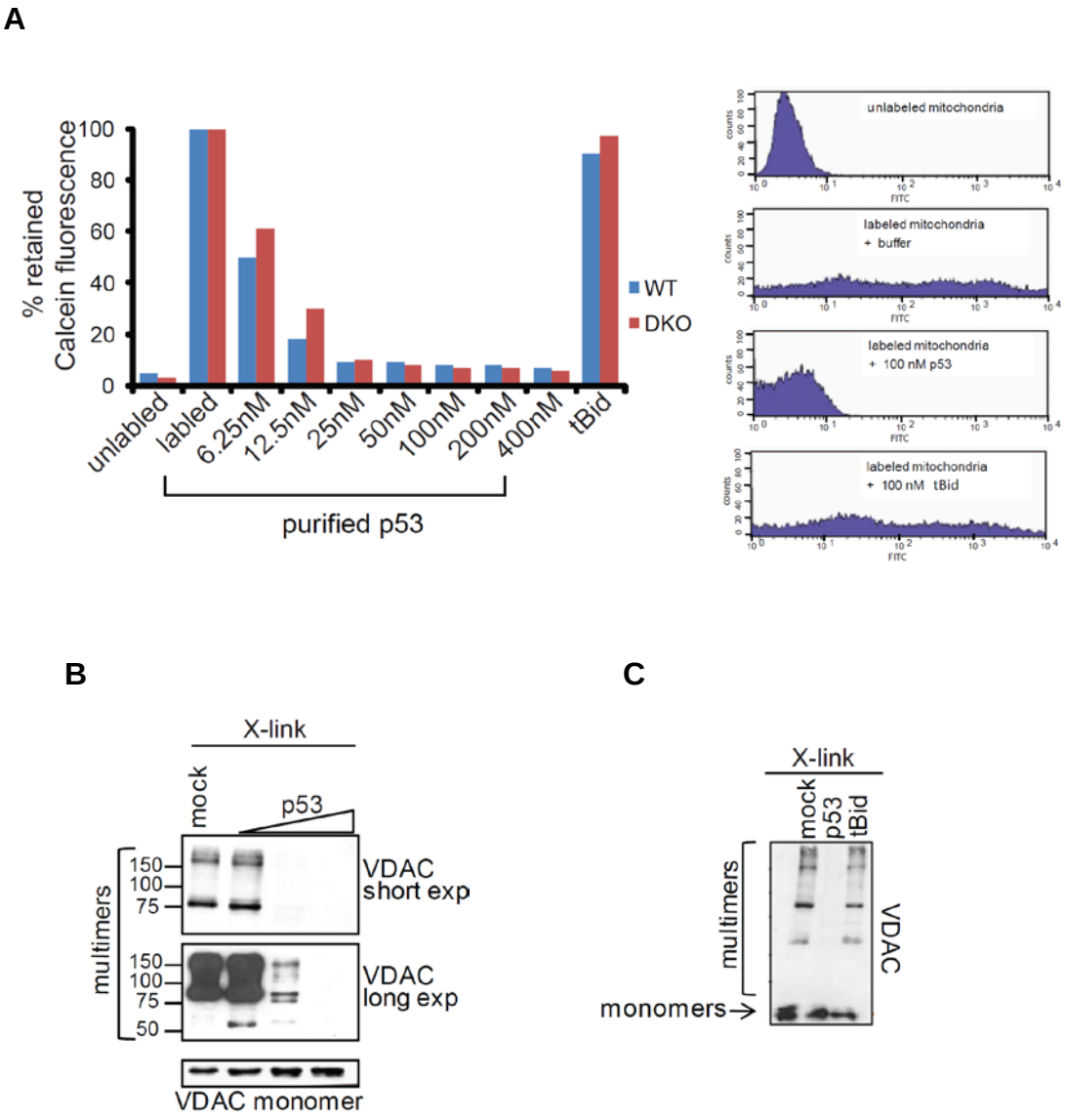

Figure 22. p53, but not tBid opens the PTP and induces physical alterations of VDAC. (A) p53 protein, but not tBid induces calcein release from WT and DKO mitochondria. Mitochondria from WT or DKO MEFs were labeled with calcein-AM prior to adding purified p53 (6.25-400 nM) or tBid (400 nM). PTP opening was measured by FACS as loss of retained mitochondrial fluorescence. **(B)** p53 drives VDAC-containing complexes ranging from ~ 60 to 300 kDa into high molecular weight complexes that no longer enter the gel. Liver mitochondria were incubated with BSA (mock) or 10, 40 and 100 nM of purified p53 prior to chemically crosslinking and immunoblotting. Co-existing monomeric VDAC as input control. **(C)** p53, but not tBid drives VDAC into high molecular weight complexes. Analysis as in B with p53 and tBid proteins at 100 nM each.

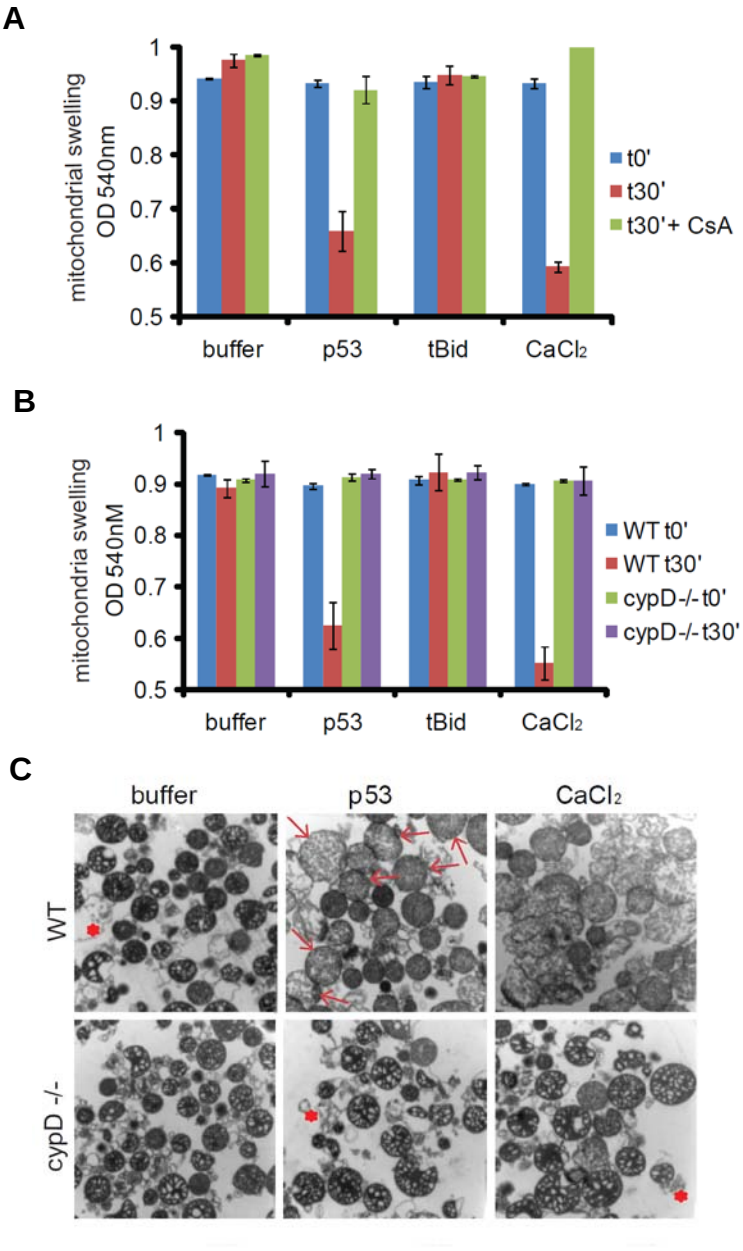

Figure 23. p53, but not tBid induces mitochondrial swelling in a CypD-dependent and Bax/Bak-independent manner. (A) Mitochondria isolated from Bax/Bak DKO MEFs were incubated with buffer, 50 nM purified p53 or tBid, or 50 μM $CaCl_2$ for 30 min. CypD inhibitor CsA (5 μM) was added prior to proteins or $CaCl_2$ where indicated. Mitochondrial swelling was measured at optical density of 540 nM. **(B)** Mitochondria from WT or cypD-/- MEFs were treated as in **A**. Four replicates ± standard error. **(C)** Electron microscopy images of WT or cypD-/- mitochondria treated as in **A**. p53 induces swelling in WT but not CypD-/- mitochondria which appear large and pale (see arrows). * denotes debris due to the isolation procedure.

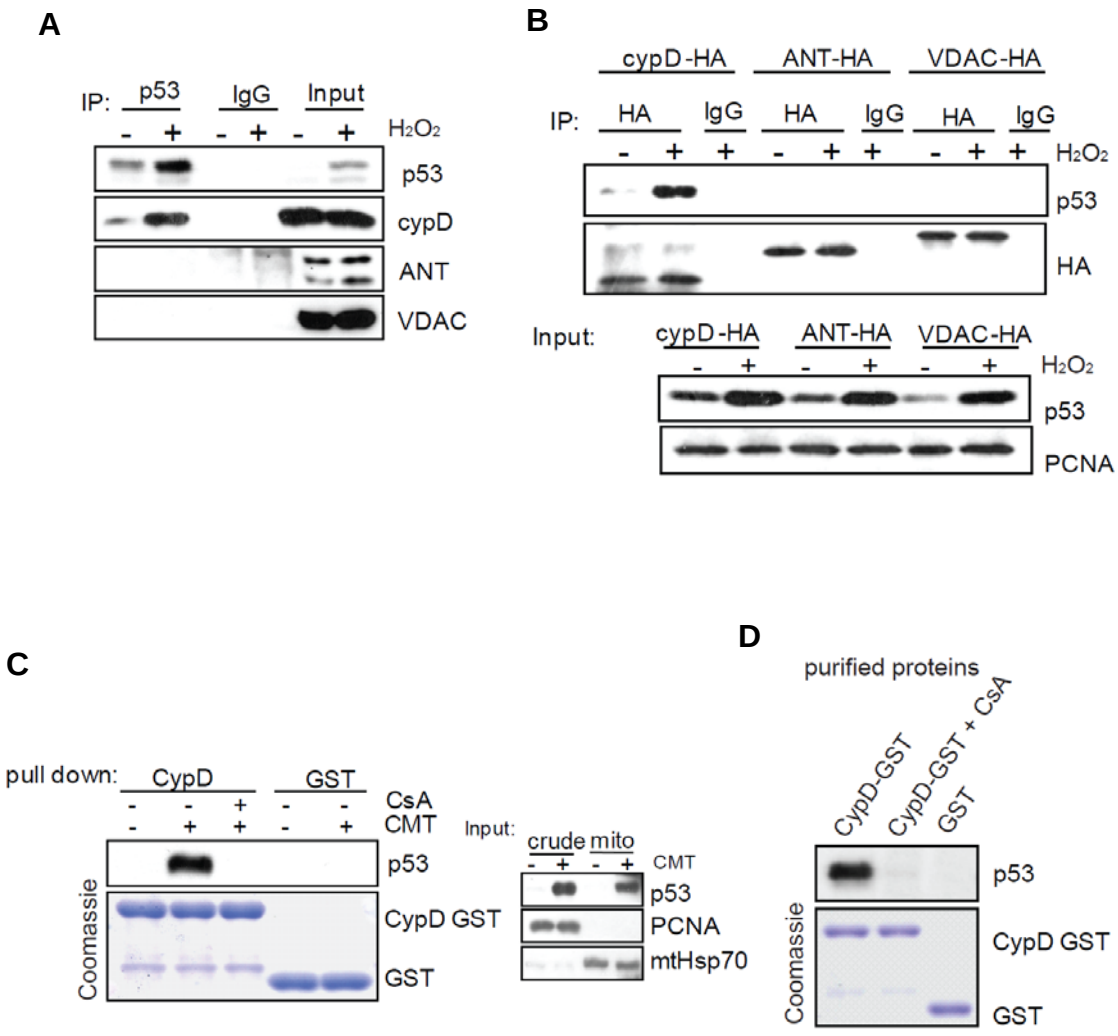

Figure 24. Mitochondrial p53 Interacts with CypD, but not with VDAC or ANT. (A) p53 forms a prominent oxidative stress-induced endogenous complex with CypD, but not with VDAC or ANT. HCT116 p53 +/+ cells were treated with H_2O_2, mitochondria were isolated, lysed and immunoprecipitated with p53 antibody or IgG followed by immunoblotting. **(B)** CypD but not VDAC or ANT binds to p53. HCT116 p53+/+ cells expressing HA-tagged CypD, ANT or VDAC were treated with H_2O_2 for 6 hrs, lysed and immunoprecipitated with anti-HA followed by immunoblotting. **(C)** p53 binds to CypD. Binding is blocked by the CypD inhibitor CsA. Mitochondrial lysates of HCT116 p53 +/+ cells (inset) treated with 5 μM Camptothecin (CMT) for 3 hrs were incubated with CypD-GST or GST alone (Coomassie) ± CsA (5 μM), washed and immunoblotted for p53. **(D)** Direct interaction between recombinant p53 and CypD proteins is CsA-dependent. Purified p53 and CypD-GST proteins were used in GST-pull down assays with 5 μM CsA where indicated.

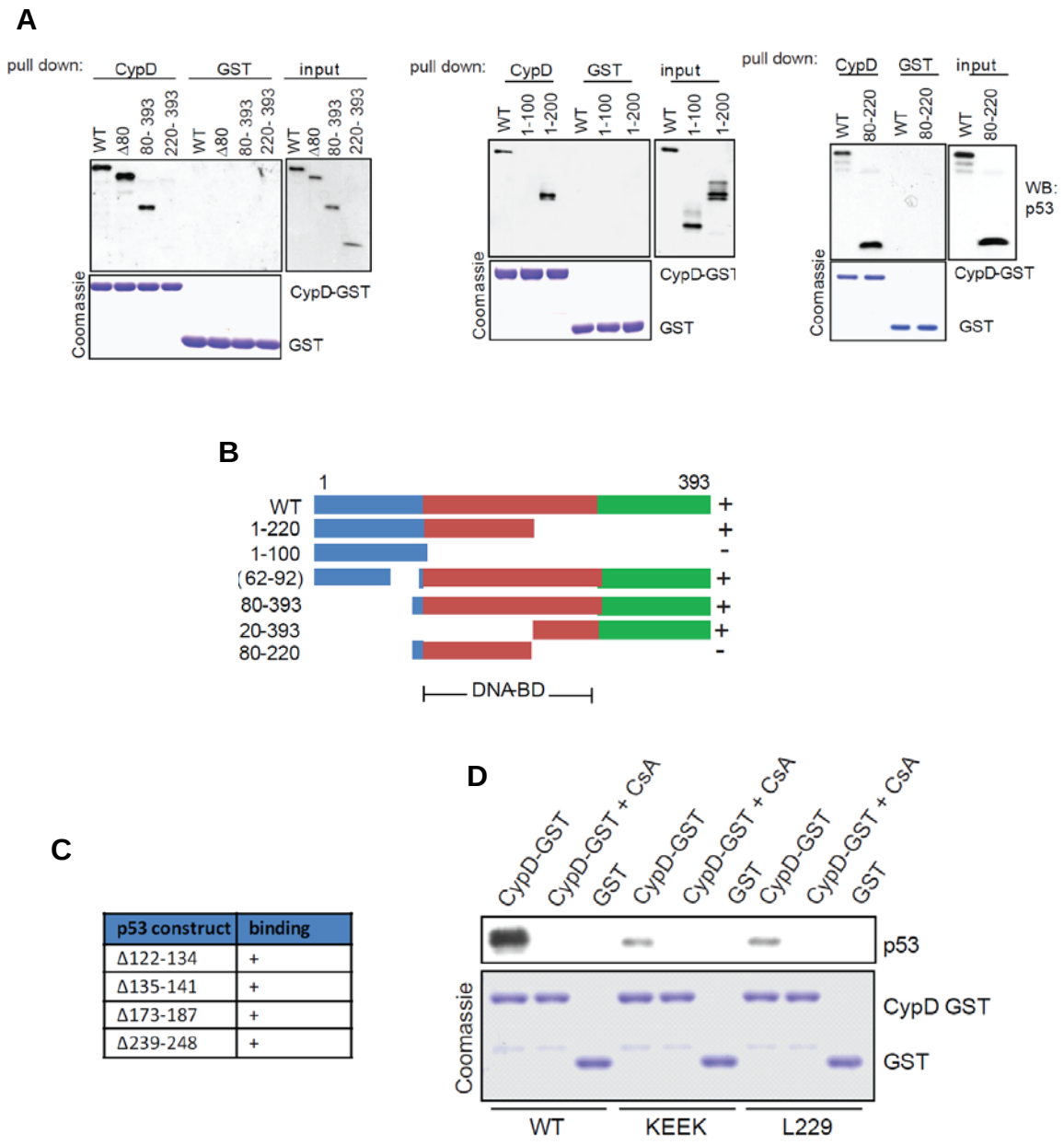

Figure 25. Mapping the CypD interaction on p53. (A) The indicated p53 deletion constructs were transfected into HCT116 p53 -/- cells. Binding was analyzed with purified CypD-GST or empty GST proteins (Coomassie) in pull-down assays. **(B)** Summary of the results in A. Lack (-) or presence (+) of binding is indicated. **(C)** The contact domains on p53 required for direct interaction with BclxL/Bcl2 proteins are not required for interaction with CypD. **(D)** Tetrameric p53 is the preferred partner for CypD interaction. Purified wild-type, monomeric (KEEK, for F341K, L344E, L348E, A355K) or dimeric (L229K) p53 mutants were used in pull-down assays with purified CypD-GST.

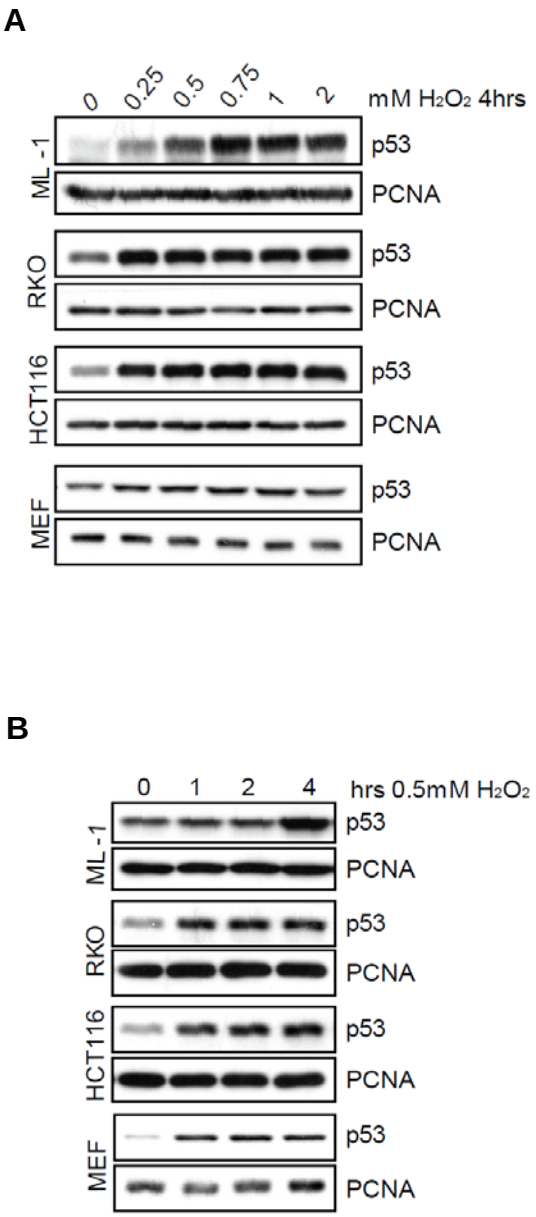

Figure 26. Upon oxidative stress p53 is rapidly stabilized. (A) Robust accumulation of p53 in primary and cancer cell lines treated with different doses of H_2O_2 for 4 hrs. Indicated cell lines were treated with H_2O_2 and protein levels assessed by Western blotting. **(B)** Treatment of primary and cancer cell lines with H_2O_2 causes rapid accumulation of p53. Indicated cell lines were treated with 0.5 mM H_2O_2 for the indicated time points and protein levels assessed by Western blotting.

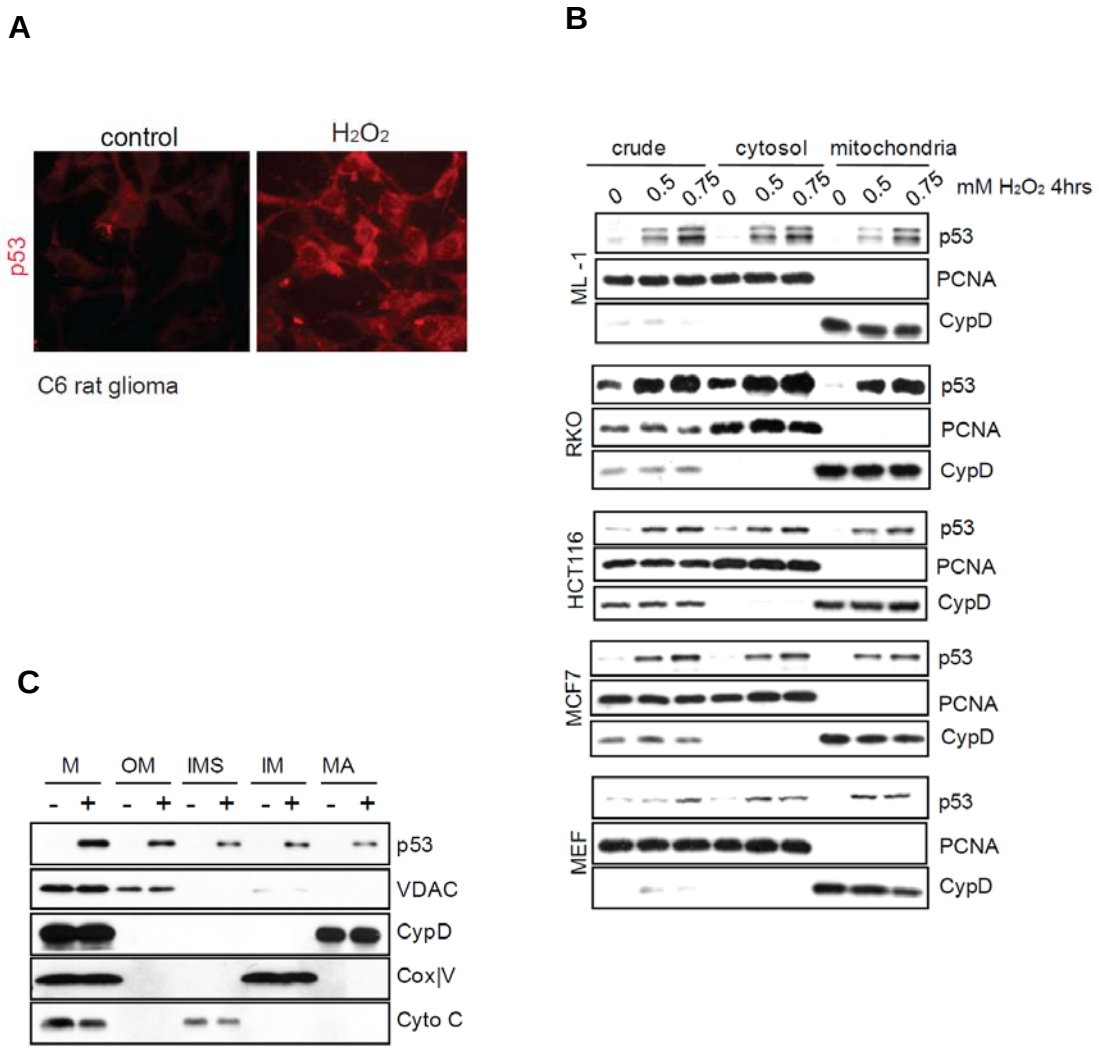

Figure 27. Upon oxidative stress p53 translocates to mitochondria. (A) p53 accumulates in a punctuate cytosolic pattern in C6 rat glioma cells treated with 0.4 mM H_2O_2 for 4 hrs. p53 immunofluorescence. **(B)** Rapid mitochondrial p53 accumulation upon oxidative stress. Cells were treated with H_2O_2 for 4 hrs. Mitochondrial fractions were prepared by sucrose gradient ultracentrifugation. PCNA serves as indicator of purity of mitochondrial fractions and as loading control for crude and cytosolic fractions. CypD serves as mitochondrial marker and loading control for mitochondrial fractions. **(C)** Upon oxidative stress, p53 accumulates in the mitochondrial matrix. Isolated mitochondria from HCT116 p53 +/+ cells treated with 0.5 mM H_2O_2 for 4 hrs were subjected to submitochondrial fractionation. M, crude mitochondrial; OM, outer membrane; IMS, intermembrane space; IM, inner membrane; MA, matrix.

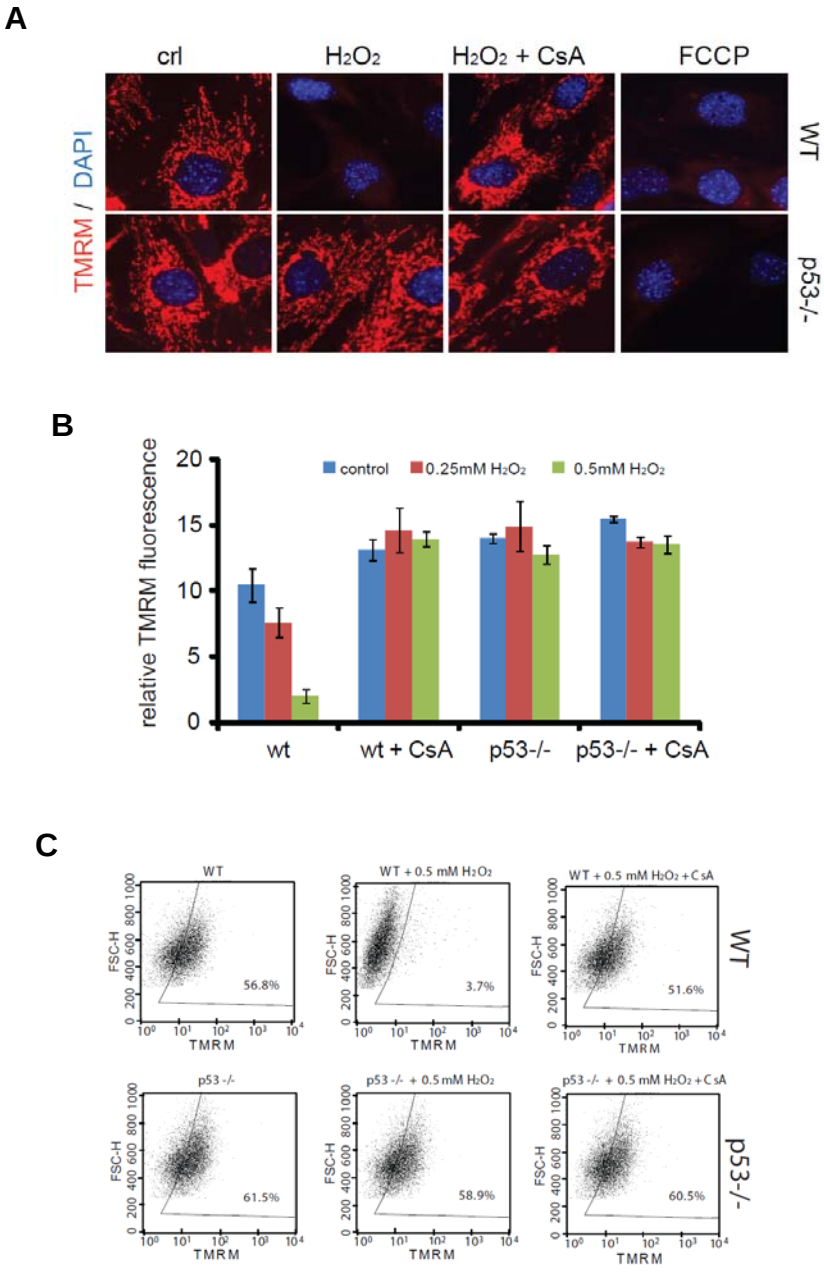

Figure 28. p53 deficiency renders cells resistant to H_2O_2-induced and CsA-dependent loss of mitochondrial membrane potential (ΔΨm). WT and p53 -/- MEFs were treated with 0.4 mM H_2O_2 for 8 hrs ± 2 µM CsA and stained with the ΔΨm -sensitive dye TMRM (Tetramethyl Rhodamine Methyl Ester). **(A)** TMRM assessed by fluorescence microscopy. Protonophore FCCP as control. **(B)** Mean TMRM fluorescence of 3 independent experiments ± SD measured by AxioVision Automatic Quantitation. **(C)** TMRM fluorescence of MEFs treated as in A, measured by FACS.

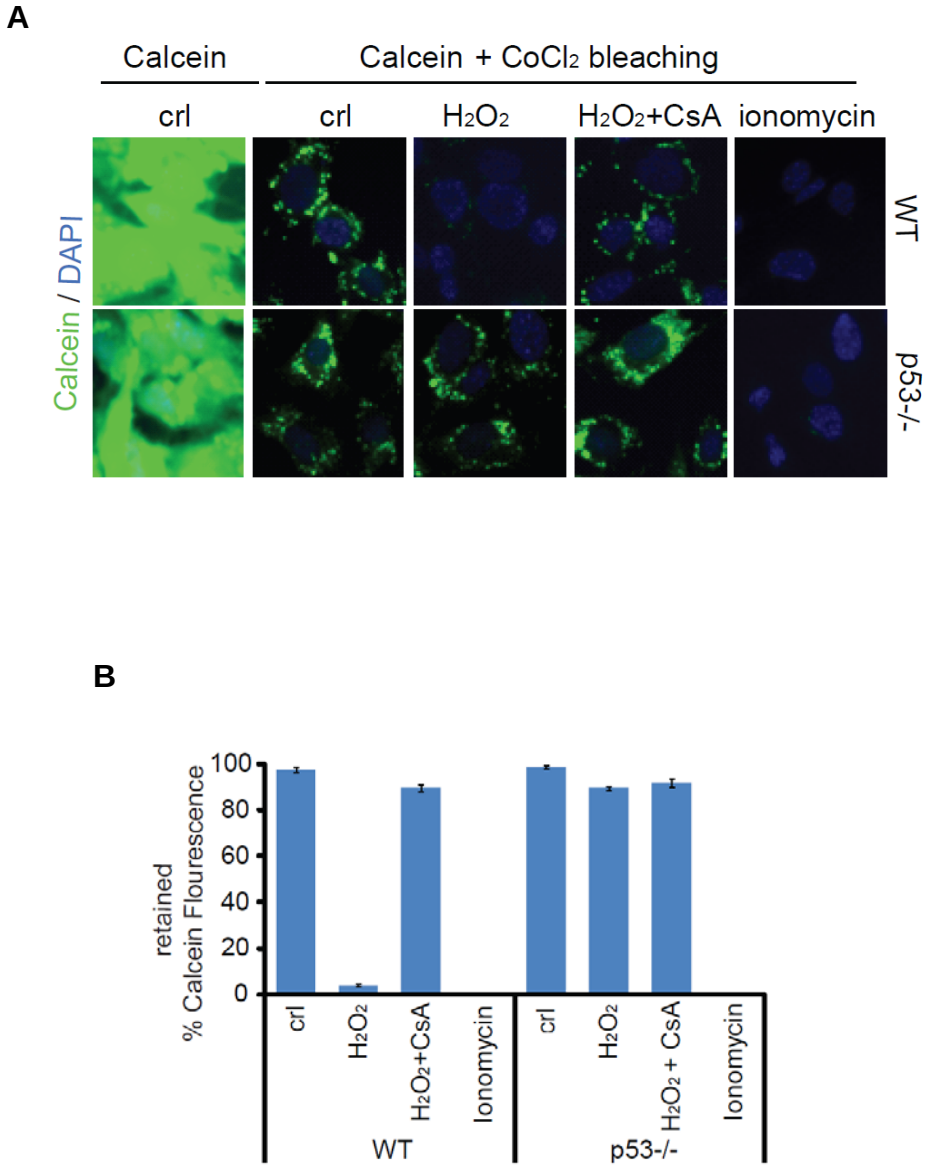

Figure 29. p53 deficiency renders primary MEFs resistant to PTP opening. WT and p53 -/- MEFs were treated with 0.4 mM H_2O_2 for 8 hrs ± 2 μM CsA. Calcein release assay. **(A)** Representative images by fluorescence microscopy. **(B)** Mean Calcein fluorescence from 3 independent experiments ± SD, measured by FACS. Ionophore Ionomycin as a control.

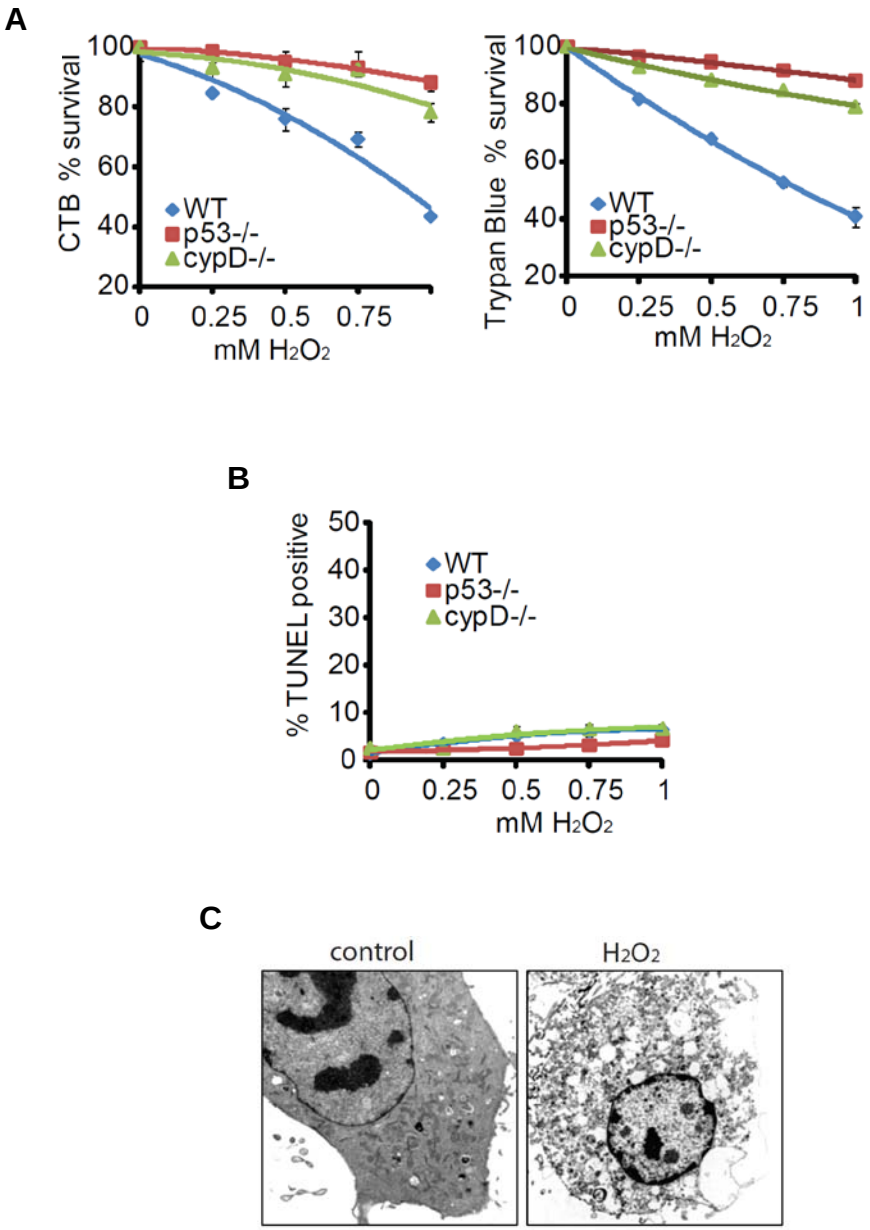

Figure 30. In primary MEFs, oxidative stress induces necrosis that depends on p53 and CypD. (A) p53 -/- and CypD -/- MEFs are resistant to H_2O_2-induced cell death. Primary MEFs of the indicated genotype were treated with H_2O_2 for 24 hrs. Cell death was measured by CTB viability (left) or trypan blue exclusion assays (right). **(B)** H_2O_2 does not induce significant apoptosis. Primary MEFs were treated with H_2O_2 for 24 hrs as in (A). Apoptosis was assessed by TUNEL assays. **(C)** WT MEFs were treated with 0.5 mM H_2O_2 for 24 hrs and the morphological hallmarks of necrotic cell death confirmed by electron microscopy.

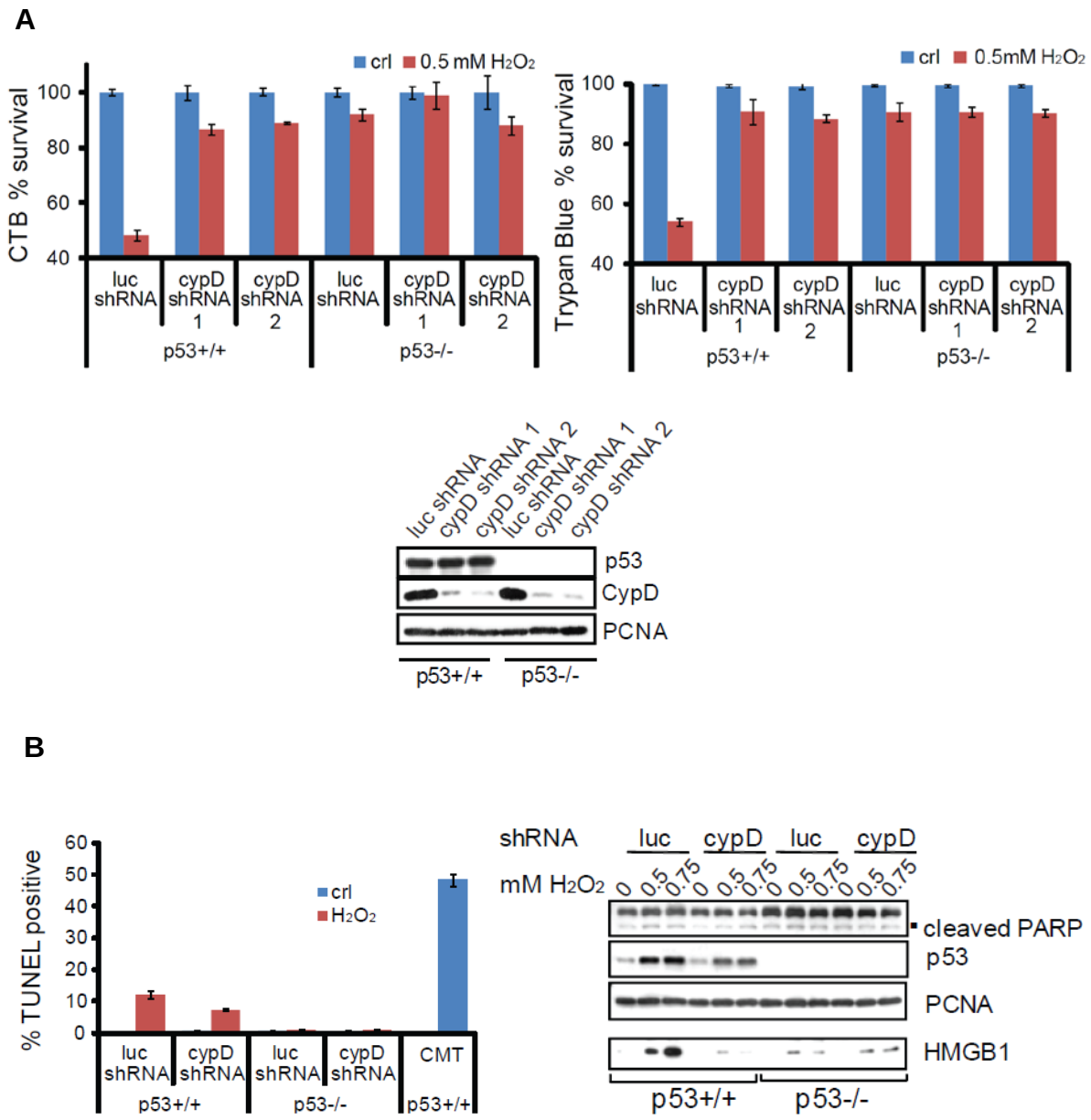

Figure 31. p53 deficiency and silencing of CypD protects HCT116 cells from H_2O_2-induced necrosis. (A) Cell death of HCT116 p53 +/+ versus HCT116 p53 -/- cells treated with H_2O_2 for 24 hrs in the presence of control shRNA (luc) or two independent cypD shRNAs. CTB viability (top left) and trypan blue exclusion assays (top right). Bottom, levels of CypD silencing upon introduction of shRNA. **(B)** Absence of significant apoptosis in cells from A, as measured by TUNEL (left) and absence of PARP cleavage (right). In contrast, H_2O_2-treated cells release large quantities of necrosis indicator HMGB1 into the medium in a dose-, p53- and CypD-dependent manner. Immunoblot.

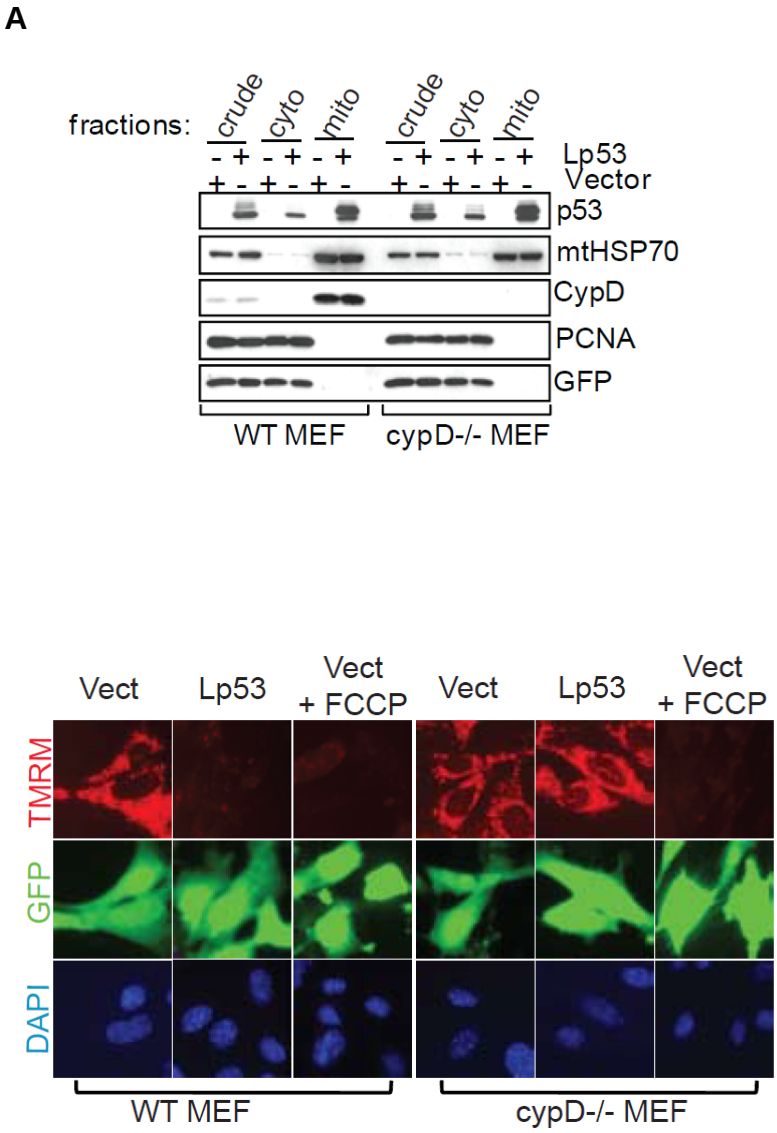

Figure 32. Mitochondrial matrix-targeted p53 (Leader p53-Lp53) reduces ΔΨm in a CypD dependent manner. (A) Mitochondria preparations from WT and cypD -/- MEFs infected with Leader p53 construct showing localization of leader p53 at mitochondria. **(B)** Mitochondrial matrix-targeted p53 causes collapse of ΔΨm in WT but not cypD -/- MEFs. Left, WT and cypD-/- MEFs were infected with vector Ad5-GFP or Leader p53 construct (Ad5-Lp53-GFP, wt p53 fused to the mitochondrial import leader sequence of ornithine transcarbamylase) designed to target p53 to mitochondrial matrix. 24 hrs after infection, TMRM was added to the media to visualize changes in ΔΨm.

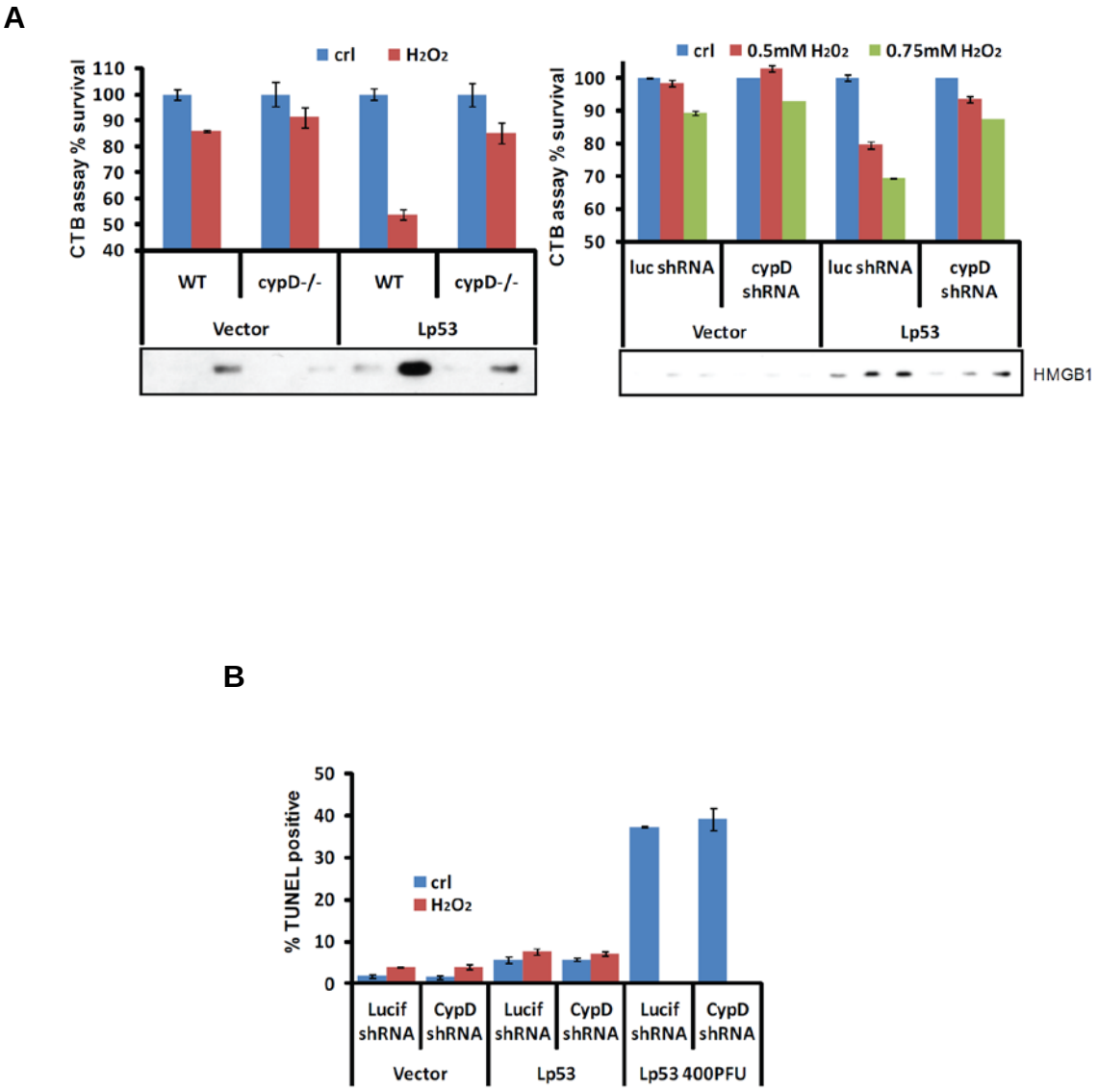

Figure 33. Mitochondrial matrix-targeted p53 (Lp53) renders p53-/- cells more sensitive to H_2O_2-induced necrotic death in a CypD dependent manner. (A) Survival and HMGB1 release in media of SV-40 immortalized WT or cypD-/- MEFs (left) or HCT116 p53 -/- cells (right) infected with 100PFU Lp53 or vector alone and treated with 0.5 mM H_2O_2 for 12 hrs. **(B)** Levels of apoptosis measured by TUNEL of HCT117p53-/- cells treated as in A. Infection with 400PFU virus for 48 hrs used as positive control.

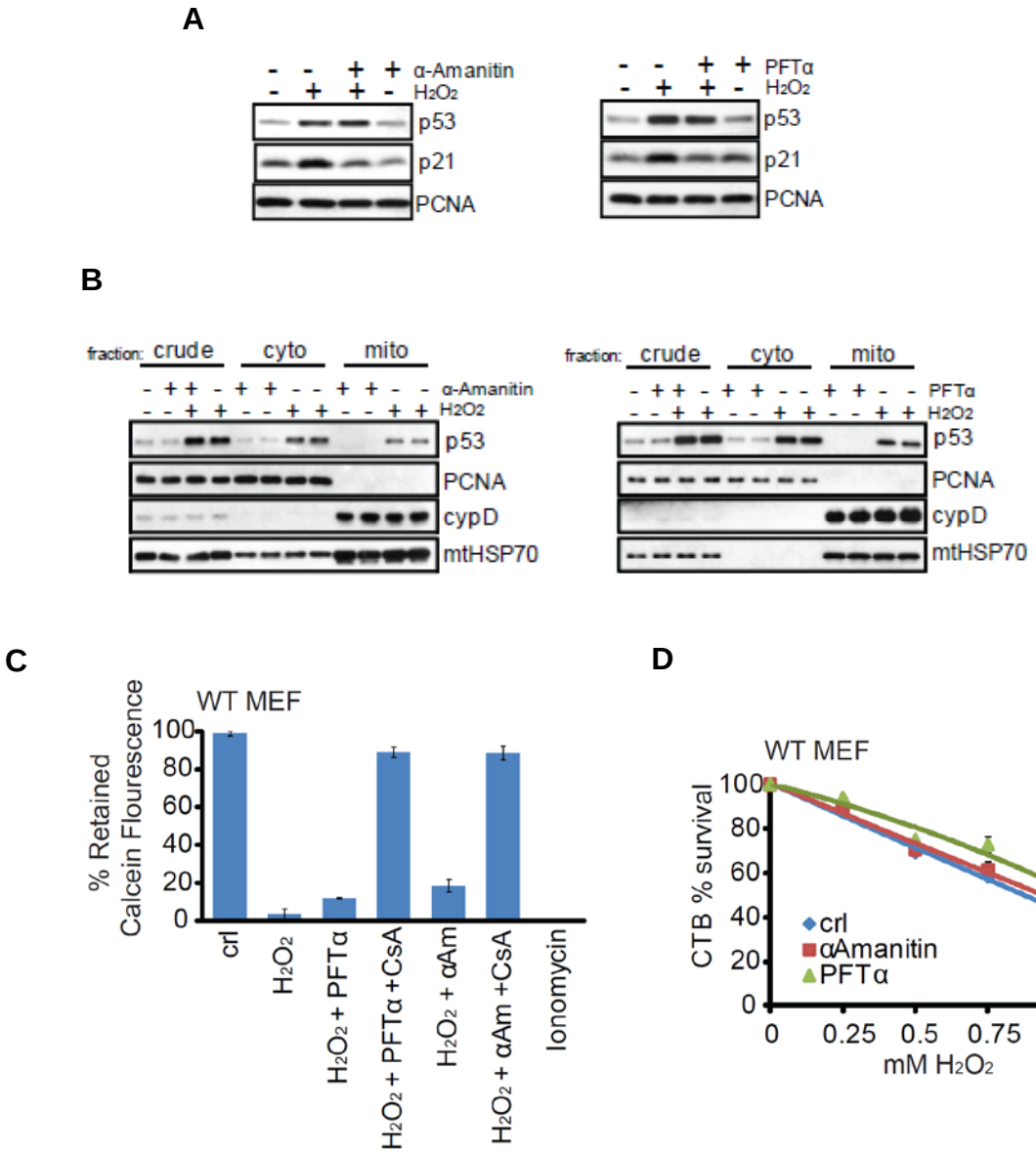

Figure 34. Blocking of transcription does not prevent H_2O_2 -induced PTP opening or cell death. (A) Pretreatment with αAmanitin or PFTα inhibits H_2O_2-induced transcription, but does not affect p53 levels. WT MEFs were treated with the inhibitors before adding H_2O_2. p21 and p53 protein levels measured by Western blotting. **(B)** Pretreatment with αAmanitin or PFTα does not inhibit H_2O_2-induced mitochondrial p53 translocation. WT MEFs were treated as in A, mitochondria isolated and p53 levels analyzed by Western blotting. **(C)** Calcein fluorescence measured by FACS after treatment of WT MEFs with 0.5 mM H_2O_2 for 8 hrs in the presence of αAmanitin or PFTα. **(D)** Survival of WT MEFs treated with the indicated doses of H_2O_2 for 24 hrs, measured by Cell Titer Blue viability assay.

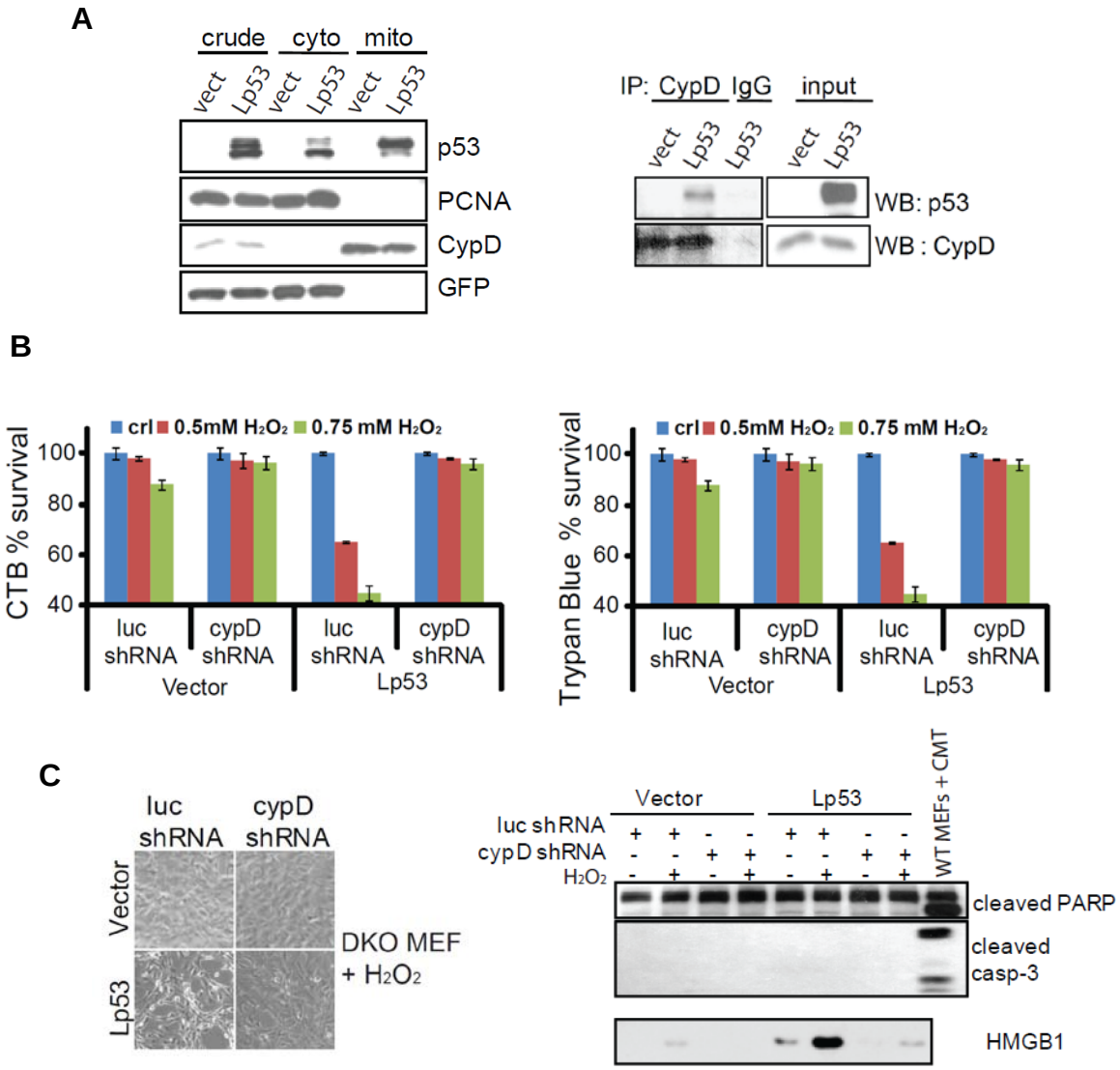

Figure 35. Lp53 renders Bax/Bak double knock out MEFs sensitive to oxidative stress in a CypD dependent manner. (A) Lp53 forms a complex with CypD. Left, mitochondrial localization of Lp53. Right, Lp53 binds to CypD. CypD was immunoprecipitated using CypD antibody from Lp53-infected Bax/Bak DKO MEF mitochondrial lysates. **(B)** Lp53 rendenrs Bax/Bak DKO MEFs more sensitive to H_2O_2 in a CypD dependent manner. Bax/Bak DKO MEFs stably expressing cypD or luciferase shRNAs were infected with Lp53 or vector alone and treated with H_2O_2 12 hrs. Cell viability was measured by CTB (right) or trypan blue exclusion assay (left). **(C)** Cell death caused by Lp53 and H_2O_2 is not apoptosis, but necrosis. Left, bright field image of Lp53- or vector-infected Bax/Bak DKO stably expressing cypD or luciferase shRNA treated with H_2O_2. Right, lack of PARP or caspase-3 cleavage, but strong HMGB1 release into the media in the presence of Lp53 and H_2O_2, reversed by cypD shRNA. Bax/Bak DKO MEFs were treated as in B and processes for western blotting. WT MEFs treated with Camptothecin serve as positive control for PARP and Caspase-3 cleavage.

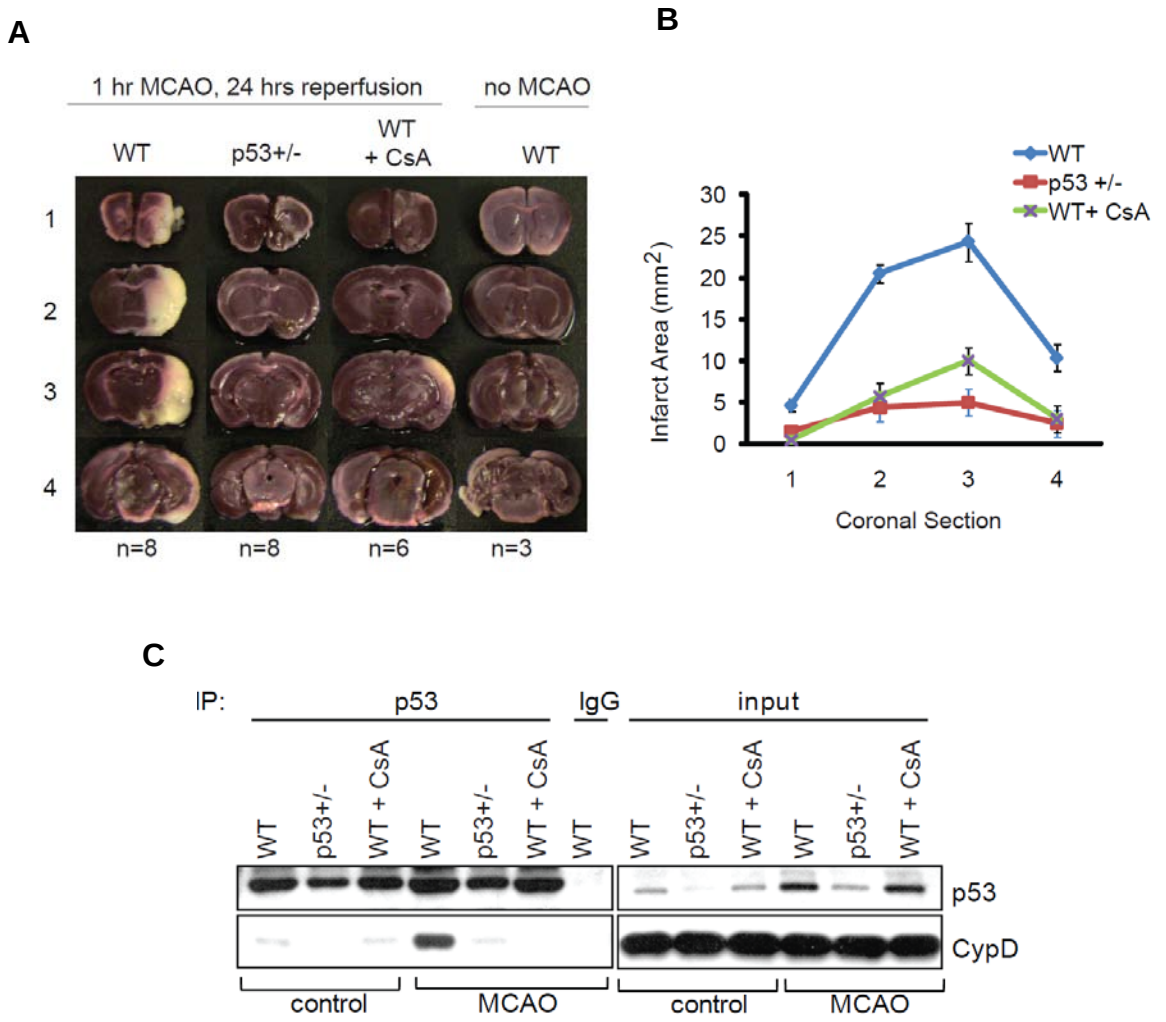

Figure 36. The p53-CypD complex has a pathophysiologic role in ischemic stroke. WT, heterozygous p53+/- and WT control mice pre-treated with CsA (15 mg/kg i.p, 15 min prior to MCAO) were subjected to middle cerebral artery occlusion (MCAO, right side) for 1 hr followed by reperfusion for 24 hrs under cerebral blood flow and temperature-controlled conditions. **(A)** Representative TTC-stained coronal brain sections; **(B)** Mean infarct size ± SD. In contrast to infarcted WT brains, p53 +/- brains are strongly stroke-protected and phenocopy the brain protection seen in cyclosporine A-pretreated WT mice. **(C)** Stroke protection correlates with the absence of an ischemia-induced p53-CypD complex in brain tissue. Co-immunoprecipitation with p53 antibody or non-specific IgG from the 25 hrs injured or corresponding contralateral control hemispheres from representative brains treated as in A. immunoblotting for CypD. Input is shown.

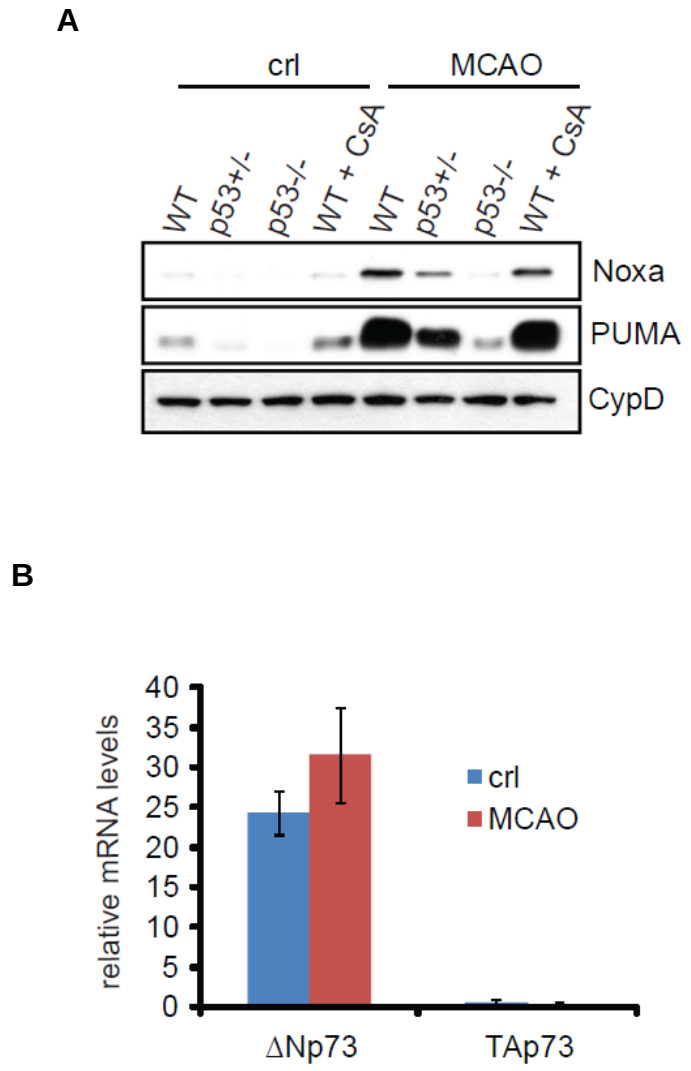

Figure 37. Expression of apoptotic proteins PUMA and Noxa and p73 family members upon MCAO. (A) Brain tissue lysates from 25 hrs-injured (MCAO) or corresponding contralateral control hemispheres from representative brains, treated as in Figure 36. Immunoblot for Noxa and PUMA. CypD is a loading control. **(B)** mRNA expression of ΔNp73 and TAp73 in brain tissues from injured (MCAO) or corresponding contralateral control hemispheres from representative WT brains, treated as in Figure 36. qRT-PCR normalized for GAPDH.